ENERGY LABORATORY

MASSACHUSETTS INSTITUTE
OF TECHNOLOGY

ANALYSIS OF STRATEGIES FOR IMPROVING URANIUM UTILIZATION IN PRESSURIZED WATER REACTORS

by

Joseph A. Sefcik
Michael J. Driscoll
David D. Lanning

DOE Contract No. DE-AC02-79ET34022 (Nuclear Engineering Department Report No. MITNE-234, Energy Laboratory Report MIT-EL-80-032). January, 1981.

DOE/ET/34022-1
MITNE-234
MIT-EL-80-032

ANALYSIS OF STRATEGIES FOR IMPROVING URANIUM UTILIZATION IN PRESSURIZED WATER REACTORS

by

Joseph A. Sefcik
Michael J. Driscoll
David D. Lanning

DOE Contract No. DE-AC02-79ET34022 (Nuclear Engineering Department Report No. MITNE-234, Energy Laboratory Report MIT-EL-80-032). January, 1981.

DOE/ET/34022-1

ANALYSIS OF STRATEGIES FOR IMPROVING URANIUM UTILIZATION IN PRESSURIZED WATER REACTORS

by

Joseph A. Sefcik
Michael J. Driscoll
David D. Lanning

Annual Technical Progress Report/Principal Topical Report
For FY 1980

Department of Nuclear Engineering
and
Energy Laboratory
MASSACHUSETTS INSTITUTE OF TECHNOLOGY
Cambridge, Massachusetts 02139

Sponsored by

U.S. Department of Energy
Division of Energy Technology
Under Contract No. DE-AC02-79ET34022

NOTICE

Printed in the United States of America

Available from

National Technical Information Service
U.S. Department of Commerce
5285 Port Royal Road
Springfield, VA 22151

USDOE LWR TECHNOLOGY PROGRAM
IMPROVED URANIUM UTILIZATION
SPECIALIZED DISTRIBUTION LIST

Mr. John R. Jensen
Mechanical Engineering Division
American Electric Power Service Corp.
2 Broadway
New York, NY 10004

Mr. Benjamin L. Dow, Jr.
Arkansas Power and Light Company
P. O. Box 551
Little Rock, AR 72203

Mr. J. Tulenko
Babcock & Wilcox Company
Nuclear Power Generation Div.
P. O. Box 1260
Lynchburg, VA 24505

Mr. Thomas A. Coleman
Babcock & Wilcox Company
Nuclear Power Generation Div.
P.O. Box 1260
Lynchburg, VA 24505

Mr. M. S. Freshley
Battelle-Pacific Northwest Laboratory
Battelle Boulevard
P.O. Box 999
Richland, WA 99352

Mr. C. L. Mohr, Manager
Nuclear Fuels
Battelle-Pacific Northwest Laboratory
P.O. Box 999
Richland, WA 99352

Dr. W. A. Weinreich
Bettis Atomic Power Laboratory (W)
Box 79
West Mifflin, PA 15122

Mr. R. N. Duncan
Combustion Engineering, Inc.
1000 Prospect Hill Road
Windsor, CT 06095

Mr. W. M. Kiefer
Commonwealth Edison Company
P. O. Box 767
Chicago, IL 06090

Mr. D. O'Boyle
Commonwealth Edison Co.
P. O. Box 767
Chicago, IL 60690

Dr. Min L. Lee
Chief Nuclear Engineer
Consolidated Edison Company
of New York, Inc.
4 Irving Place
New York, NY 10003

Mr. F. W. Buckman
Consumers Power Company
212 W. Michigan Avenue
Jackson, MI 49201

Mr. D. B. Wehmeyer
Detroit Edison Co.
2000 Second Avenue
Detroit, MI 48226

Mr. J. D. Kortheuer
Duke Power Company
P. O. Box 33189
Charlotte, NC 28242

Mr. T. Snead
Duke Power Company
P. O. Box 33189
Charlotte, NC 28242

Mr. R. G. Snipes
Duke Power Company
P.O. Box 33189
Charlotte, NC 28242

Mr. Floyd E. Gelhaus
Electric Power Research Inst.
P. O. Box 10412
Palo Alto, CA 94303

Dr. J. T. A. Roberts
Electric Power Research Inst.
P. O. Box 10412
Palo Alto, CA 94303

Mr. C. E. Crouthamel
Exxon Nuclear Company, Inc.
2595 George Washington Way
Richland, WA 99352

Dr. G. A. Sofer
Nuclear Fuels Engineering
Exxon Nuclear Company, Inc.
2101 Horn Rapids Road
Richland, WA 99352

Dr. K. N. Woods
2595 George Washington Way
Exxon Nuclear Company, Inc.
Richland, WA 99352

Mr. J. R. Tomonto
Florida Power & Light Company
P. O. Box 3100
Miami, FL 33101

Dr. S. Armijo
General Electric Company
Nuclear Energy Division
175 Curtner Avenue
San Jose, CA 95125

Dr. H. W. Schadler, Manager
Metallurgy Laboratory
General Electric Company
Research and Development Center
P. O. Box 8
Schenectady, NY 12301

Mr. Gordon Bond
GPU Service Corp.
260 Cherry Hill Road
Parsippany, NJ 07054

Mr. D. J. Groetch
Manager, Advanced Development Activity
Knolls Atomic Power Laboratory
Box 1072, F3, 12
Schenectady, NY 12301

Mr. William J. Tunney
Long Island Lighting Company
175 E. Old Country Road
Hicksville, NY 11801

Mr. S. W. Wilczek, Jr.
Niagara Mohawk Power Corp.
300 Erie Boulevard West
Syracuse, NY 13202

Mr. John Hallam
Manager, Computer Engineering
Quadrex Corporation
1700 Dell Avenue
Campbell, CA 95008

Mr. I. Spiewak
Oak Ridge National Laboratory
P. O. Box X, Building 9201-3
Oak Ridge, TN 37830

Mr. G. F. Daebeler
Philadelphia Electric Company
2301 Market Street
P. O. Box 8699
Philadelphia, PA 19101

Mr. B. H. Koske
Energy Conversion Engineer
Public Service Company of
New Mexico
P.O. Box 2267
Albuquerque, NM 87103

Mr. Kashmiri L. Mahna
Public Service Electric
and Gas Company
P.O. Box 570, Room 3347
Newark, NJ 07101

Mr. Richard R. O'Laughlin
Nuclear Fuel Manager
Public Service Company of Indiana
1000 East Main Street
Plainfield, IN 46168

Dr. William V. Johnston
Chief, Fuel Behavior Research Branch
Division of Reactor Safety Research
U.S. Nuclear Regulatory Commission
Washington, D.C. 20555

Mr. D. L. Larkin
Washington Public Power Supply System
P. O. Box 968
Richland, WA 99352

Mr. R. S. Miller
Westinghouse Electric Corp.
Nuclear Fuel Division
Box 355
Pittsburgh, PA 15230

Dr. Joseph K. Gasper
Manager, Reactor and Computer Technical Services
Omaha Public Power District
1623 Harney
Omaha, NE 68102

Dr. U. Decher
Combustion Engineering
1000 Prospect Hill Road
P.O. Box 500
Windsor, CT 06095

Mr. Martin L. Bowling
Virginia Electric and Power Company
Seventh and Franklin Streets
P.O. Box 1194
Richmond, VA 23209

Professor A. Sesonske
School of Engineering
Purdue University
West Lafayette, IN 47907

Mr. Philip D. Brown
Nuclear Engineer, Fuel Cycle Services
409 Krystal Building
Chattanooga, TN 37401

Mr. Daniel D. Whitney
Sacramento Municipal Utility District
6201 S. Street
Box 15830
Sacramento, CA 95813

Mr. Michael Driscoll
Massachusetts Institute of Technology
138 Albany Street
Cambridge, MA 02139

Dr. J. C. Turnage
Yankee Atomic Electric Company
20 Turnpike Road
Westborough, MA 01581

Mr. Peter A. Aucoin
Nuclear Assurance Corporation
24 Executive Park West
Atlanta, GA 30329

Mr. Howard L. Sobel
Section Head, Nuclear Materials and Fuel Management Section
American Electric Power Service Corporation
2 Broadway
New York, NY 10004

Mr. T. D. Chikalla, Manager
Ceramics and Graphite
Battelle-Pacific Northwest Laboratory
P.O. Box 999
Richland, WA 99352

Mr. R. L. Horowitz
General Electric - Research and
Development Corporate
P.O. Box 8
Schenectady, NY 12345

Dr. Elwyn Roberts
Manager, Irradiation Testing
Westinghouse Electric Corporation
P.O. Box 355
Pittsburgh, PA 15230

R. Crowther
Project Manager
General Electric Company
175 Curtner Company
San Jose, California 95125

Dr. Peter M. Lang, Chief
LWR Branch
Division of Nuclear Power Development
U.S. Dept. of Energy, Mail Stop B-107
Washington, D.C. 20545 (5 copies)

N.L. Shapiro
Manager, Advanced Design Projects
Combustion Engineering, Inc.
1000 Prospect Hill Road
Windsor, CT 06095

W.L. Orr
Manager of Product Development Support
Nuclear Fuel Division
Westinghouse Electric Corp.
P.O. Box 355
Pittsburgh, PA 15230

Dr. Richard B. Stout
Nuclear Fuels Engineering Dept.
Exxon Nuclear
2101 Horn Rapids Road
Richland, WA 99352

V. Uotinen
Project Manager
The Babcock & Wilcox Co.
P.O. Box 1260
Lynchburg, VA 24505

ABSTRACT

Systematic procedures have been devised and applied to evaluate core design and fuel management strategies for improving uranium utilization in Pressurized Water Reactors operated on a once-through fuel cycle. A principal objective has been the evaluation of suggested improvements on a self-consistent basis, allowing for concurrent changes in dependent variables such as core leakage and batch power histories, which might otherwise obscure the sometimes subtle effects of interest. Two levels of evaluation have been devised: a simple but accurate analytic model based on the observed linear variations in assembly reactivity as a function of burnup; and a numerical approach, embodied in a computer program, which relaxes this assumption and combines it with empirical prescriptions for assembly (or batch) power as a function of reactivity, and core leakage as a function of peripheral assembly power. State-of-the-art physics methods, such as PDQ-7, were used to verify and supplement these techniques.

These methods have been applied to evaluate several suggested improvements: (1) axial blankets of low-enriched or depleted uranium, and of beryllium metal, (2) radial natural uranium blankets, (3) low-leakage radial fuel management, (4) high burnup fuels, (5) optimized H/U atom ratio, (6) annular fuel, and (7) mechanical spectral shift (i.e. variable fuel-to-moderator ratio) concepts such as those involving pin pulling and bundle reconstitution.

The potential savings in uranium requirements compared to current practice were found to be as follows: (1) ∿0-3%, (2) negative, (3) 2-3%; possibly 5%, (4) ∿15%, (5) 0-2.5%, (6) no inherent advantage, (7) ∿10%. Total savings should not be assumed to be additive; and thermal/hydraulic or mechanical design restrictions may preclude full realization of some of the potential improvements.

ACKNOWLEDGEMENTS

The work presented in this report has been performed primarily by the principal author, Joseph A. Sefcik, who has submitted substantially the same report in partial fulfillment of the requirements for the Ph.D degree in Nuclear Engineering at M.I.T.

The present work was supported by a Department of Energy (DOE) contract administered through the M.I.T. Energy Laboratory. Computer calculations were carried out at the M.I.T. Information Processing Center and the Laboratory for Nuclear Science.

The authors would like to acknowledge the cooperation of Dr. Edward Pilat and employees of the Yankee Atomic Electric Company in facilitating the acquisition of descriptive data from publicly available documentation on the Maine Yankee Reactor. The information in this report cited as deriving from "Maine Yankee", however, should not be considered as representing that actual system in its current or projected operating configuration, but as an idealization thereof. In particular, the results so identified in this report have not been either reviewed or approved by the Yankee organization.

The majority of the typing was ably handled by Ms. Maureen Walsh, with the assistence of Ms. Carolyn Rose and Ms. Christal Whelan.

TABLE OF CONTENTS

Table of Contents - Cont.

Table of Contents - Cont.

LIST OF FIGURES

LIST OF FIGURES

LIST OF FIGURES

LIST OF FIGURES

LIST OF TABLES

LIST OF TABLES

LIST OF TABLES

CHAPTER 1

BACKGROUND AND PREVIOUS RESEARCH

1.1 INTRODUCTION

The efficient use of fuel resources is an important goal for any energy technology. This objective has been assigned higher priority in the past several years with respect to natural uranium consumption by light water reactors (LWR's). Several reasons have motivated this attention: the rising price of uranium on the domestic and world market; the deceleration of the breeder development/deployment program; and the deferral of plans to recycle plutonium in LWR's. The deferral of recycle is largely due to concerns over linkage to weapons proliferation.

The work described in this report was undertaken under the LWR Technology Program for Improved Uranium Utilization sponsored by the United States Department of Energy. It continues earlier MIT efforts along the same general lines undertaken as part of the Nonproliferation Alternative Systems Assessment Program (NASAP) (N-1) which in turn, provided input to the International Nuclear Fuel Cycle Evaluation (INFCE) (I-1). The general goal of the present work has been to develop, test, and apply self-consistent methods for the evaluation of improvements in core design and fuel management strategy in pressurized

water reactors as they apply to increasing the energy generated per unit mass of natural uranium mined.

The MIT effort has focused on pressurized water reactors (PWRs) because they comprise nearly 2/3 of the nuclear power plant capacity operable, under construction, or on order in the U.S. and over 1/2 of the worldwide nuclear capacity (see Table 1.1). However, it is expected that much of the work can be readily extended to the boiling water reactors (BWRs), which account for most of the remaining capacity. Similarly, the emphasis has been on concepts which can be retro-fit into current system designs, operating on the once-thru fuel cycle, since only items in this category have credible prospects for making a substantial impact through rapid and widespread deployment.

1.2 BACKGROUND

Several major studies have been completed over the past few years which delineate the potential uranium savings which can be achieved in pressurized water reactors. Table 1.2 summarizes some of the uranium saving techniques which have been identified, the potential savings, and the time interval needed for their introduction. The uranium-conserving strategies range from very simple to very complicated, and even though large savings are available in some cases (e.g. through reprocessing), the economics and politics of the situation may dictate against their use. It should also be noted that the various sav-

TABLE 1.1 NUCLEAR POWER PLANTS

(Operable, under construction, or on order (≥30 MWe)
as of 6/30/80)

TYPE (COOL/MOD.)		U.S.	WORLD
PWR	LWR (H_2O)	113 (63.5%)	280 (53.2%)
BWR	LWR (H_2O)	61 (34.3%)	119 (22.6%)
LWBR	LWR (H_2O)		
PHWR (CANDU)	(D_2O)		36
LWCHWR	(D_2O)		2
HWBLWR	(D_2O)		2 (8.0%)
GCHWR	(D_2O)		2
GCR	GRAPHITE		36
AGR	GRAPHITE		15
LGR	GRAPHITE	1	23 (14.4%)
HTGR	GRAPHITE	1	1
THTR	GRAPHITE		1
LMFBR (Na)		1	8
TOTAL UNITS		178	526
TOTAL GWE		171	400
TOTAL OPERABLE		74	229
GWE OPERABLE		54	125

KEY: PWR = Pressurized Water Reactor
BWR = Boiling Water Reactor
PHWR = Pressurized Heavy Water Moderated and Cooled Reactor
LWBR = Light Water Breeder Reactor
LWCHWR = Light Water Cooled, Heavy Water Moderated Reactor
HWBLWR = Heavy Water Moderated Boiling Light Water Cooled Reactor
GCHWR = Gas Cooled Heavy Water Moderated Reactor
GCR = Gas Cooled Reactor
AGR = Advanced Gas-Cooled Reactor
LGR = Light Water Cooled, Graphite Moderated Reactor
HTGR = High Temperature Gas Cooled Reactor
THTR = Thorium High Temperature Reactor
LMFBR = Liquid Metal Cooled Fast Breeder Reactor

Source: Reference (N-2)

TABLE 1.2 REPRESENTATIVE LIST OF SOME STRATEGIES FOR FUEL CONSERVATION IN A PWR

Tactic	Percent Saving (approx.)	Time to Introduce	References	Comments
Reprocessing	20-30	10 years	G-2	Economic uncertainties Politically undesirable under current conditions
Increased Number of Batches	10	5 years	F-1,D-1, S-2	Constant discharge burnup would require more frequent refueling and would decrease capacity factor
Increased Discharge Burnup	10	5-15 years	F-1,D-1, S-2,M-2	Must assess materials problems
Reduced Radial Leakage	5-7	3-5 years	D-1,S-2, S-3	Commonly known as low-leakage fuel management; adverse power peaking is created
Axial Blankets	1-3	3-5 years	K-1,D-1, S-2	Leads to power peaking problems
Reduced Axial Leakage	1-2	5-10 years	K-1	Requires use of zirconium core support structures
Routine Coastdown	5-15	1-2 years	F-1,D-1, M-1,S-2, M-2,D-2 L-1	High savings if coastdown is done to economic breakeven
Variable Fuel to Moderator Ratio	5-15	10 years	R-1	Ore savings depend on strategy used (e.g. pin pulling); may lead to thermal-hydraulic problems; fuel reassembly required

TABLE 1.2 (Cont.)

Tactic	Percent Saving (approx.)	Time to Introduce	References	Comments
D_2O Spectral Shift	10-15	10 years	C-1,G-1	Poison control is reduced; D_2O is expensive and losses are significant
Optimized Fixed Fuel/Moderator ratio (e.g. change lattice pitch, pin diameter or use annular fuel)	~2-3	5 years	R-1,B-1	Applicability depends on specific reactor design

ings may not be additive when combined into a single design.

Current pressurized water reactors operate on a cycle which is one year in length, following which they are shut down for about six weeks for refueling. The mean discharge burnup is about 33000 MWD/MT. Every year one third of the core is replaced with fresh fuel which has an enrichment of about 3 w/o U-235. The fuel design characteristics and operating conditions of a reference PWR (Maine Yankee) are listed in Appendix A.

Increasing the number of staggered in-core batches results in a decrease in the cycle reactivity swing, which decreases the uranium enrichment required to meet the same energy output. The increased number of batches necessitates an increase in the number of refuelings in a given calendar period. An increased refueling frequency decreases plant capacity factor and thereby adversely affects the cost of electricity.

If the number of batches were held constant and the reload enrichment raised, the discharge burnup would be increased and the time between refuelings would be increased. The higher reactivity of the fresher batches permits the older batches to be driven deeper along the reactivity vs. burnup curve. Current pressurized water reactor owners are seriously considering switching to 18 month cycles with discharge burnups in the vicinity

of 36000 MWD/MT. The attendant increase in capacity factor helps reduce the cost of the generated electricity.

Employing both higher discharge burnup and an increased number of batches (e.g. 60000 MWD/MT, five batches) would reduce yellowcake consumption by 20%. There are potential difficulties, however, in implementing extended burnup, which are primarily related to the structural components of the fuel. The cladding faces increased corrosion on the water side during the long residence times and an increased internal pressure from fission product gas buildup. In-reactor experiments are under way at this time to assess the consequences of driving fuel to higher burnup.

Axial and radial leakage can account for neutron losses as high as four or five percent of total neutron production. Various schemes have been proposed for minimizing the losses. "Low-leakage" fuel management is a strategy whereby the fresh fuel is not loaded on the core periphery (as has been customary), but is instead scattered among older fuel in the core interior, while once or twice burned fuel is loaded on the periphery. The reduced peripheral power results in lower neutron losses, but higher radial power peaking factors throughout the reactor's burnup cycle.

The use of axial blankets of natural uranium or enrichment zoning in the axial direction can reduce axial leakage but, once again, power peaking factors are in-

creased. Neutron losses can be reduced without adversely affecting radial and axial peaking factors if stainless steel core support structures and/or core shrouds and barrels are replaced with zirconium structures.

Coastdown is a technique which relies on a reduction of moderator and fuel temperatures of the reactor, by reducing the coolant temperature and/or reactor power level to insert positive reactivity and thereby extend the length of the operating cycle. The electrical power output of the reactor is decreased in a ramp or stepwise fashion until the coastdown is terminated. The length of the coastdown period can be optimized to maximize the overall economics of the utility's electrical grid. Coastdown always reduces $U_3 O_8$ consumption. Under economically optimum conditions the reduction typically ranges from 5 to 8 percent. Coastdown to economic breakeven generates larger savings, around 12 percent.

The D_2O spectral shift concept uses a mixture of light and heavy water to change the neutron spectrum during the reactor's operating cycle, substantially reducing boron control requirements. At the beginning of the cycle, a 50% H_2O, 50% D_2O mixture is introduced into the reactor and the harder (more epithermal) spectrum increases absorption in U-238 which decreases reactivity in the short term but increases Pu-239 production. H_2O is added during the cycle to provide the reactivity needed to compensate for burnup. In-

decreased plutonium production and decreased losses to boron control poisons account for the improved neutron economy and increased fuel efficiency. D_2O is expensive, however, and losses can be quite costly. The separation of the H_2O and the D_2O may be more difficult than a utility would desire. Increased tritium production would complicate plant operation and maintenance. Hence, overall economics may preclude the use of this scheme.

Variable fuel-to-moderator ratio schemes seek to accomplish the same spectral shift as the D_2O-H_2O method but by mechanical means. The fuel begins in a tight pitch configuration with a lower reactivity than normal and an increased conversion ratio. At end-of-cycle, the rods are moved in some fashion to create a "wetter" configuration and in this manner, reactivity is inserted. Several of these schemes call for mechanical movement of the fuel, or fuel bundle disassembly and reassembly. The uranium savings are dependent upon whether the mechanical manipulation is done before or after the refueling (as will be discussed in a later chapter of this report). The thermal-hydraulic problems of both the fresh and reconstituted lattices involved in these schemes for producing a mechanical spectral shift may be severe.

The lattices of current generation pressurized water reactors were optimized under different constraints than those which apply at present: ore was cheaper and recycle

was assumed. As a result, the lattices may be slightly "dry" relative to the optimum fuel to moderator ratio for a high-burnup once-through cycle. A slight wettening of the lattice (through the use of annular fuel, reduced fuel density, etc.) may permit better fuel utilization on the once-thru cycle without violating safety criteria such as the need for a negative moderator temperature coefficient.

1.3 RESEARCH OBJECTIVES

To progress beyond the obvious gains obtained from increasing burnup and the number of fuel batches, it is generally believed that a large number of small, incremental improvements must be accumulated. This puts a severe strain on computational methodology: simple methods are too crude to discern the often subtle effects at issue and the use of full-fledged state-of-the-art computer capabilities involves far too much detail to be economically justified and, more importantly, admits so much increased flexibility that one can never be sure that comparisons are being made on an "all-else-being-equal" basis. Apparently innocuous simplifications or constraints can often perturb the comparison to the point where the effect of interest can be obscured.

This fundamental dilemma became clear early in the course of the present work, and led to the identification of the first major subtask -- the development of a simple scoping model which was capable of evaluating small changes

in core design and fuel management on a consistent basis and in a transparent manner. As developed, the model relies heavily on an analytically improved version of the linear reactivity model of core behavior, and on heuristic models benchmarked against more detailed computer results.

The second major focus of the present work has been on the evaluation of a number of contemporary candidate changes which have been suggested as ways to improve uranium utilization: the use of annular fuel pellets, axial and radial blankets, low leakage fuel management, and variable fuel-to-moderator-ratio concepts in several guises, such as pin-pulling and bundle reconstitution.

1.4 ORGANIZATION OF REPORT

The work reported here is organized as follows. Chapter two provides an outline of the computer methods used in this research. The calculational models used in these programs are also be discussed along with their applicability and limitations.

Chapter three contains an introduction to the linear reactivity model of core behavior. The model is extended to include the effects of leakage and power sharing as they occur in actual LWR fuel management schemes. An optimization process is developed and used to demonstrate that spatial and temporal criteria exist which can improve uranium ore use.

In chapter four, the use of simplified "group-and-one-half" methods and some heuristic observations of computer-calculated reactor core maps leads to the development of simplified power sharing and core leakage algorithms for inclusion in the methodology developed in the previous chapter.

Chapter five reports on the application of the subject methods to axial fuel management. The basic analytic relationships and static bundle results are examined to determine the best approach for more sophisticated computer calculations. Several of the most promising candidates are examined in detail.

In chapter six the methodology is applied to discern the relative advantages of low-leakage fuel management and natural uranium radial blankets. Several core configurations are examined.

Chapter seven deals with variable fuel-to-moderator ratio concepts. The analytical additions and extensions of the advanced linear reactivity model necessary to calculate uranium savings for a wide range of options are developed. In addition, some modifications to the LEOPARD computer program are required to adequately model the spectral shift concepts. Optimization criteria are presented and a final design proposed, one that is consistent with current perceptions of the thermal-hydraulic limitations.

Chapter eight summarizes the present work: the methods development effort and the several applications. The potential for the application of the same approach to other uranium saving strategies not analyzed here is discussed.

Several appendices are included to provide detail and supporting evidence and to document the computer program used to implement the screening of the various fuel design options.

CHAPTER 2

COMPUTER METHODS

2.1 INTRODUCTION

A central problem of nuclear reactor fuel management is the accurate determination of reaction rates and isotopic distributions at all points in space and time. The development of large and complex computer programs has simplified this task greatly. It is possible, in principle, to calculate the flux and isotopic concentrations in a nuclear reactor by using hundreds of energy groups, thousands of spatial points, and a multitude of time increments. However, practical considerations such as the size of today's computer memories and the costs associated with running long programs intervene to impose various constraints.

The evolution of computer programs in the nuclear fuel management sector reflects a continuing reduction of conservatisms imposed by safety requirements by a trade-off between cost and accuracy. Fortunately, acceptably accurate answers can be obtained without the necessity of complete pointwise modeling of the core. Thus, available "state-of-the-art" programs could be used to provide a sound foundation for the recent work.

The computer codes used in this research (primarily LEOPARD and PDQ-7) are employed either individually or in combination to make comparisons between various fuel manage-

ment strategies. The codes have been benchmarked against experimental data, and for certain regions of interest can be considered quite accurate.

Since there are several references which describe the methods associated with LWR fuel management (A-1,D-3,H-1,D-3) we can be brief in regard to generalities and concentrate on specifics in the exposition which follows. Even more germane, previous workers at MIT: namely, Garel (G-2), Fujita (F-1), and Correa (C-2) have used these same codes and documented both the general features of the programs and their experience with their use for applications similar to those of present concern.

The methodology of LWR fuel management can be thought of as two coupled, yet distinct, phases: the neutron spectrum calculation and the neutron diffusion calculation as depicted in Figure 2.1. In the pressurized water reactor, the broad features of the ambient neutron spectrum (e.g. fast, epithermal, thermal regimes) within the confines of a given fuel assembly depend primarily on burnup status. Thus, for a given fuel design at a specific burnup, the few-group cross-sections and the concentrations of the isotopes, along with their attendant neutron spectrum, may be considered to be "state or state vector functions" of the burnup.

In non-fuel regions the cross-sections will not vary appreciably over the life of the fuel. In common practice, the cross-sections for both types of regions are generally "collapsed" into only two groups (fast and thermal) from the

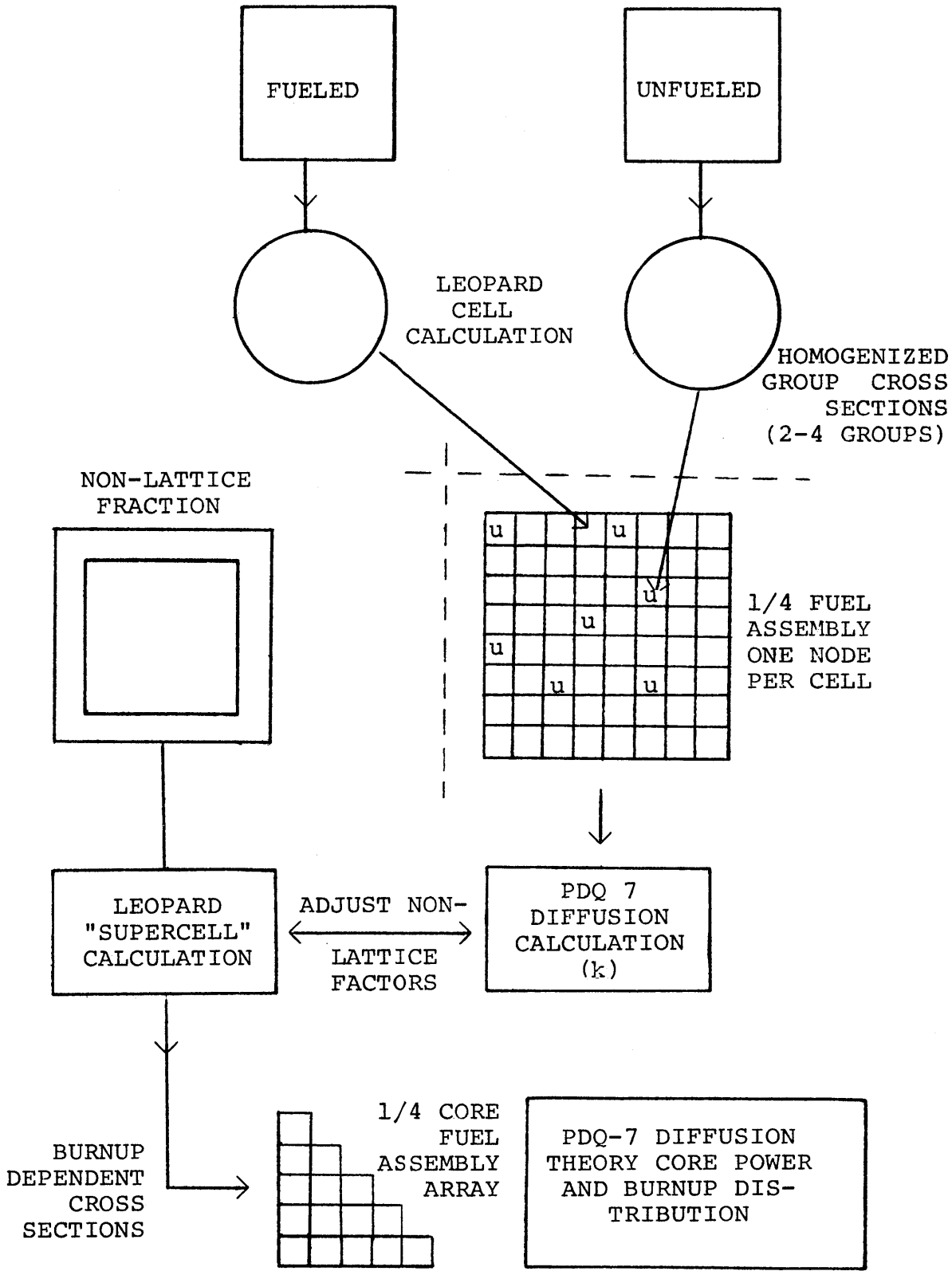

FIG. 2.1 FLOW CHART FOR LEOPARD AND PDQ CORE POWER CALCULATIONS

several hundred energy groups used in the unit cell spectrum calculation.

The burnup achieved at each point in the reactor depends on the local neutron flux level, and hence on local and near-neighborhood power levels. The flux level is determined by solving the spatial finite-difference equations (using the two-group spectrum) over a given time period. At each burnup time step the fine group spectrum calculation of the unit fuel cell is used to provide the collapsed two-group cross-sections used by the spatial calculation and the spatial flux shape is solved for again. The new flux levels are then applied once again to deplete the isotopes appropriately at each point. The process is continued in a successive fashion until the target energy production is achieved.

2.2 The LEOPARD Code (B-2)

The LEOPARD code calculates the spectrum for a "unit fuel cell" consisting of fuel, gap, cladding, moderator, and, in some cases, an "extra" region representing fuel assembly structure. In addition, neutron cross-sections can be calculated for unfueled regions. The cross-sections for the EPRI-LEOPARD version used in the present work are obtained from ENDF/B-IV data sets.

Material compositions, number densities, geometry, temperatures and pressures are input parameters to the code. A "zero-dimensional" (homogenized) calculation is performed to

determine the spectrum. An input buckling can be included to account for global leakage effects. In the thermal regime (E_n <0.625 eV) 172 energy groups are calculated over a Wigner-Wilkins spectrum using a SOFOCATE-type treatment (A-2), and disadvantage factors are calculated by a modification of the ABH method (A-3).

The fast spectrum calculation (in 54 groups) uses the self-consistent B-1 approximation in the MUFT treatment (B-3). The resonance parameters are calculated using the procedures described by Strawbridge and Barry (S-4).

The few group cross-sections (2-4 groups) generated by LEOPARD apply to a properly "homogenized" cell and hence can be input directly into coarse spatial mesh calculations.

The cross-section sets used in this research are either fast and thermal, or fast and thermal mixed number density (MND) (B-4). The MND model uses neutron activation continuity as a boundary condition rather than flux continuity. The thermal ($E_n < 0.625$ eV) values of Σ_a and Σ_f are averaged over a Wigner-Wilkins spectrum, whereas the thermal value of the diffusion coefficient, D, is averaged over Maxwellian spectrum.

The LEOPARD unit cell geometry is shown in Fig. 2.2. At the beginning of each time step, the neutron spectrum is recomputed and isotopic depletion during a time step is based on this spectrum. Boron concentration can be varied as a function of time, as can the D_2O/H_2O ratio to model spectral

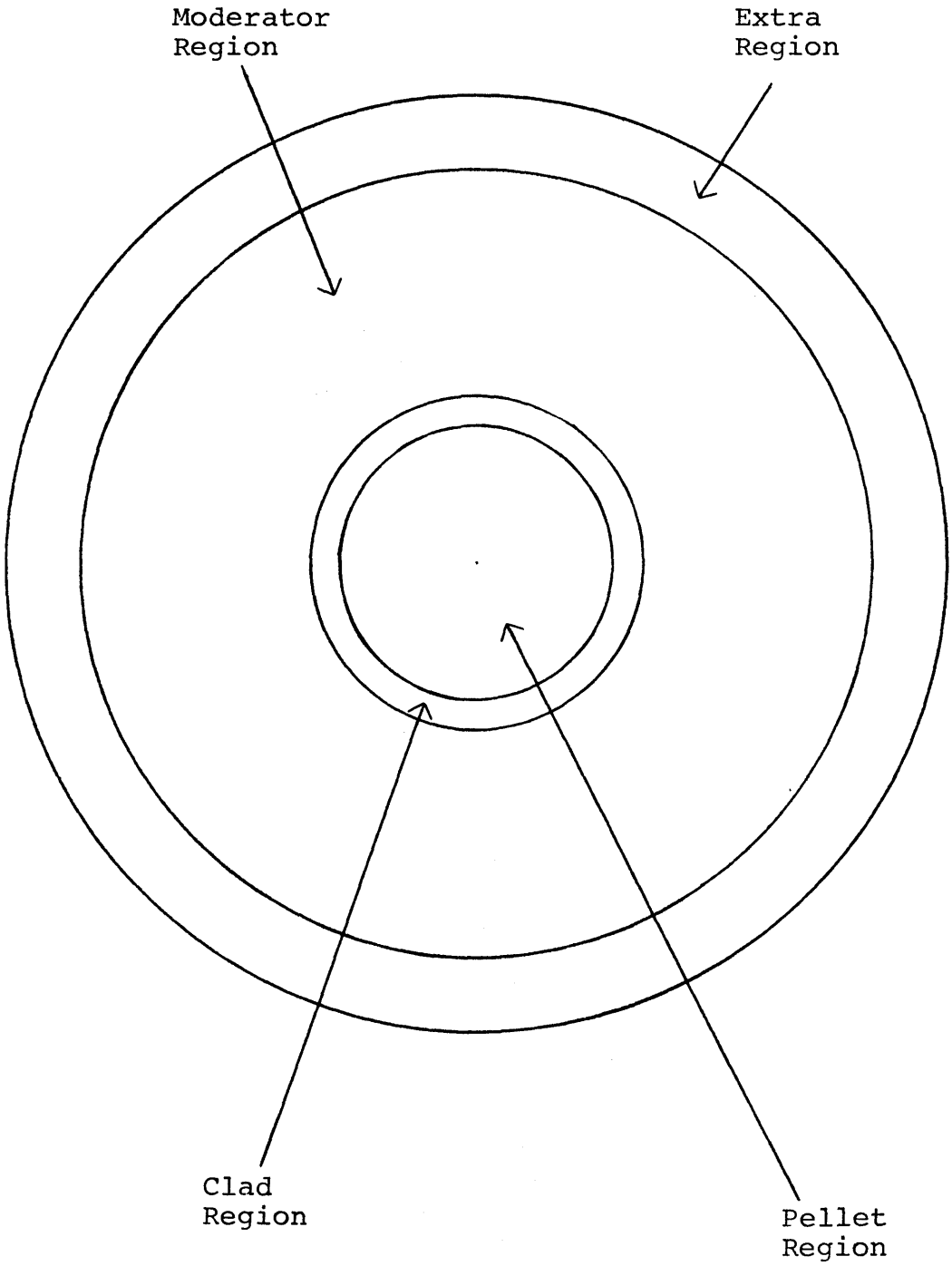

FIG. 2.2 LEOPARD UNIT CELL GEOMETRY

shift effects. A fission product scale factor can be adjusted to allow for the effects of variation in uranium or plutonium isotopic content. A discussion of some of the characteristics of the LEOPARD results (and some salient operational points) is included in Appendix B.

Correa (C-2) has benchmarked EPRI-LEOPARD (with its ENDF/B-IV based cross sections) at MIT. Whereas the primary emphasis of the calculations was tight pitch U-233/ThO_2 and Pu/ThO_2 cores, twenty-six U-235/UO_2 lattices were examined. The average k value for the critical experiments and the range of parameters investigated is shown in Table 2.1.

2.3 The CHIMP Code

The large number of flux-weighted microscopic cross-sections produced by LEOPARD at each time step are processed by the CHIMP code, which was developed by the Yankee Atomic Electric Company (C-2). The LEOPARD output at each time step can be routed directly to cards, tape, or disk and this data can be directly manipulated by the CHIMP code to prepare cross section sets usable by PDQ-7, the spatial depletion code used in this research and described later in this chapter.

2.4 The HAMMER System (S-5)

The HAMMER system is a set of linked reactor physics programs for the calculation of infinite lattice parameters using multigroup transport theory, and composite reactor

TABLE 2.1 SUMMARY OF BENCHMARK COMPARISONS

Fuel:	$U\text{-}233/ThO_2$	$U\text{-}235/ThO_2$	$U\text{-}235/UO_2$	U-235/U	$U\text{-}235/UO_2$	Pu/UO_2
ε (w/o)	3.00	3.78 - 6.33	3.00 - 4.02	0.7 - 1.5	1.3 - 4.1	1.5 - 6.6
F/M	0.01 - 1.00	0.11 - 0.78	0.23 - 2.32	0.15 - 1.69	0.1 - 1.3	0.1 - 0.9
(H+D)/U-238 (or/Th-232)	3.4 - 403.	4.7 - 36.	1.31 - 14.6	0.8 - 5.7	2.9 - 1.3	3.5 - 39.
$\Phi 1/\Phi 2$	0.3 - 21.	1.7 - 23.	2.4 - 50.	1.3 - 12.	1.6 - 12.	1.2 - 20.
D_2O (%)	0. - 99.34	0. - 81.96	0. - 89.14	--	--	--
Boron (PPM)	--	--	--	--	0. - 3400.	--
$\bar{k}$	1.003 $\pm$0.012	1.009 $\pm$0.016	0.998 $\pm$0.006	1.006 $\pm$0.011	1.003 $\pm$0.012	1.018 $\pm$0.014
# of cases	16	16	26	82	63	42

*Reference C-2

parameters by few group diffusion theory. In this research, only the infinite lattice calculations were utilized. The relevant unit cell geometry is shown in Figure 2.3. The difference between this method of calculation and the LEOPARD methodology is the inclusion of spatial transport calculations to treat the unit cell geometry. In addition, in the HAMMER system most heavy metal isotopes are self-shielded whereas LEOPARD only self-shields the most abundant heavy isotope. This is quite important, for example, in the analysis of mixed thorium-uranium unit cell configurations.

Two components of the HAMMER program library are of particular interest. The THERMOS program (H-2) performs a multigroup calculation of the thermal flux distribution ($E_n < .625$ eV) by using integral transport theory. Unlike LEOPARD, the assumption of space-energy separability is not made. THERMOS uses an integral form of the transport equation to calculate the spatially dependent thermal neutron spectrum in a cell characterized by one-dimensional symmetry (D-3).

The HAMLET program performs a multigroup spatial calculation of the flux in the energy range from 0.625 eV to 10 MeV. Collision probabilities are calculated under the assumption of cosine currents crossing region boundaries and the energy spectrum during moderation is calculated as in the MUFT code.

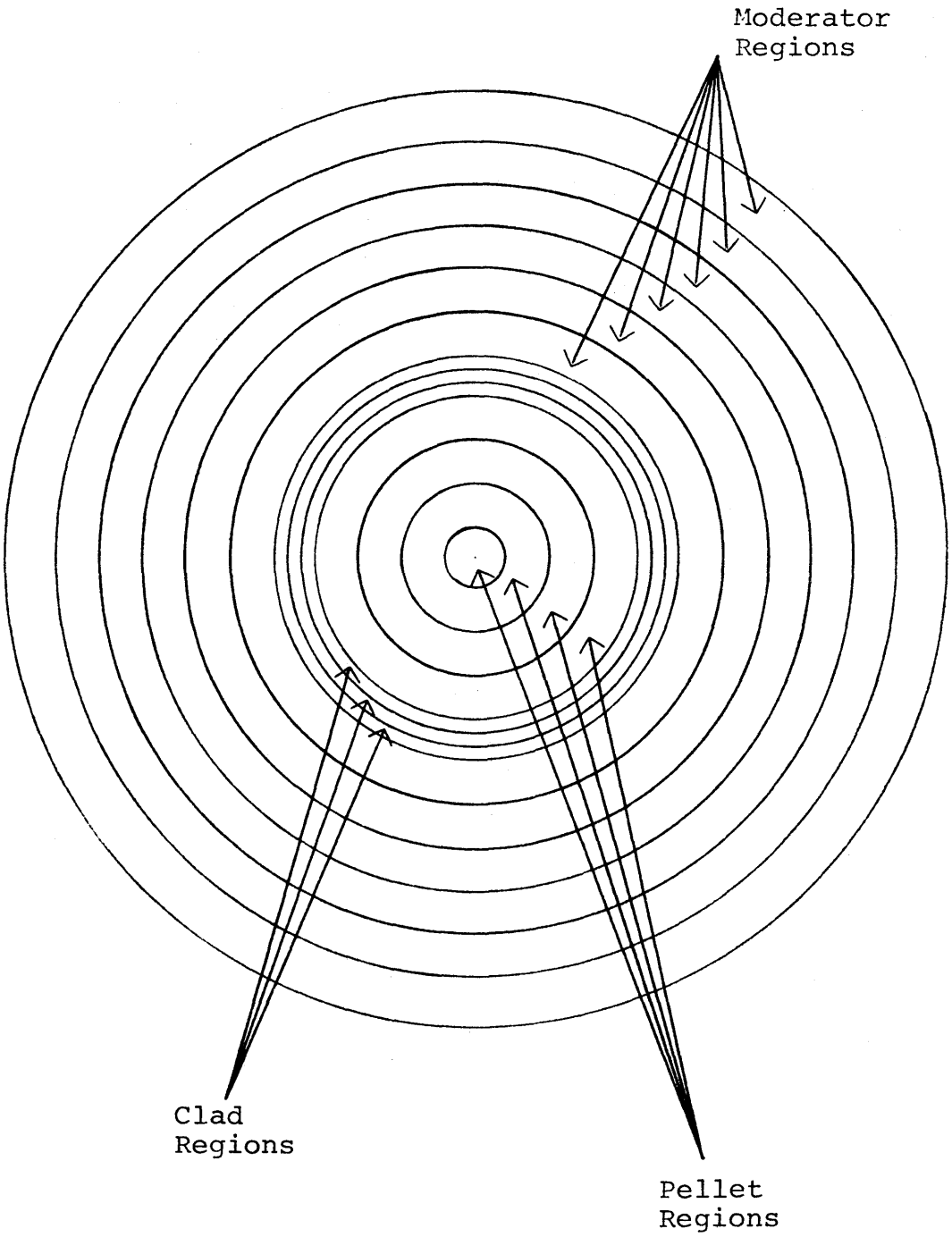

FIG. 2.3 HAMMER UNIT CELL GEOMETRY

2.5 PDQ-7, HARMONY

The PDQ-7 code (C-3, H-3) is designed to perform the spatial diffusion calculation in one, two, or three dimensions. It has been used widely by the nuclear industry for the licensing of reload cores (A-4, A-1). In this research, two energy groups are used, whereas, as many as five energy groups can be handled by the program. Solutions to the eigenvalue equation can be obtained in rectangular, cylindrical, spherical, or hexagonal geometry. Zero flux or zero current boundary conditions are admissible.

The multigroup diffusion equation is solved by discretizing the energy variable and finite-differencing the spatial variable over a variable or constant mesh size.

The one dimensional group equations are solved by Gauss elimination, and the two dimensional equations are solved by using a single-line cyclic Chebyshev semi-iterative technique. A block Gauss-Seidel procedure is used in three dimensions. In the present work, however, three dimensional PDQ-7 analyses were not performed.

The actual depletion chain manipulation and cross-section data management is performed by the HARMONY system (B-5). The depletion chains are user inputs and the cross-section tables are obtained from the LEOPARD code after appropriate massaging by the CHIMP code.

The fluxes are normalized based on the power level input by the user. The cross-sections are fitted to the

concentrations of the isotopes with time via a high order polynomial. At the end of each depletion time step, the PDQ-7 code solves for the spatial flux shape and these values of the flux levels are used in the following time step. The depletion can be done on a "point" or "block" basis. Various options available in the code and used in this research will be discussed as the need arises.

2.6 Chapter Summary

In this chapter the computer methods used in the present research have been outlined. An accurate determination of the neutron spectrum and the spatial flux shape is essential for the determination of uranium consumption. The suggested improvements in core design and fuel management which have to be evaluated involve perturbations of the neutron spectrum, and the arrangement of fuel in patterns which generate flux shapes quite different from those encountered in current designs. Hence we will routinely fall back upon state-of-the art, well-benchmarked methods to provide a solid base upon which to build further analyses.

CHAPTER 3

A POWER WEIGHTING ALGORITHM FOR ESTIMATION OF SYSTEM REACTIVITY

3.1 Introduction

First approximations to nuclear fuel management problems are often made using models in which either reactivity, ρ, (or multiplication factor, k) vary linearly (or quadratically) with burnup [G-3, N-3, S-6, S-7].

In this chapter a pragmatic case will be made for the use of ρ versus burnup as opposed to k_∞ versus burnup. An analysis will be carried out to demonstrate that the reactivity of fuel bundles in nuclear reactors should be weighted not merely by their mass or volume fractions, but rather by their power fractions. The linear reactivity model is extended to include these effects, and computer-generated results are analyzed to verify the analytical models.

Further extension of the linear reactivity model is made to account for core leakage. This extension is also checked and found to be consistent with more detailed computer studies. Finally, an illustrative example is presented, showing the application of the model to discern the differences between uranium utilization in the "out-in" and "low-leakage" fuel management schemes.

3.2 The Linear Reactivity Model

The time-dependent evolution of the reactor or region-wise eigenvalue is an extremely useful integral measure of the neutronic status of the reactor fuel. Many researchers in the field of PWR fuel management have made good use of the empirical observation that the plot of eigenvalue versus burnup is approximately linear [G-3, N-3].

It is not widely recognized, however, that reactivity is a considerably more linear function of burnup than the eigenvalue (or k), that is:

$$\rho_\infty = \frac{k_\infty - 1}{k_\infty} = \rho_o - AB \qquad (3.1)$$

The Maine Yankee supercell reference lattice (see Appendix A) was analyzed using LEOPARD, for enrichment variations ranging from 1.5 w/o U-235 to 4.34 w/o U-235. Linear least squares curve-fits of k_∞ versus burnup over the range 150-50,000 MWD/MT gave an average coefficient of determination (R^2) of 0.9898, whereas linear fits of ρ_∞ versus burnup gave an average R^2 value of 0.995 (i.e., in the latter case only 0.5% of the variance is not accounted for by the correlation!)

In a one-batch PWR core the excess reactivity at the beginning of the cycle is balanced by the presence

of the soluble boron control absorber in the moderator. As the excess reactivity of the core decreases due to fuel depletion and fission product buildup, the boron is slowly withdrawn, until at end-of-cycle the excess reactivity of the core medium is equal to the fraction of neutrons that are lost to leakage. Plots of k_∞ and ρ_∞ vs. burnup for a 3.0 w/o U-235 lattice (Maine Yankee supercell) are shown in Fig. 3.1.

In the simplest version of the linear reactivity model (leakage effects not included) the reactivity, ρ, decreases linearly with burnup, and for one-batch irradiation the EOC burnup is given by:

$$B_1 = \frac{\rho_o}{A} \qquad (3.2)$$

Typical values for a 3.0 w/o U-235 enriched PWR lattice are:

$\rho_o \simeq 0.20$

$A \simeq 0.91 \times 10^{-5}$ $(MWD/MT)^{-1}$

$B_1 \simeq 22{,}000$ MWD/MT

In an N-batch steady-state core, at the end of the reactor cycle the freshest batch is burned to $B_{discharge}/N$, the next oldest batch to $2\,B_{discharge}/N$, etc. The mean reactivity of the mixture is typically estimated by simple arithmetic averaging of the EOC reactivity of each batch:

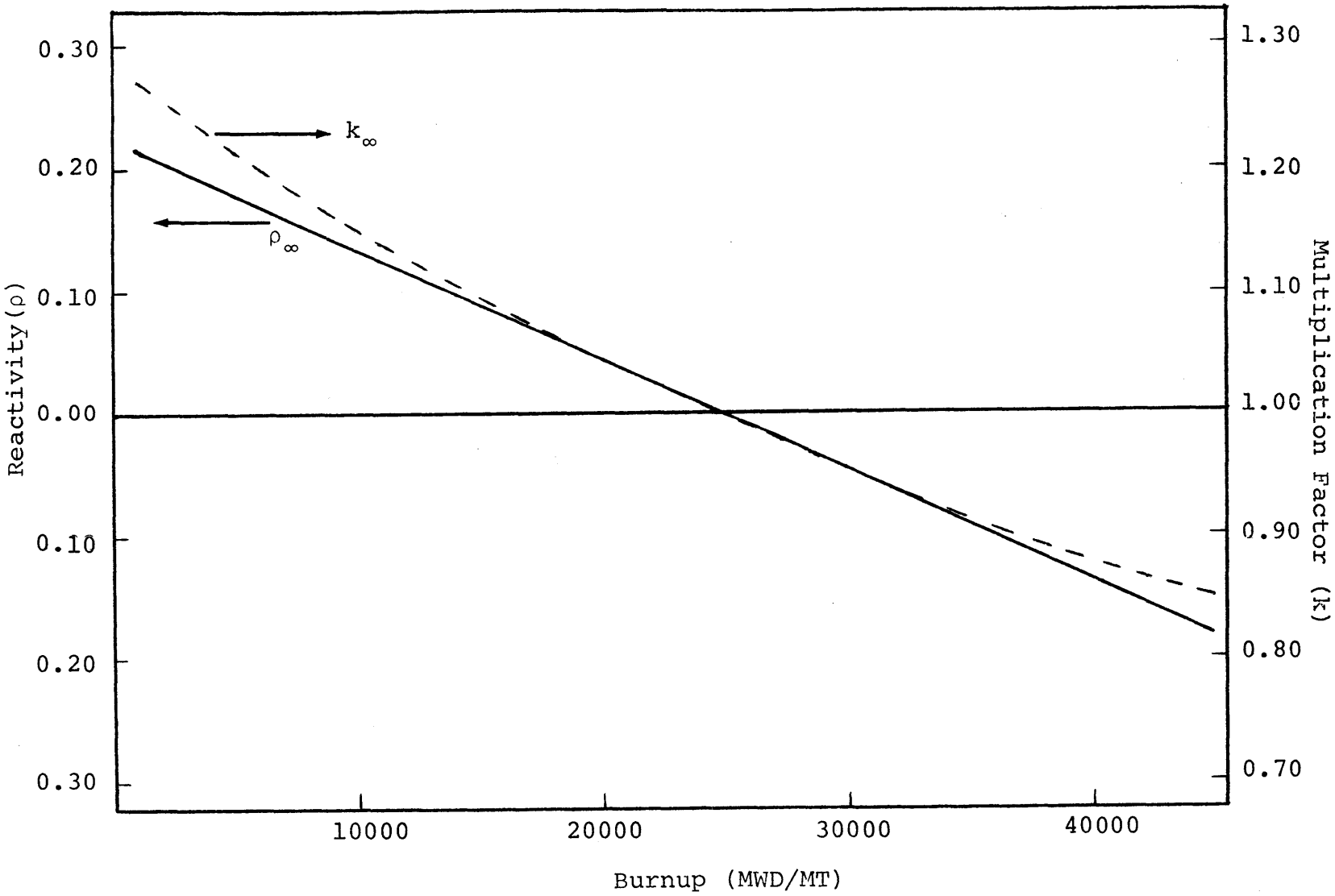

FIG. 3.1 k_∞ AND ρ_∞ AS A FUNCTION OF BURNUP FOR A 3.0 W/O U-235 MAINE YANKEE SUPERCELL

$$\rho_1 = \rho_{o,N} - \frac{1}{N} AB_{dis}$$

$$\rho_2 = \rho_{o,N} - \frac{2}{N} AB_{dis}$$

.

.

.

$$\rho_N = \rho_{o,N} - AB_{dis}$$

$$\rho = \frac{1}{N} \sum_{i=1}^{N} \rho_i = \frac{1}{N} \left\{ N \rho_{o,N} - \frac{N(N+1)}{2N} AB_{dis} \right\} = 0 \qquad (3.3)$$

Thus, the reload reactivity needed to achieve a discharge burnup of B_1 is:

$$\rho_{o,1} = \frac{N+1}{2N} AB_1 = \frac{N+1}{2N} \rho_{o,n} \qquad (3.4)$$

If, instead, the reload reactivity is kept the same, then a higher burnup can be achieved:

$$B_N = \left(\frac{2N}{N+1}\right) B_1 \qquad (3.5)$$

When the oldest batch is replaced by fresh fuel we can repeat the averaging process to find the BOC reactivity:

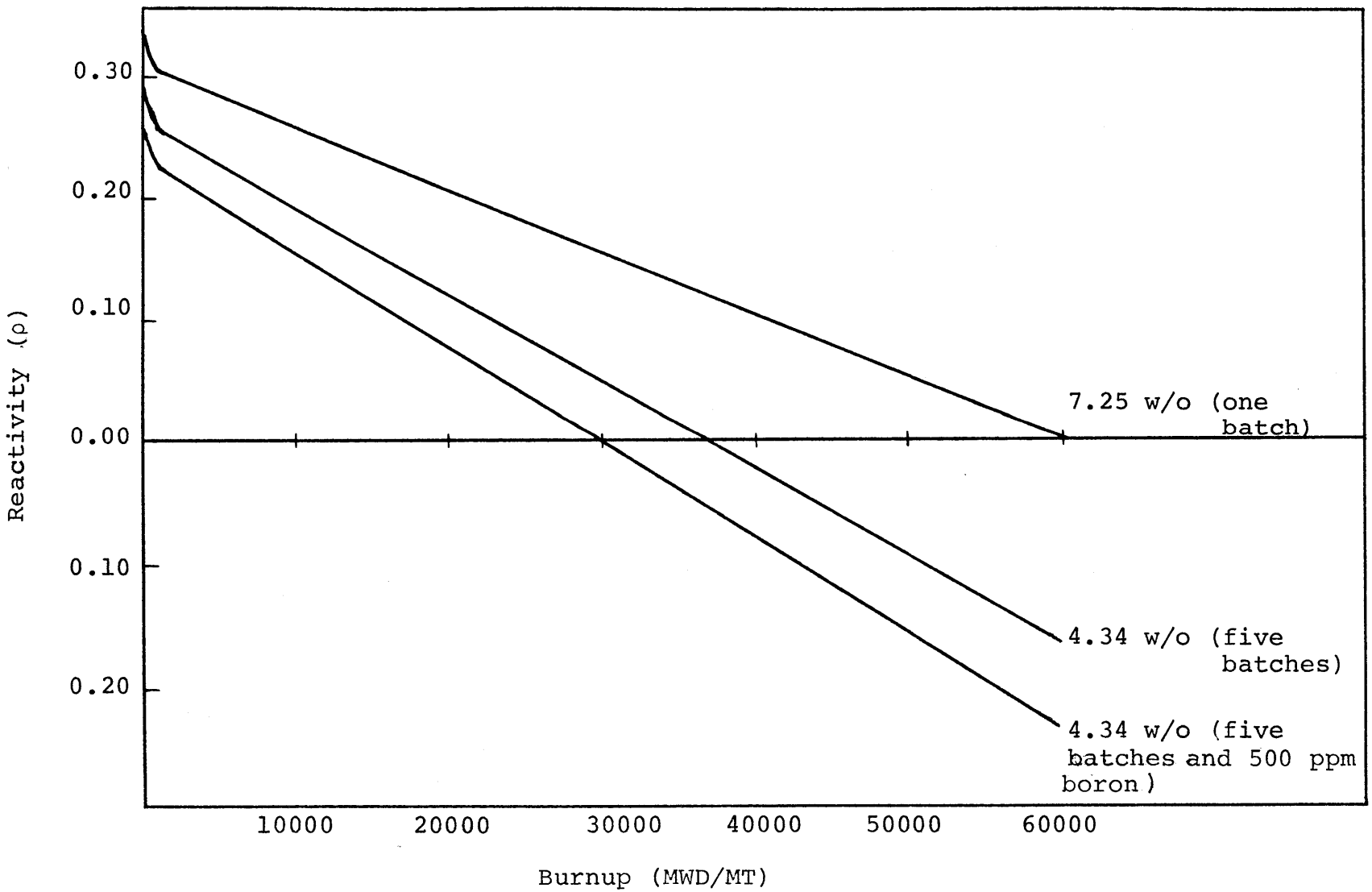

FIG. 3.2 REACTIVITY VS. BURNUP CURVES FOR FIVE BATCH FUEL MANAGEMENT SCHEME WITH 60000 MWD/MT TARGET BURNUP

$$\rho_1 = \rho_{o,N}$$

$$\rho_2 = \rho_{o,N} - \frac{AB_{dis}}{N}$$

.

.

.

$$\rho_N = \rho_{o,N} - AB_{dis}$$

$$\rho = \frac{1}{N} \sum_{i=1}^{N} \rho_i = \frac{1}{N}\left\{N\rho_{o,N} - AB_{dis}\ \left(\frac{N(N+1)}{2N} - 1\right)\right\} \qquad (3.6)$$

Hence the cycle reactivity swing ($\rho_{BOC} - \rho_{EOC}$) is given by:

$$\Delta\rho_{c,N} = \frac{1}{N}\ \rho_{o,1} = \frac{2}{N+1}\ \rho_{o,N} \qquad (3.7)$$

Figure 3.2 illustrates an application of the linear reactivity model (LRM) methodology. A 7.0 w/o U-235 enriched PWR lattice is depleted until $\rho = 0$ at 60000 MWD/MT, the target burnup for one-batch fuel management. The reload reactivity is then determined using Eq. 3.4 such that the new reload reactivity corresponds to the anticipated use of five fuel batches. If the slopes of both curves were the same, the required enrichment would be easily calculated; however, the lower enrichment cores have a steeper ρ versus B slope, so that a higher than might be anticipated enrichment (here 4.34 w/o U-235) is required to reach criticality at EOC with the fifth and final batch at a discharge burnup of 60000 MWD/MT.

In the third curve, a fixed amount of boron is added to the lattice such that $\int_{o}^{B_{dis}} \rho(B)\, dB = 0$, i.e, the net excess of neutrons above the $\rho = 0$ line is balanced by the net deficit of neutrons below the $\rho = 0$ line. The fixed amount of boron is the reactor cycle-average boron concentration. Note in the figure that except for the sudden drop of reactivity during the first 150 MWD/MT (on account of the buildup of xenon and samarium fission product poisons to their equilibrium levels) the curves are very linear over the full range of burnup.

Several implicit assumptions are present in the linear reactivity model, as usually applied, which restricts its usefulness for the purpose of this research; namely, fixed batch size, equal power sharing among batches, failure to account for leakage from the core, and treating the burnup slope as a constant over the entire range of burnup. A relaxation of these conditions is clearly desirable.

3.3 Power Weighting

In a large reactor with negligible leakage and N fuel regions, the eigenvalue equation can be written as:

$$k_{sys} = \frac{\nu\Sigma_f^{(1)}\phi^{(1)} + \nu\Sigma_f^{(2)}\phi^{(2)} + \ldots + \nu\Sigma_f^{(N)}\phi^{(N)}}{\Sigma_a^{(1)}\phi^{(1)} + \Sigma_a^{(2)}\phi^{(2)} + \ldots + \Sigma_a^{(N)}\phi^{(N)}} \qquad (3.8)$$

where $\nu\Sigma_f^{(i)}$ and $\Sigma_a^{(i)}$ are the neutron production and neutron destruction cross-sections in the i^{th} region, respectively. This equation can be rewritten:

$$k_{sys} = \frac{\nu\Sigma_f^{(1)}\phi^{(1)} + \nu\Sigma_f^{(2)}\phi^{(2)} + \ldots + \nu\Sigma_f^{(N)}\phi^{(N)}}{\frac{\nu\Sigma_f^{(1)}\phi^{(1)}}{k_\infty^{(1)}} + \frac{\nu\Sigma_f^{(2)}\phi^{(2)}}{k_\infty^{(2)}} + \ldots + \frac{\nu\Sigma_f^{(N)}\phi^{(N)}}{k_\infty^{(N)}}} \qquad (3.9)$$

Rearranging the terms gives:

$$\frac{1}{k_{sys}} = \frac{q^{(1)}}{k_\infty^{(1)}} + \frac{q^{(2)}}{k_\infty^{(2)}} + \ldots + \frac{q^{(N)}}{k_\infty^{(N)}} \qquad (3.10)$$

where $k_\infty^{(i)}$ is the infinite medium multiplication factor of the i^{th} region and $q^{(i)}$ is the fission neutron production fraction in region i:

$$q^{(i)} = \frac{\nu\Sigma_f^{(i)}\phi^{(i)}}{\sum_{i=1}^{N} \nu\Sigma_f^{(i)}\phi^{(i)}} \qquad (3.11)$$

In a pressurized water reactor, the value of κ/ν (the ratio of the average energy released per fission to the average number of neutrons released per fission) varies slightly with burnup, as shown in Fig. 3.3. Nevertheless

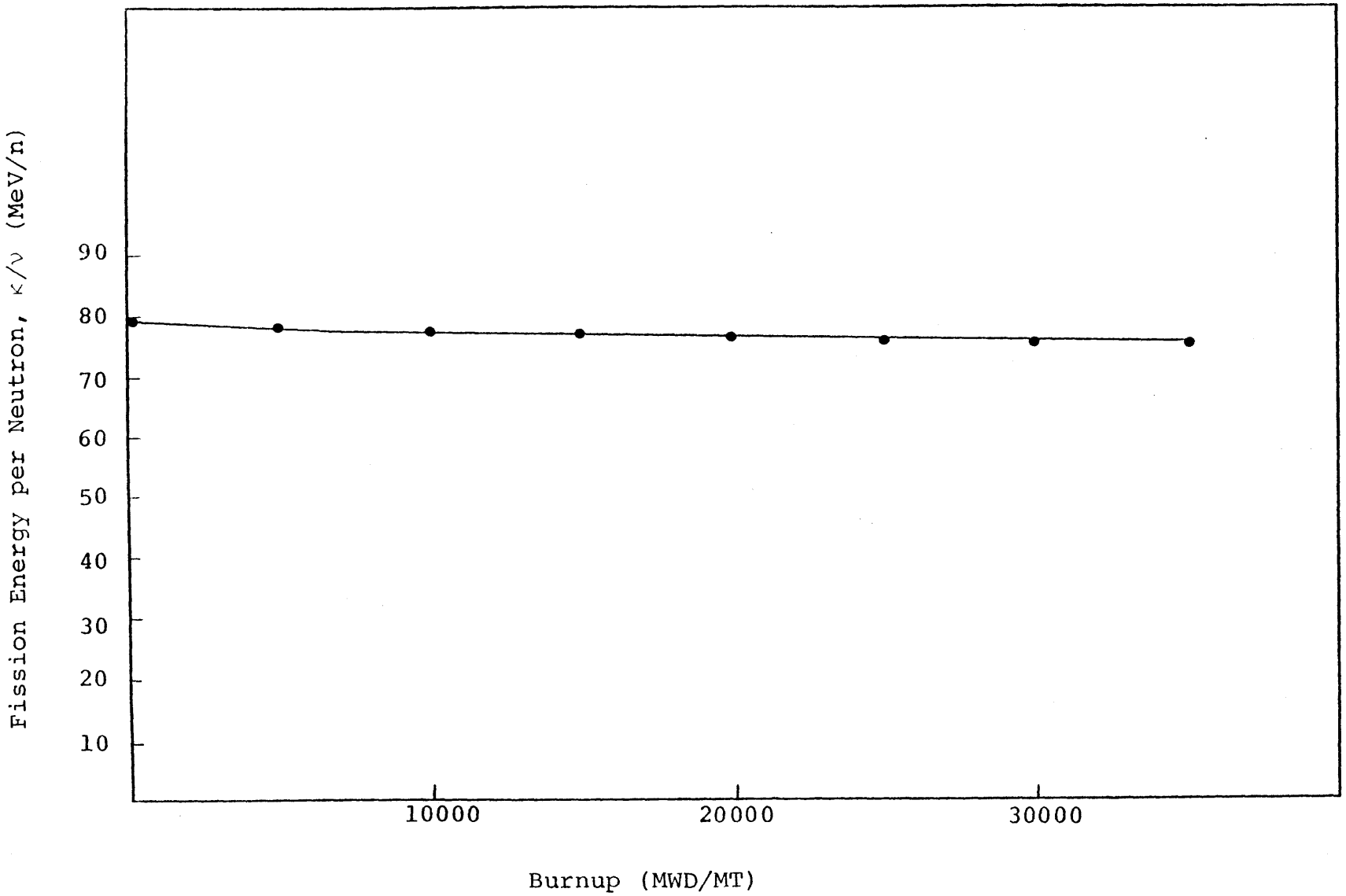

FIG. 3.3 AVERAGE ENERGY RELEASE PER FISSION NEUTRON (κ/ν) AS A FUNCTION OF FUEL BURNUP

TABLE 3.1 COMPARISON OF COMPUTED (PDQ-7) AND POWER-WEIGHTED VALUES OF k_∞ FOR A TWO-BUNDLE PROBLEM (FIG. 3.4)

k_1	k_2	$\sum_{i=1}^{2} f_i \rho_i$	k_∞(PDQ-7)	Δk
1.128962	1.073943	1.103352	1.103167	0.000185
1.128962	1.000420	1.075070	1.074255	0.000815
1.128962	0.900117	1.046842	1.044636	0.002206
1.128962	0.805563	1.028687	1.024873	0.003814
1.073943	0.805563	0.985596	0.983145	0.002451
1.073943	1.000420	1.040755	1.040527	0.000228
0.900117	1.000420	0.957598	0.957212	0.000386
0.900117	0.805563	0.860263	0.859973	0.000290

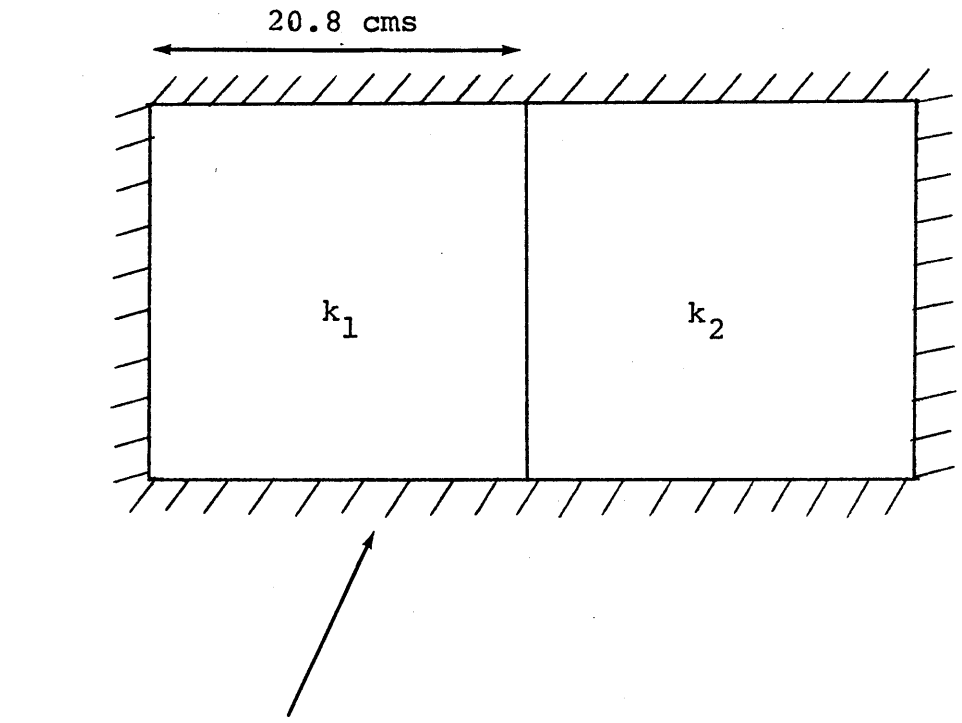

FIG. 3.4 GEOMETRY FOR TWO-BUNDLE PDQ-7 POWER SPLIT PROBLEM

if we approximate $q^{(i)}$ by the thermal power fraction, f_i, reasonable accuracy results. Equation 3.11 then becomes:

$$\frac{1}{k_{sys}} = \sum_{i=1}^{N} \frac{f_i}{k_i} \qquad (3.12)$$

Table 3.1 shows the results of a two-bundle, zero-current boundary condition, PDQ-7 problem where the k_∞ values of the bundles have been varied over a wide range. The differences between the eigenvalues calculated using Eq 3.12 and the eigenvalues computed by PDQ-7 are very small. The worst case occurs when the difference between k_1 and k_2 is the largest, and even in this case, the error is less than 0.4%. Thus, the errors associated with using an average value of κ/ν do not appear prohibitive.

Since $\rho = 1 - 1/k$, Eq 3.12 can be rewritten as:

$$\rho_{sys} = \sum_{i=1}^{N} f_i \rho_i \qquad (3.13)$$

This formula indicates that the correct algorithm for reactivity combination in a PWR core is a power-weighting scheme.

The implications of power weighting become more apparent when the reactivity balance is calculated. For an N-batch steady-state core, assuming that the power fractions remain constant over a given cycle:

$$\rho_1 = \rho_o - AB_{dis}\, f_1$$

$$\rho_2 = \rho_o - AB_{dis}\, (f_1 + f_2)$$

$$\downarrow$$

$$\rho_N = \rho_o - AB_{dis}\, (f_1 + f_2 + \ldots + f_N) \qquad (3.14)$$

At end of cycle

$$\rho = 0 = \sum_{i=1}^{N} f_i\, \rho_i \qquad (3.15)$$

from which

$$\rho = 0 = \rho_o - AB_{dis} \left\{ \sum_{i=1}^{N} \sum_{j=i}^{N} f_i\, f_j \right\} \qquad (3.16)$$

or

$$B_{dis} = \frac{\rho_o}{A\left\{ \sum_{i=1}^{N} \sum_{j=i}^{N} f_i\, f_j \right\}} \qquad (3.17)$$

The double summation in the denominator, which we will designate as the "cycle schedule index", accounts for the effect of burnup schedule (the sequence of f_i), or alternatively, the effect of a non-uniform core power distribution (since the f_i apply to one batch over its N in-core cycles, or all batches in-core during a representative cycle). Note that this effect is not included in the simplest version of the linear reactivity model. As will be shown, the lower burnup associated with non-uniform f_i degrades uranium utilization by a non-negligible amount.

3.4 Accounting for Leakage

In any finite reactor the neutron leakage is an important factor in the determination of system reactivity, hence sustainable burnup and uranium utilization. In a normal PWR operated with an out-in fuel shuffling strategy, roughly 3% to 4% of the neutrons are lost via leakage to, and absorption in, the regions surrounding the core (grids, core barrel, thermal shields, etc.).

An approximate treatment of leakage effects can be developed by considering the fast group leakage as a function of source shape. The plane geometry (or large radius cylinder) flux kernel (flux at x due to a source at x') is given by:

$$\phi(x,x') = \frac{M}{2D} \exp\left\{-\frac{(x'-x)}{M}\right\} \tag{3.18}$$

and the neutron current can be written as:

$$J = -D\frac{d\phi}{dx} = \frac{1}{2} \exp\left\{-\frac{(x'-x)}{M}\right\} \tag{3.19}$$

Consider a fuel region of total length 2H with a symmetric source shape about the origin. The fraction of neutrons which leak out the end of the region (the leakage reactivity loss) is:

$$\rho_L = \frac{\int_0^H J(x,x')\ S(x)\ dx}{\int_0^H S(x)\ dx} = \frac{\int_0^H \frac{1}{2} \exp\left[-\frac{(H-x)}{M}\right] S(x)\ dx}{\int_0^H S(x)\ dx} \tag{3.20}$$

There are three source shapes which are of immediate interest with respect to the behavior of ρ_L as a function of source shape; namely, flat ($S(x) = S_o$), cosine ($S(x) = S_o \cos \frac{\pi x}{2H}$), and flat interior with drooping ends ($S(x) = S_o(1-\exp - \frac{(H-x)}{M}$). The corresponding solutions of the leakage reactivity equations are shown in Table 3.2.

In a PWR the source shape is cosine in the axial direction at beginning of life and flat with drooping ends at end of life. Examination of the kernel equations indicates that the leakage effect is most prominent in the last few diffusion lengths of the fuel material, that is, most of the neutron loss originates in fuel regions within two or three migration lengths of the core periphery. Since this is the case, axial and radial leakage should be correlated with the power (source) in the peripheral core regions. Figure 3.5 shows the <u>axial</u> leakage reactivity loss plotted as a function of the power in the outermost 6 inches of a Maine Yankee fuel assembly in which the last six inches of the fuel have been replaced with various enrichments from 0.2 w/o U-235 to 1.0 w/o U-235, and with depleted and natural uranium fuel blankets, at various stages of assembly burnup. The calculations were made in two groups using PDQ-7 and PDQ-7-HARMONY. The correlation is linear, with an R^2 value of 0.98445. The non-zero intercept can be interpreted as a relative indication of leakage due to neutrons born in the interior.

TABLE 3.2 EFFECTS OF SOURCE SHAPE ON LEAKAGE REACTIVITY

ICE ER) PE	EQUATION FOR SOURCE	EQUATION FOR ρ_L	LEAK REACT
T	$S(x) = 1.0$	$\dfrac{\int_0^H 1/2\left[\exp-(\frac{H-x}{M})\right]dx}{\int_0^H dx}$	0.(
E	$S(x) = S_o \cos(\frac{\pi x}{2H})$	$\dfrac{\int_0^H 1/2\left[\exp-(\frac{H-x}{M})\right]\cos\frac{\pi x}{2H}\,dx}{\int_0^H \cos\frac{\pi x}{2H}\,dx}$	0.(
ITH ING	$S(x) = S_o(1-\exp-(\frac{H-x}{M}))$	$\dfrac{\int_0^H 1/2\left[\exp-(\frac{H-x}{M})\right]-1/2\left[\exp-2(\frac{H-x}{M})\right]dx}{\int_0^H 1-\exp-(\frac{H-x}{M})\,dx}$	0.(

presentative parameter values, M=7.5 cms, H=175.2 cms.

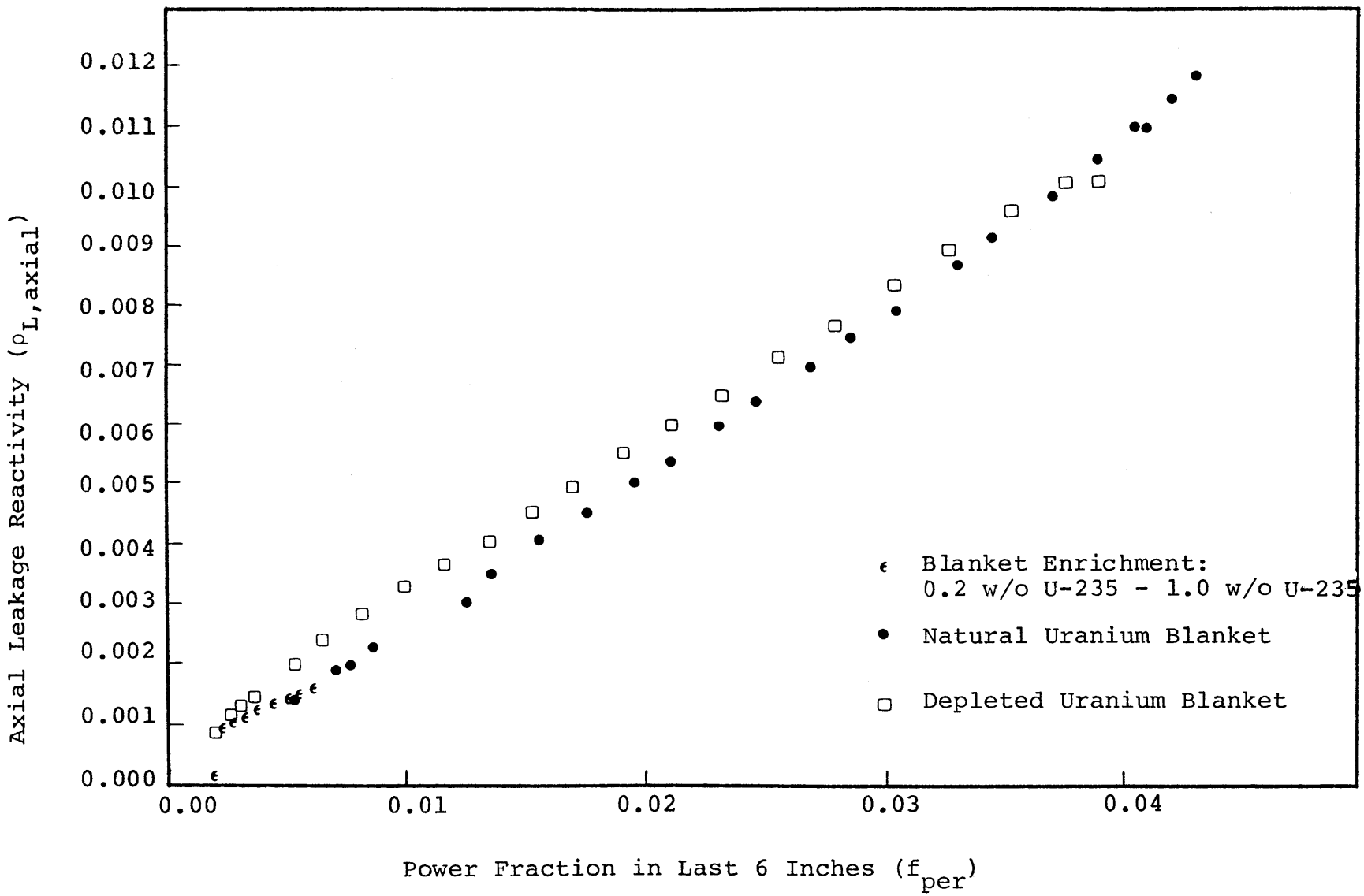

FIG. 3.5 AXIAL LEAKAGE REACTIVITY VS. POWER FRACTION IN OUTERMOST 6 INCHES OF THE FUELED REGION IN A MAINE YANKEE REACTOR ASSEMBLY

Figure 3.6 shows the radial leakage reactivity loss as a function of the power in the peripheral fuel assemblies of the Maine Yankee reactor, again using PDQ-7 static calculations. The peripheral power was varied by successively shuffling the four fuel batches in the core between the periphery and the interior. The lowest power case represents 4th cycle fuel on the core periphery, whereas the highest power case represents fresh fuel loaded on the core periphery. The absorption fraction in non-fuel, ex-core materials was used to measure the leakage reactivity.

For the comparison of various fuel management schemes, the axial and radial leakage will be assumed to be "decoupled", i.e., changes in radial leakage will not affect the axial losses and vice versa. As shown, both leakage components can be correlated as linear functions, where:

$$\rho_L = \alpha + \beta\, f_{per} \tag{3.21}$$

The values of α and β depend on the specific reactor design; f_{per} is the fraction of the core power generated in the peripheral fuel region.

System reactivity can be defined as:

$$\rho_{sys} = \frac{\left\{\sum_{i=1}^{N} (F_i - A_i)\right\} - A_R}{\sum_{i=1}^{N} F_i} = \left\{\sum_{i=1}^{N} f_i\, \rho_i\right\} - \frac{A_R}{\sum_{i=1}^{N} F_i} \tag{3.22}$$

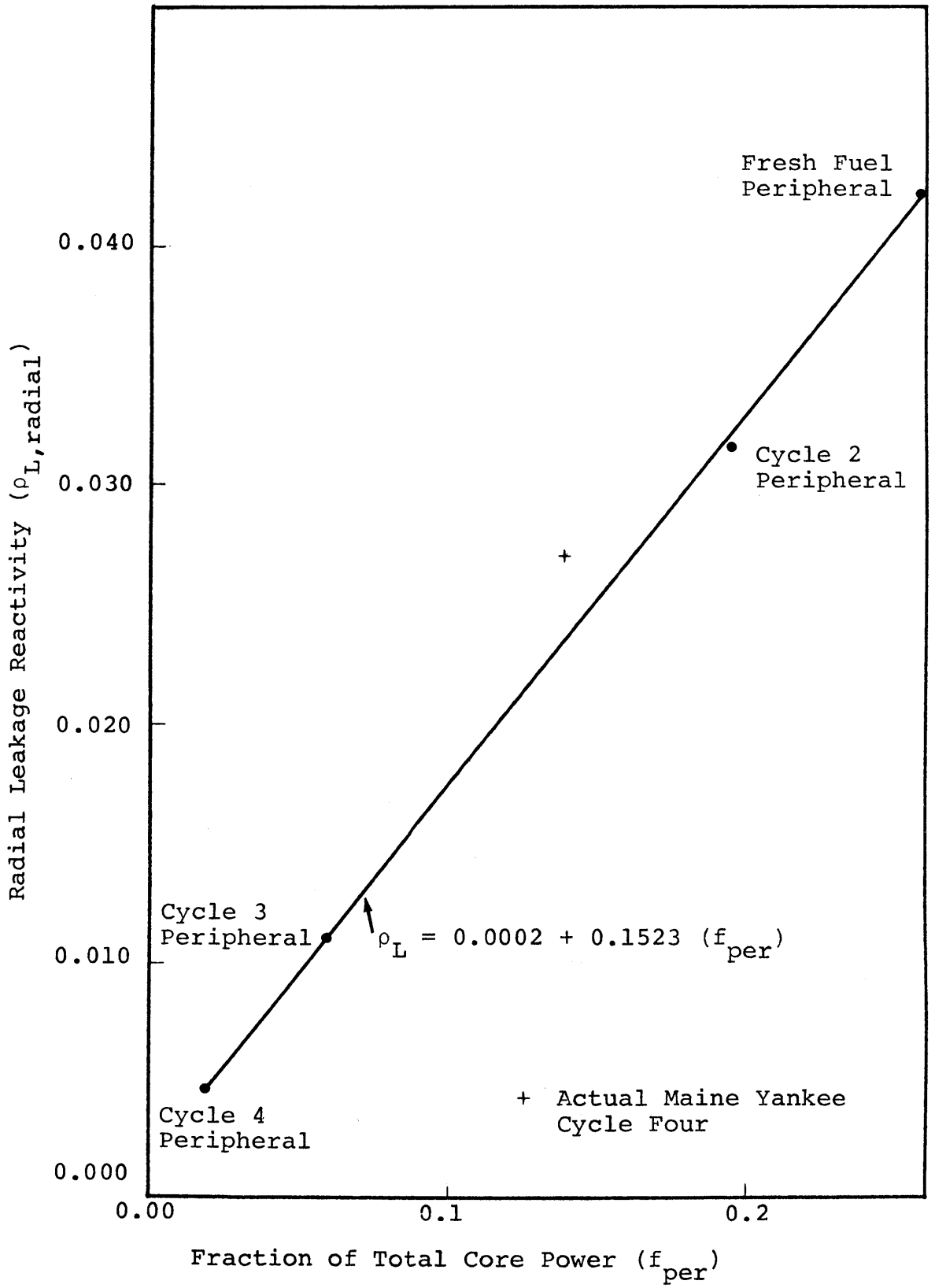

FIG. 3.6 RADIAL LEAKAGE REACTIVITY FOR M.Y. REACTOR VS. FRACTION OF CORE POWER GENERATED IN PERIPHERAL ASSEMBLIES

where ρ_i is the assembly reactivity, $\frac{(F_i - A_i)}{(F_i)}$, F_i is the neutron production by fission in fuel region i, A_i is the neutron loss by absorption in fuel region i and A_R is the absorption in the non-fuel, ex-core regions. The term $\frac{A_R}{\sum_{i=1}^{N} F_i}$ can be identified as the leakage reactivity.

Thus,

$$\rho_{sys} = \left\{ \sum_{i=1}^{N} f_i \rho_i \right\} - \rho_L \tag{3.23}$$

and the discharge burnup can be calculated as:

$$B_{dis} = \frac{\rho_o - \rho_L}{A\left\{ \sum_{i=1}^{N} \sum_{j=i}^{N} f_i f_j \right\}} \tag{3.24}$$

If the reactivity decrement associated with axial leakage is combined with the fuel reactivity:

$$\rho'_o = \rho_o - \rho_{L,axial} \tag{3.25}$$

then the radial leakage correlation can be included in Eq. 3.24 to give:

$$B_{discharge} = \frac{\rho'_o - \alpha - \beta f_{per}}{A\left\{ \sum_{i=1}^{N} \sum_{j=i}^{N} f_i f_j \right\}} \tag{3.26}$$

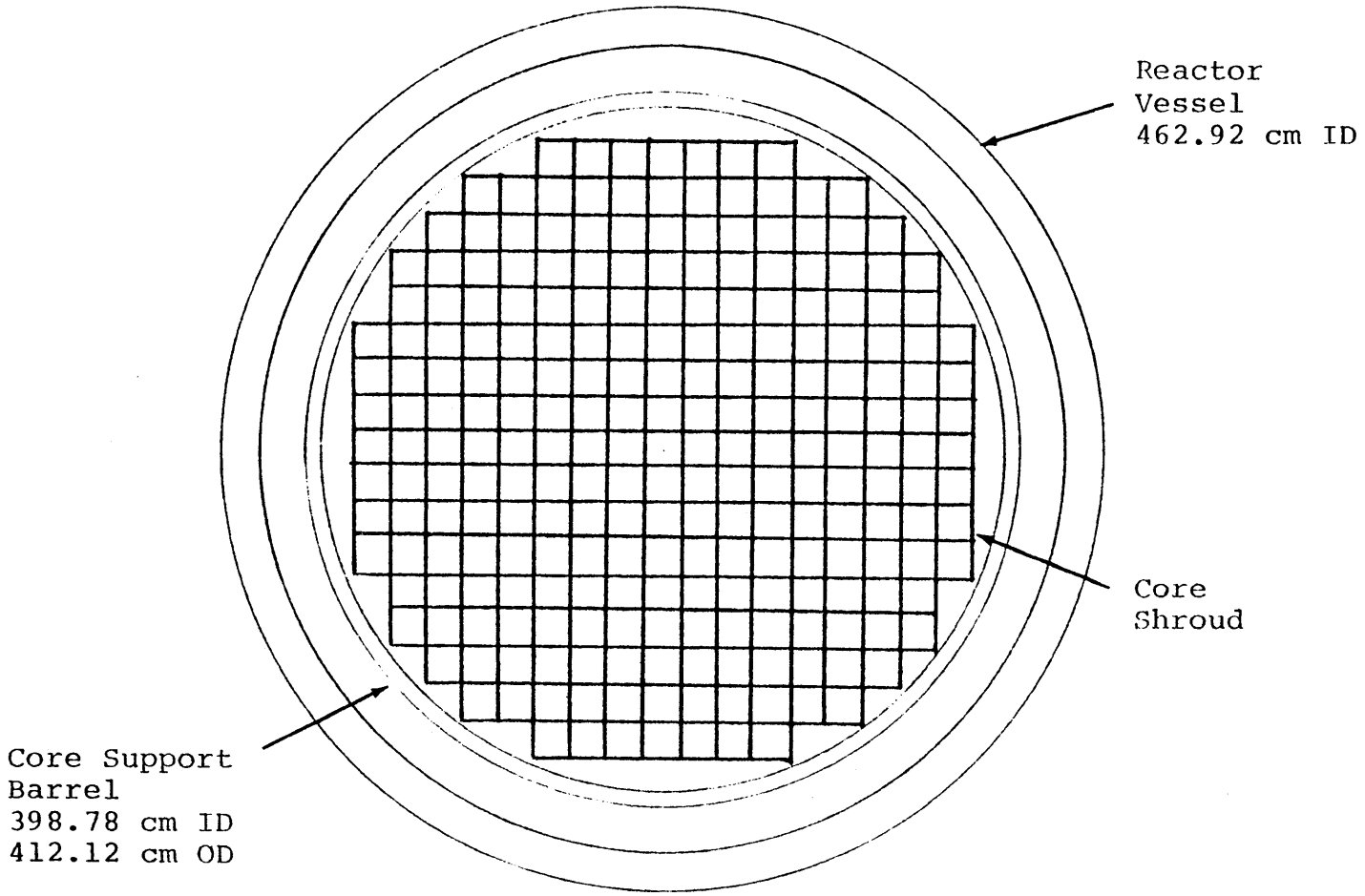

FIG. 3.7 C-E SYSTEM 80™ CORE DESIGN
(241 FUEL ASSEMBLIES)

3.5 An Application of The Advanced Linear Reactivity Model: Low Leakage Fuel Mangement

One of the benefits of the Advanced Linear Reactivity Model (ALRM) is its ability to calculate the differences in uranium utilization between fuel management schemes where the application of simpler linear reactivity models fails to discern any difference. In addition, the competing effects of leakage and fuel power history factors can be separated and quantified.

Consider five-batch, extended burnup, "out-in" fuel management versus a comparable "low-leakage" burnup schedule. The Combustion Engineering System-80 reference design shown in Fig. 3.7 will be used as the core model. The reactor has 241 assemblies with 48 peripheral assembly locations. Published data (M-3) for low-leakage and out-in fuel management allows us to correlate leakage reactivity with peripheral power fraction, as the core approaches its equilibrium cycle, as shown in Fig. 3.8.

$$\rho_L = 0.01126 + 0.2214\ f_{per} \tag{3.27}$$

The power fractions for each of the five batches under "equilibrium" cycle conditions are shown in Table 3.2.

Typical lattice parameters for 5-batch, extended burnup fuel management are:

$$\rho_o \simeq 0.2661$$

$$A \simeq 0.7154 \times 10^{-5}\ (\text{MWD/MT})^{-1}$$

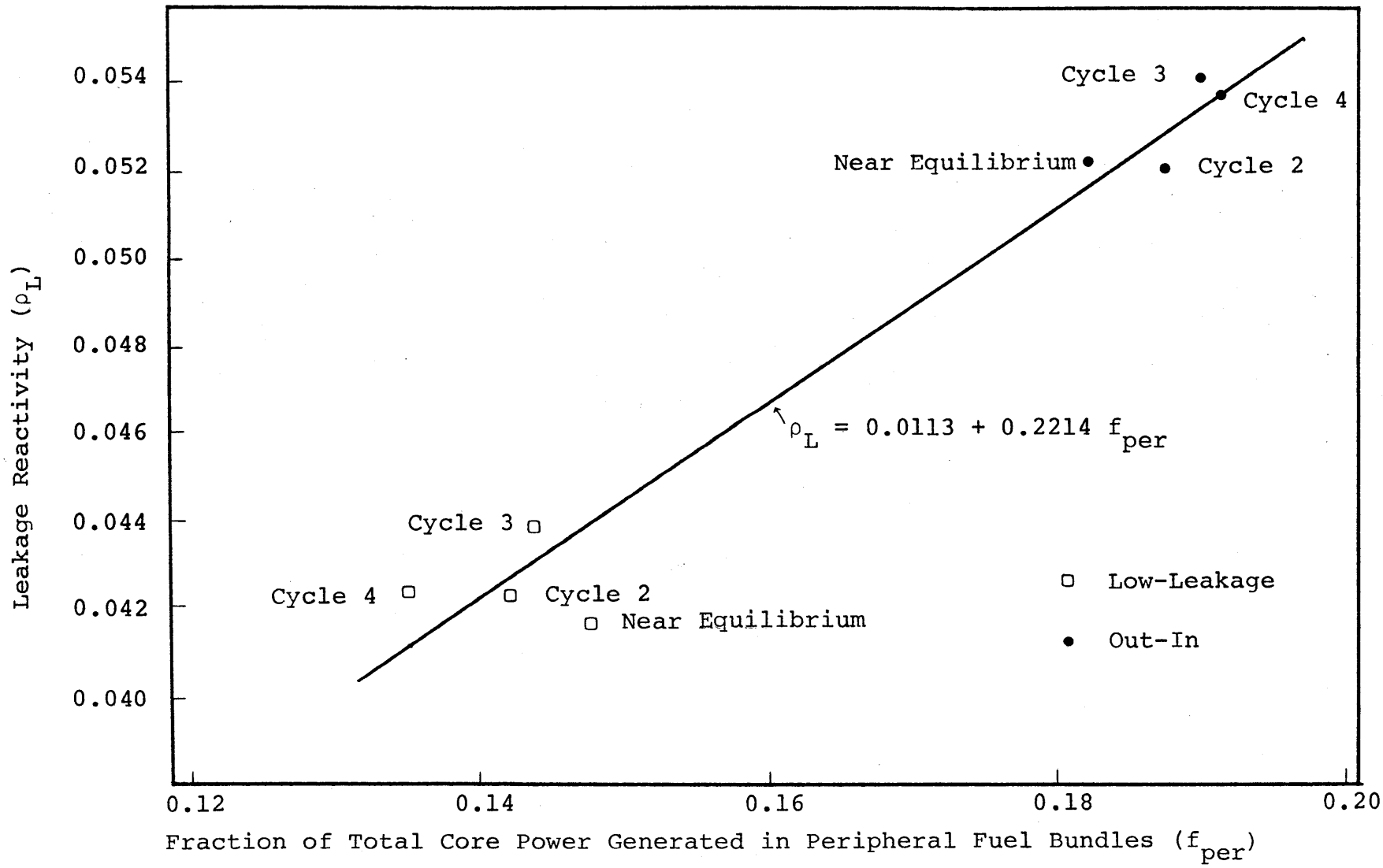

FIG. 3.8 LEAKAGE REACTIVITY FOR C-E SYSTEM-80^{TM} REACTOR VS. FRACTION OF POWER GENERATED IN PERIPHERAL ASSEMBLIES (FIVE BATCH FUEL MANAGEMENT, HIGH BURNUP)

The equation for the discharge burnup becomes:

$$B_{dis} = \frac{0.2661 - 0.01126 - 0.2214\ f_{per}}{(0.7154 \times 10^{-5}) \left\{ \sum_{i=1}^{5} \sum_{j=i}^{5} f_i\ f_j \right\}} \qquad (3.28)$$

For the power fractions listed in Table 3.3, the low-leakage fuel arrangement achieves an average discharge burnup of 51542 MWD/MT, whereas the out-in fuel management scheme achieves a burnup of 49790 MWD/MT; a net advantage to low leakage management under equilibrium cycle conditions of 3.52%. This value neglects the presence of residual shim worth associated with the use of burnable poison to suppress the high assembly power peaking factors encountered in the low-leakage fuel arrangements. Under equilibrium conditions it is predicted (M-3) that the shim residual worth would drop to 0.5% $\Delta\rho$. Equation 3.28 then becomes:

$$B_{dis} = \frac{0.2661 - 0.01126 - 0.2214\ f_{per} - \Delta\rho_{res}}{(0.7154 \times 10^{-3}) \left\{ \sum_{i=1}^{N} \sum_{j=i}^{N} f_i\ f_j \right\}} \qquad (3.29)$$

where $\Delta\rho_{res}$ = +0.005. Under these conditions the discharge burnup becomes 50381 MWD/MT for the low-leakage scheme and the relative advantage in discharge burnup, hence uranium utilization is 1.2%. The equilibrium cycle uranium savings predicted by CE using detailed computer calculations is 2.34%. The difference is caused by the use of a leakage

TABLE 3.3 EQUILIBRIUM CYCLE POWER FRACTIONS FOR 5 BATCH OUT-IN AND LOW-LEAKAGE FUEL MANAGEMENT SCHEMES*

	POWER FRACTION	
BATCH NUMBER	OUT-IN	LOW-LEAKAGE
1	0.1860**	0.2514
2	0.2400	0.1612**
3	0.2140	0.2063
4	0.1960	0.1971
5	0.1640	0.1840
PERIPHERAL POWER FRACTION	0.1831	0.1480

* Ref. (M-3).

** Principal Peripheral Batch.

correlation based on an approach to equilibrium cycle whereas the CE results are based on achieving the equilibrium cycle leakage profiles. In view of the simplicity of the ALRM, the agreement must be considered good; and it could probably be improved upon with experience in interfacing the ALRM and the results of computer modeling.

For both fuel management schemes, the burnup schedule index $\sum_{i=1}^{N} \sum_{j=i}^{N} f_i f_j$ is approximately 0.602. (The minimum burnup schedule index occurs when all f_i are equal (see Appendix C). Under these conditions, the schedule index becomes 0.600, and the discharge burnup for a perfectly power flattened core becomes 49054 MWD/MT. This represents a 1.5% disadvantage vs. the conventional out-in fuel management strategy and a 3.8% disadvantage vs. the low-leakage scheme, because of the much higher radial leakage.) This clearly demonstrates the importance of the leakage and cycle schedule index in uranium utilization calculations, even though such perfectly flat distributions probably cannot be attained in a real reactor, at least not without encountering compensatory losses from residual burnable poison.

3.6 Chapter Summary

In this chapter, the linear reactivity model has been extended to include the effects of inter-batch power sharing and neutron leakage losses from the core. Its

application to a detailed design study indicates reasonably good agreement for such a simple model, and serves to highlight the importance of the cycle schedule index and leakage in burnup calculations. While useful in principle, the ALRM, as presented so far, is restricted in practice by the need for sufficiently accurate specification of the batch power sharing fractions, f_i. If detailed PDQ computations were needed to supply this information one might question whether much was accomplished in then applying a simple model. Thus we must also stress the need for developing a sufficiently accurate but simply implemented power sharing algorithm. This task will be addressed in the next chapter, where other restrictions on the model will also be relaxed.

CHAPTER 4

A POWER SHARING ALGORITHM FOR PWR FUEL BUNDLES

4.1 Introduction

In the previous chapter, the influence of the cycle schedule index on uranium utilization was demonstrated. The power fractions used in the calculations were extracted from detailed computer results. In this chapter, an empirical relation will be proposed to describe the power sharing among in-core batches in a PWR. This will provide the remaining ingredient necessary for a simple model which can stand on its own.

Using a "group-and-one-half" model, and the assumption that the fast flux in a bundle is proportional to $k_\infty^{\theta-1}$, leads to a prescription for bundle power as a function only of the k_∞ values of the bundles involved.

In this chapter two and nine-bundle, zero-current boundary condition problems are analyzed with PDQ-7, and θ values are calculated and compared. Then quarter-core results are analyzed and a heuristic algorithm for batch power fractions is developed. Finally, the linearity condition on the ρ vs B curve is relaxed, and a computer program is described which calculates equilibrium cycle fuel discharge burnups, including the effects of leakage, variable batch size, and cycle schedule index.

4.2 "Group and One-Half" Model

In the two-group formulation, the thermal power in a region can be written as:

$$q = \kappa\Sigma_{f1}\ \phi_1 + \kappa\Sigma_{f2}\ \phi_2 \tag{4.1}$$

If the assumption $\Sigma_{12}\ \phi_1 = \Sigma_{a2}\ \phi_2$ is made, and the leakage effects are neglected, where Σ_{12} is the macroscopic down-scatter cross-section from group one (the fast group) to group two (the thermal group), Eq. 4.1 becomes:

$$q = \kappa \left\{ \Sigma_{f1}\ \phi_1 + \Sigma_{f2} \frac{\Sigma_{12}}{\Sigma_{a2}}\ \phi_1 \right\} \tag{4.2}$$

The two-group value of k_∞ can be written as:

$$k_\infty = \frac{\nu\Sigma_{f1}}{\Sigma_{a1} + \Sigma_{12}} + \frac{\Sigma_{12}}{\Sigma_{a1} + \Sigma_{12}} \frac{\nu\Sigma_{f2}}{\Sigma_{a2}} \tag{4.3}$$

Thus, the power can be written as:

$$q = \frac{\kappa}{\nu}(\Sigma_{a1} + \Sigma_{12})\ k_\infty\ \phi_1 \tag{4.4}$$

If the quantity $\frac{\kappa}{\nu}(\Sigma_a + \Sigma_{12})$ is assumed to be constant, and the empirical relation $\phi_1 \simeq k_\infty^{\theta-1}$ is invoked (see Appendix D), a formula for q can be proposed as:

$$q = Ck_\infty^{\theta} \tag{4.5}$$

4.3 Results of Two-Bundle Calculations

Consider the two-bundle, zero-current boundary condition problems discussed in Section 3.3. If the power in bundle one is Ck_1^N and the power in bundle two is Ck_2^N, then the power weighting algorithm gives a combined system reactivity of:

$$k_{sys} = \frac{k_1^M + k_2^N}{k_1^{M-1} + k_2^{N-1}} \tag{4.6}$$

It can be shown (see Appendix D) that for such a system a single number, G, can be found such that:

$$k_{sys} = \frac{k_1^G + k_2^G}{k_1^{G-1} + k_2^{G-1}} \tag{4.7}$$

In this case, the power fraction can be approximated as:

$$f_1 = \frac{k_1^G}{k_1^G + k_2^G} \tag{4.8}$$

Table 4.1 shows the results of a series of two-bundle, zero-current boundary condition problems. The burnup of the bundles was varied to provide a number of test cases with different values of k_1 and k_2. In all cases, the G

TABLE 4.1 ACTUAL AND ESTIMATED POWER FRACTIONS FOR TWO BUNDLE,* ZERO CURRENT BOUNDARY CONDITION PROBLEMS

PDQ RESULTS					G = 3.6	
k_1	k_2	f_1	f_2	G	f_1	f_2
1.3117	1.2094	0.5754	0.4246	3.75	0.5726	0.4274
1.3117	0.9638	0.7449	0.2550	3.48	0.7520	0.2480
1.1289	1.0739	0.5469	0.4531	3.77	0.5448	0.4552
1.1289	1.0004	0.6099	0.3901	3.70	0.6071	0.3929
1.1289	0.9001	0.6915	0.3085	3.56	0.6933	0.3067
1.1289	0.8056	0.7572	0.2428	3.37	0.7711	0.2289
1.0739	0.8056	0.7309	0.2691	3.48	0.7379	0.2621
1.0739	1.0004	0.5661	0.4339	3.75	0.5635	0.4365
0.9001	1.0004	0.4013	0.5987	3.79	0.4060	0.5940
0.9001	0.8056	0.6053	0.3947	3.85	0.5985	0.4015

* Configuration: Fig. 3.4.

factor was calculated which reproduced the exact (PDQ-7 computed) answer. An average G factor of 3.6 was then adopted for all cases and the errors associated with this assumption determined.

As shown in the table, the errors associated with assuming an "average" value of G of 3.6 are very small: averaging less than 1.3%.

It can also be seen that the larger the difference $(k_1 - k_2)$, the smaller the G value becomes. The largest errors in estimating the power fractions occur when the actual G value is farthest from the average value of G = 3.6.

In a power-flattened PWR core, high k_∞ bundles are surrounded by low k_∞ bundles in a well shuffled pattern. To determine a θ value more representative of such cores, the configuration and boundary conditions shown in Fig. 4.1 were used in a second series of PDQ-7 calculations. Three successive constant values of k_2 (0.9, 1.0, 1.2) were used and the values of k_1 were varied (as shown in Table 4.2) over a wide range of enrichments, burnups, fuel-to-moderator ratios, and boron concentrations. Fig. 4.2 shows a plot of $\ln\left\{\frac{q_1}{q_{avg}}\right\}$ versus $\ln\left\{\frac{k_1}{k_{sys}}\right\}$. The plot is linear, with a coefficient of determination (R^2) equal to 0.975. The formula for the best least square fit is:

$$\frac{q_1}{\bar{q}} = 0.94 \left\{\frac{k_1}{\bar{k}}\right\}^{1.55} \qquad (4.9)$$

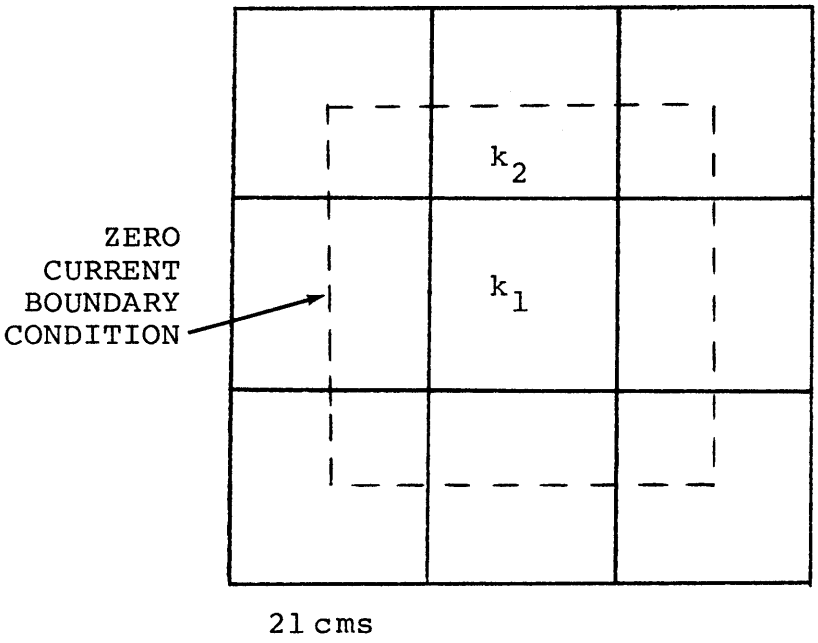

FIGURE 4.1 ASSEMBLY CONFIGURATION FOR DETERMINATION OF θ FOR PWR CORE INTERIOR CONDITIONS

TABLE 4.2 CASES ANALYZED TO DETERMINE POWER SHARING AMONG PWR BUNDLES

RELOAD ENRICHMENT (W/O)	BURNUP (MWD/MT)	PIN PITCH (IN.)	BORON (PPM)
4.3	150	0.580	0
4.3	10,000	0.580	0
4.3	25,000	0.580	0
4.3	40,000	0.580	0
3.0	0	0.580	200
3.0	0	0.580	400
3.0	0	0.580	600
3.0	0	0.680	800
3.0	20,000	0.580	0
3.0	30,000	0.580	0
3.0	40,000	0.580	0
4.0	0	0.580	0
3.5	0	0.580	0
2.5	0	0.580	0
2.0	0	0.580	0
3.0	0	0.500	0
3.0	0	0.575	0
3.0	0	0.600	0

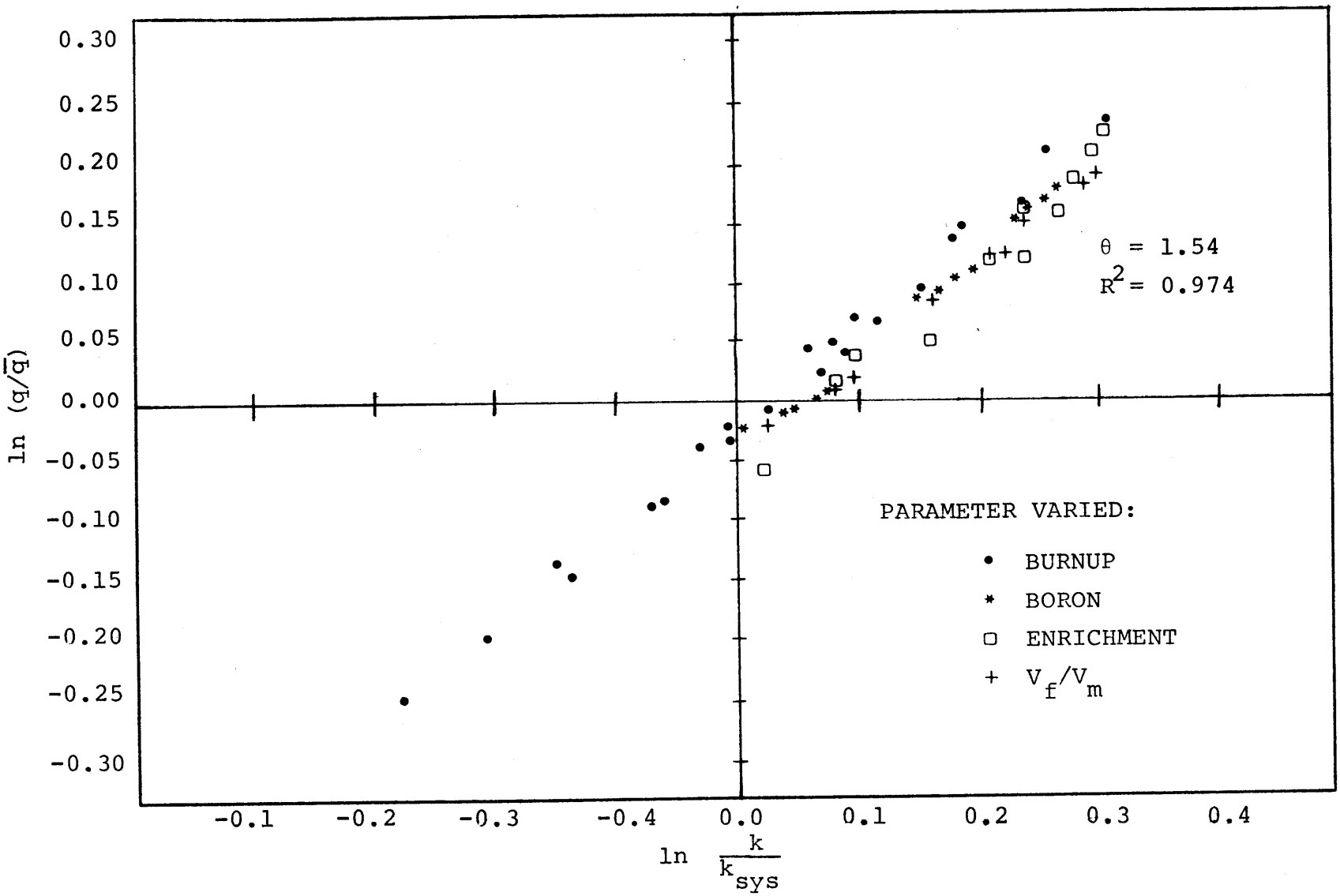

FIG. 4.2 NINE-BUNDLE POWER - k_∞ CORRELATION

4.4 Whole Core Results

The results of the simple nine-bundle zero-current boundary condition problem suggest that the power in the interior assembly can be written as:

$$q_{int} = C\left\{\frac{k_{int}}{\bar{k}}\right\}^{\theta} \bar{q} \qquad (4.10)$$

where $\bar{q}$ represents the average power in the nine assemblies and $\bar{K}$ represents the effective value of k for the nine assembly cluster.

The natural logarithms of interior assembly powers as a function of the natural logarithm of assembly k_∞ values are plotted in Figs. 4.3 and 4.4 for a C-E System 80™ core (W-1) and the Maine Yankee cycle-four reload design (D-4), respectively. The least squares fit for the System 80™ assembly data is given by the equation

$$q_i = 1.026\, k_i^{1.782} \qquad (4.11)$$

whereas the Maine Yankee assembly data can be fit by the equation

$$q_i = 1.003\, k_i^{1.487} \qquad (4.12)$$

The wide scatter among the assembly data is evident from the figures. This is testified to in a quantitative sense

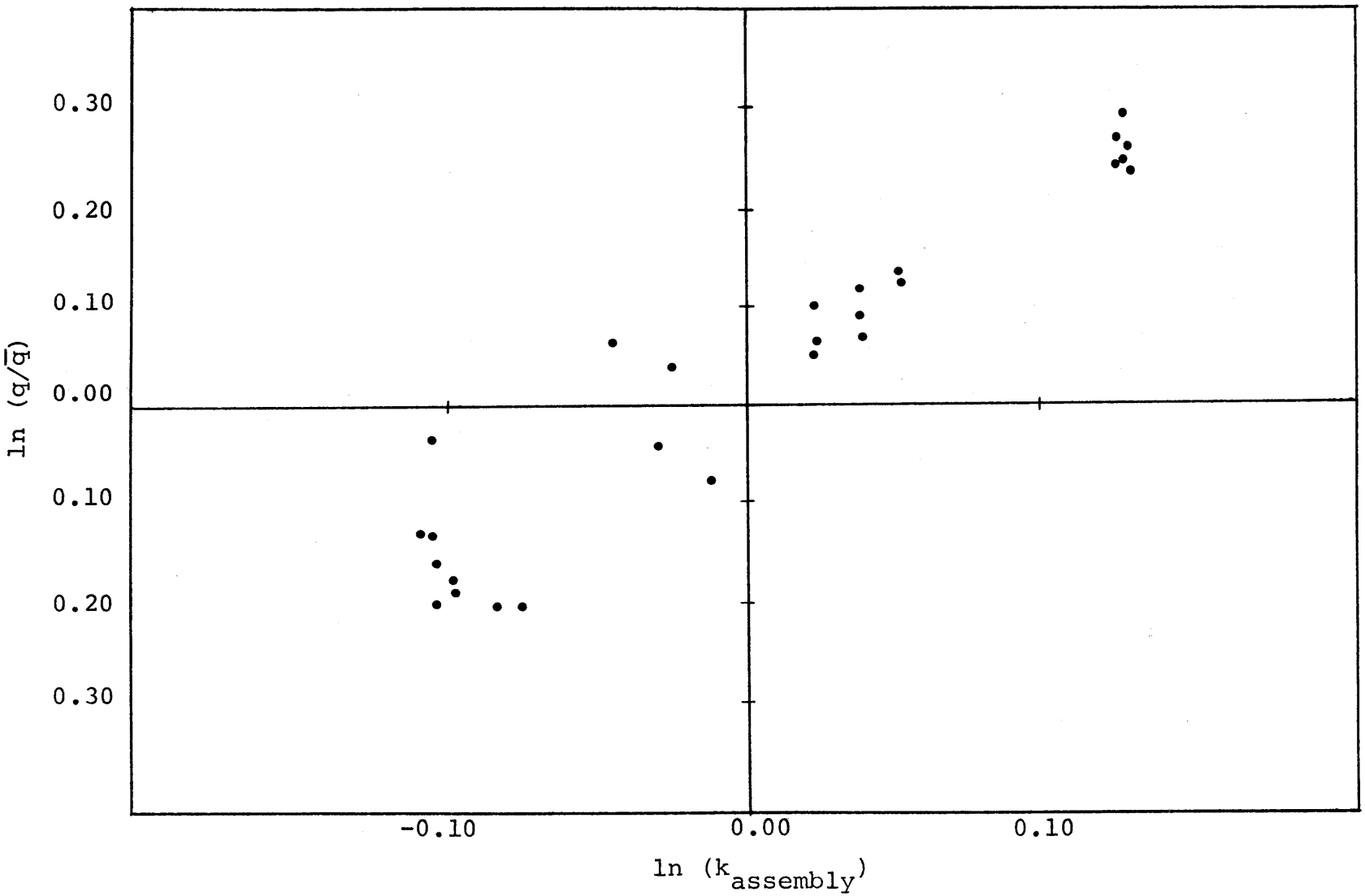

FIG. 4.3 ASSEMBLY POWER VS. k PLOT FOR INTERIOR ASSEMBLIES IN A C-E CORE

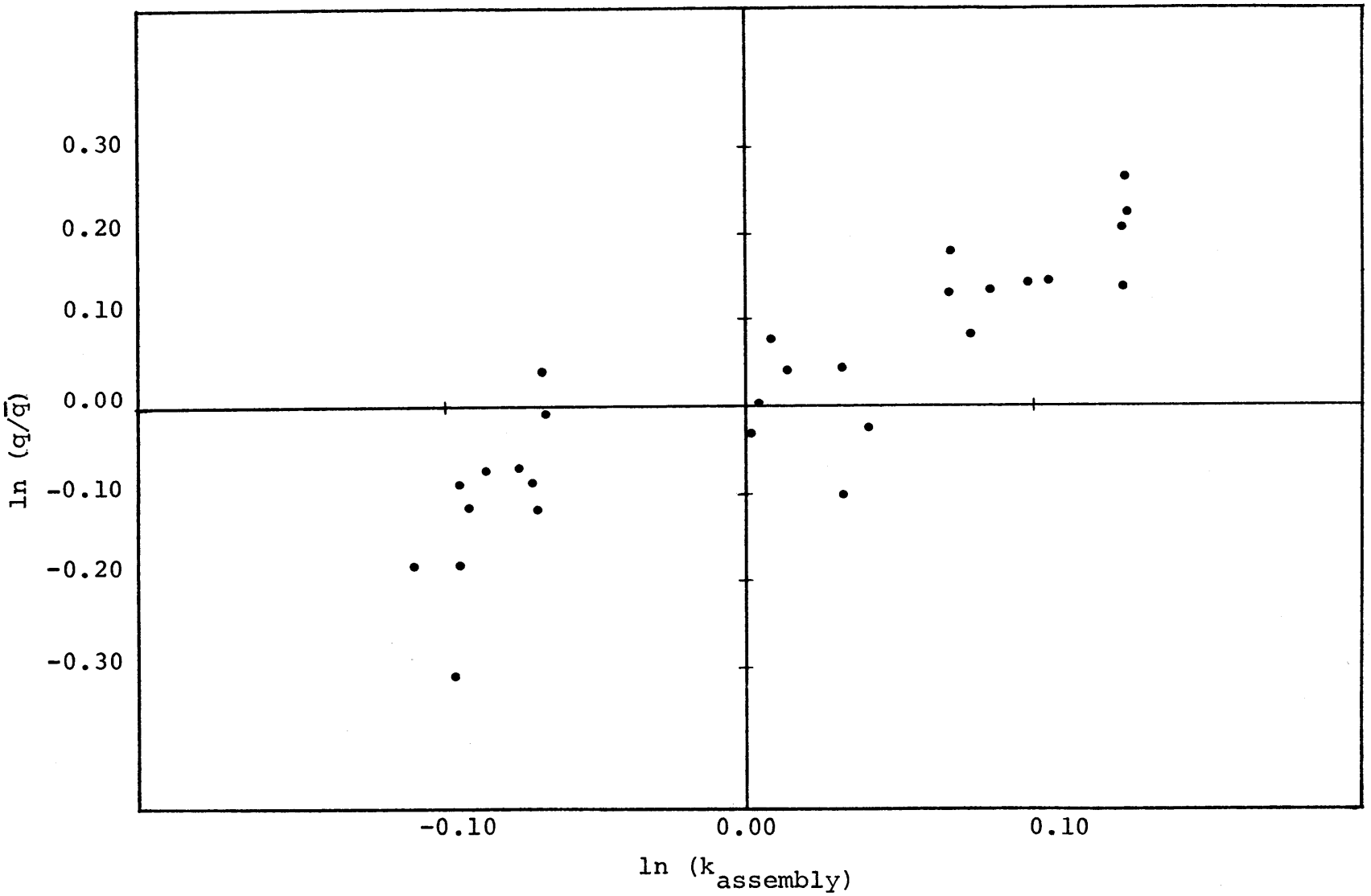

FIG. 4.4 ASSEMBLY POWER VS. k PLOT FOR INTERIOR ASSEMBLIES IN THE MAINE YANKEE CYCLE 4 RELOAD DESIGN

by the coefficient of determination R^2, which for both sets of data is in the range 0.6-0.7. However, for present purposes it is more relevant to plot the data for assemblies grouped into a batch. The results for the Maine Yankee cycle 4 reload core design are shown in Fig. 4.5. The best-fit line can be described by the equation

$$\frac{q_{batch}}{q_{average}} = 1.003 \left\{k_{batch}\right\}^{1.49} \qquad (4.13)$$

The coefficient of determination (R^2) for this plot is 0.985. Thus, even though individual assembly power cannot be predicted accurately, the batch-wise power splits can be determined to the level of accuracy required for detailed fuel management analysis. A similar analysis for the CE core yielded a θ value of 1.79 with an R^2 value of 0.996. The plot for the batches is shown in Fig. 4.6. These values for θ are consistent with the value of θ determined from the nine-assembly calculations, 1.55.

The core maps for the two designs analyzed in this section are shown in Figs. 4.7 and 4.8. We have, however, to this point, excluded the assemblies which are grouped on the core periphery. Estimating the powers of the assemblies grouped on the core periphery is crucial to estimation of the core leakage reactivity, and hence, the fuel discharge burnup. For the peripheral batch, the multiplication factor, k_{eff}, can be defined as:

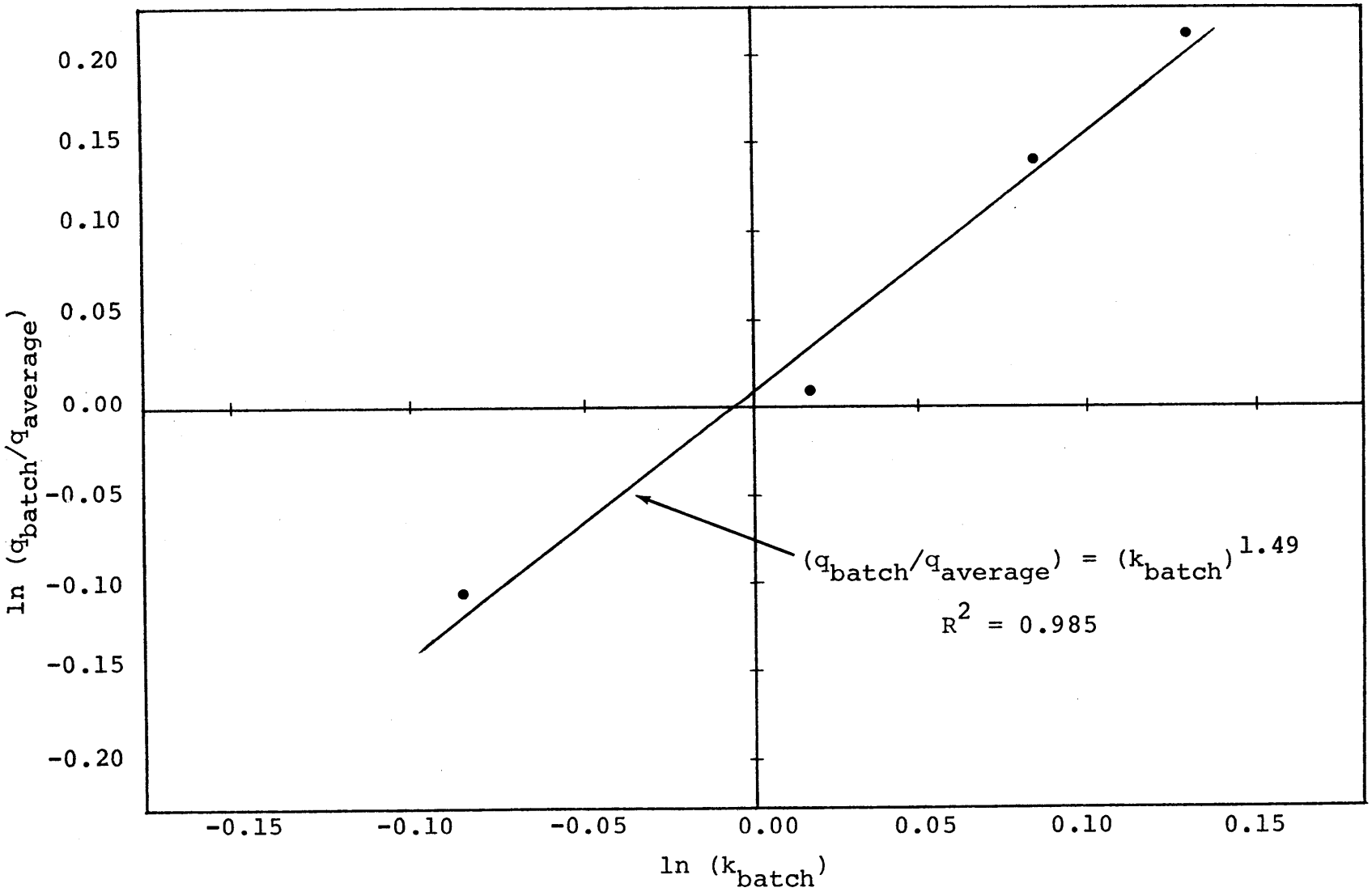

FIG. 4.5 POWER-MULTIPLICATION FACTOR REGRESSION LINE FOR MAINE YANKEE FUEL BATCHES

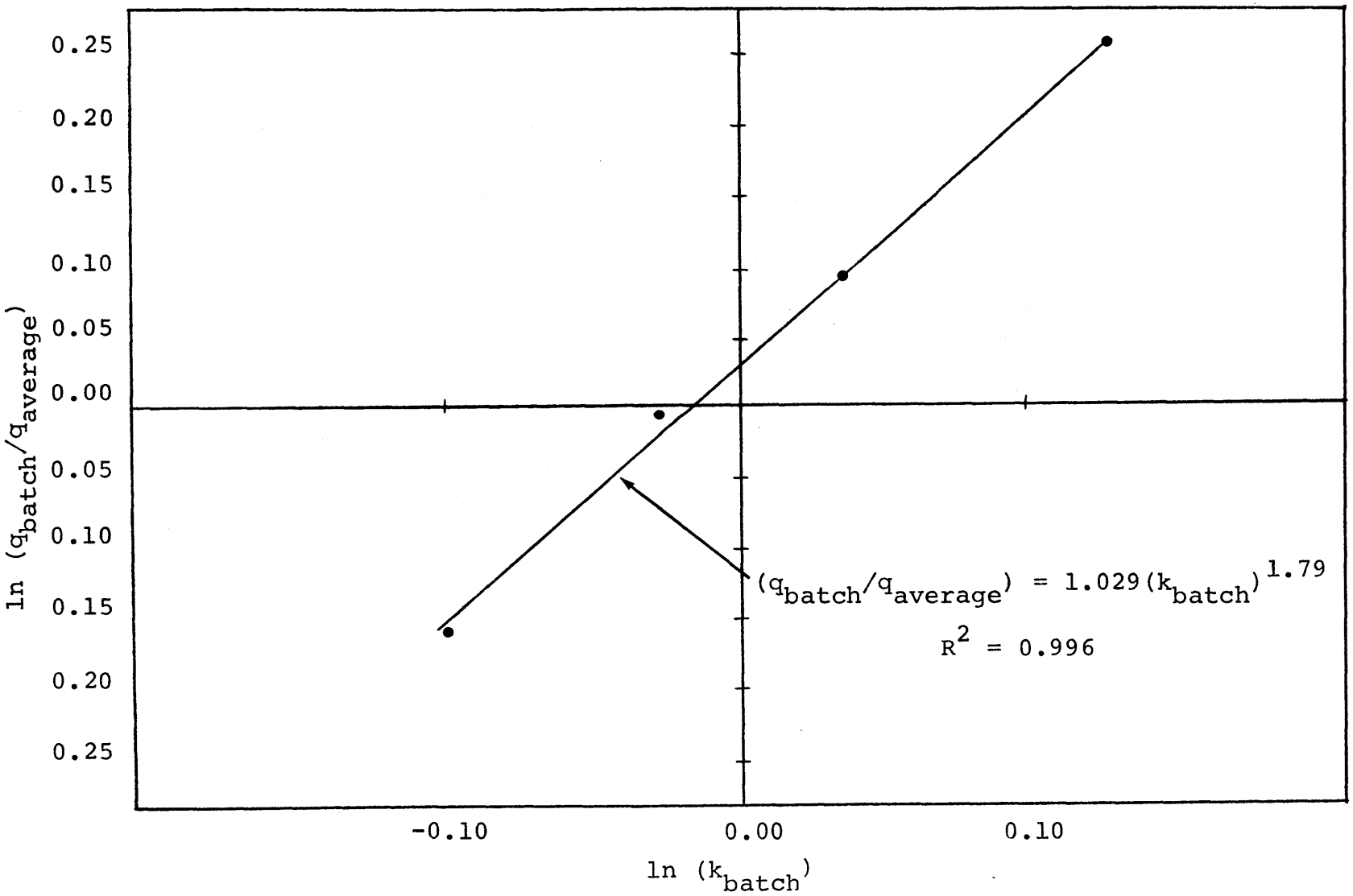

FIG. 4.6 POWER-MULTIPLICATION FACTOR REGRESSION LINE FOR C-E SYSTEM-80™ BATCHES

k / $q/\bar{q}$								
							1.194 0.689	1.194 0.949
				1.194 0.698	1.194 0.927	1.194 1.101	0.909 0.952	1.134 1.324
			1.194 0.843	1.138 1.153	0.934 0.891	0.928 0.943	1.139 1.280	0.935 1.062
		1.194 0.840	1.138 1.284	0.936 0.987	1.088 1.148	1.003 0.986	0.906 0.937	1.036 1.080
	1.194 0.696	1.138 1.152	0.936 0.991	1.075 1.200	1.016 1.040	0.917 0.935	1.103 1.179	1.011 1.097
	1.194 0.920	1.934 0.833	1.089 1.150	1.016 1.045	0.932 0.916	1.109 1.161	0.912 0.896	1.075 1.152
	1.195 1.087	0.928 0.931	1.003 0.972	0.917 0.929	1.110 1.161	1.908 0.914	1.082 1.090	1.006 1.010
1.194 0.680	0.909 0.936	1.140 1.251	0.896 0.791	1.103 1.158	0.912 0.889	1.082 1.090	0.910 0.832	1.037 0.907
1.195 0.934	1.139 1.300	0.935 1.039	1.036 1.049	1.011 1.078	1.075 1.041	1.006 1.005	1.036 0.905	0.908 0.734

FIG. 4.7 CORE MAP FOR MAINE YANKEE CYCLE 4 REDESIGN

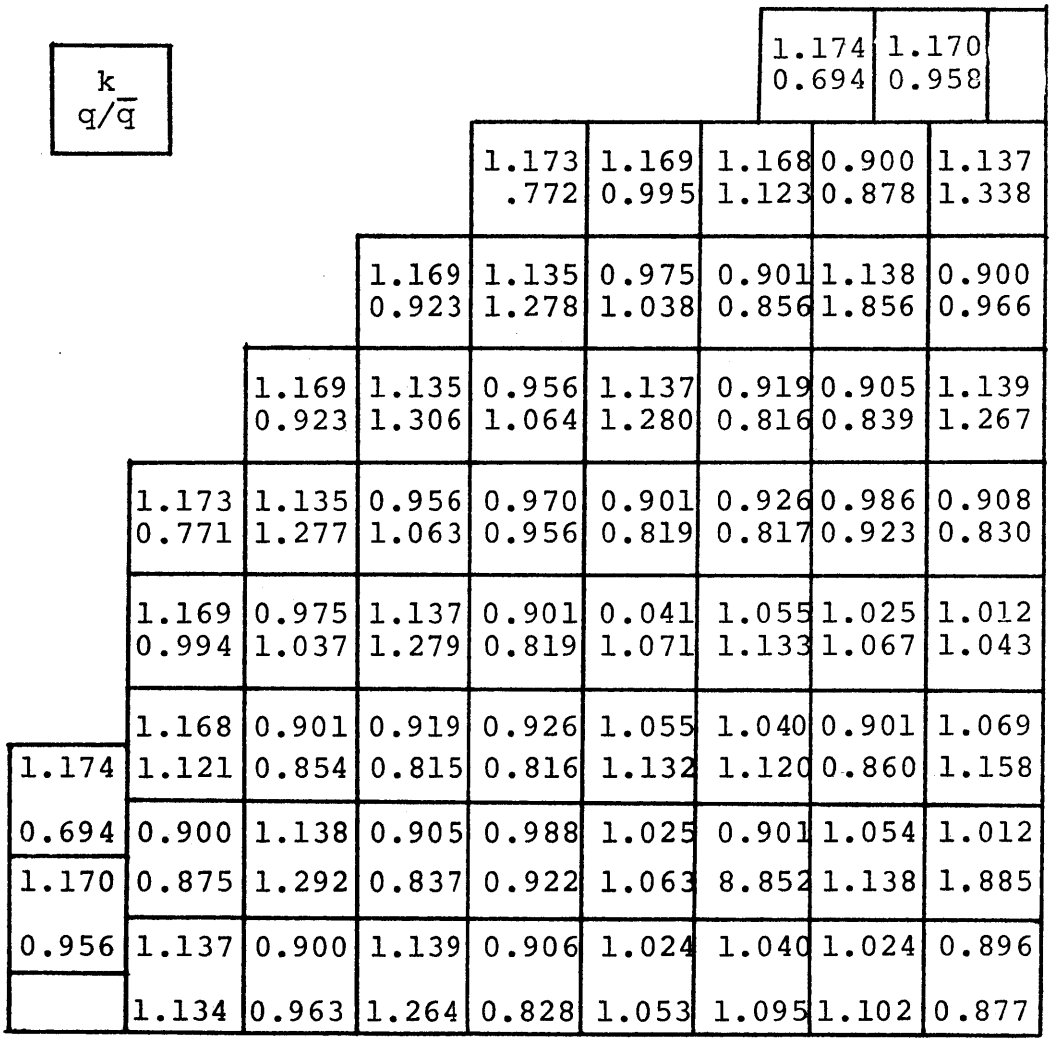

FIG. 4.8 CORE MAP FOR COMBUSTION ENGINEERING SYSTEM-80™ CORE

$$k_{eff} = (PNL)\ k_{\infty} \tag{4.14}$$

where PNL is the non-leakage probability for the peripheral zone; and the peripheral zone power can be written as

$$\frac{q}{\bar{q}} = C\ \left\{(PNL)\ k_{\infty}\right\}^{\theta_p} \tag{4.15}$$

where C is a constant and θ_p is the value of θ which is appropriate for peripheral batches. Estimation of θ_p and PNL for peripheral batches is a somewhat empirical exercise at present, but the limited data base suggests that $\theta_p \simeq 2.0$ and PNL $\simeq 0.77$. Thus, the power sharing formula for batch i in an N batch core with M_i assemblies in batch i is given by:

$$f_i = \frac{\frac{M_{i,per}}{M_i}\ (PNL_i k_i)^{\theta_{per}} + \frac{M_{i,int}}{M_i}\ (k_i)^{\theta_{int}}}{\sum_{i=1}^{N}\left\{\frac{M_{i,per}}{M_i}(PNL_i k_i)^{\theta_{per}} + \frac{M_{i,int}}{M_i}\ (k_i)^{\theta_{int}}\right\}} \tag{4.16}$$

where f_i is the fraction of the total core power generated in batch i, M_i is the number of assemblies in batch i, $M_{i,per}$ is the number of peripheral assemblies in batch i, $M_{i,int}$ is the number of interior assemblies in batch i, PNL is the non-leakage probability associated with peripheral assemblies in batch i, and θ_{per} and θ_{int} are, respectively, the peripheral and interior values for θ.

The choice of the θ values and non-leakage probabilities requires some prior knowledge of the characteristics of the reactor core design and fuel management schemes under consideration. Equal power sharing among batches can be obtained by setting $\theta = 0.0$. This limit is, of course, not achievable in real core designs. At the other extreme an uneven power sharing schedule can be achieved by setting $\theta \simeq 3.0$. The adverse power sharing resulting from this choice leads to detrimental power peaking in the core interior.

For extreme perturbations from normal fuel management strategies, a static PDQ-7 2-dimensional calculation suffices to estimate representative θ values at low cost.

4.5 The ALARM (A-Linear Advanced Reactivity Model)

An automated procedure has been developed for determining the discharge burnup of fuel batches, in an N-batch reactor based on the θ-method described previously. The model includes features developed in Chapter 3 for the Advanced Linear Reactivity Method, such as a leakage correlation and power-weighted reactivity averaging. θ values for the core periphery and interior are input to permit estimation of a cycle schedule index. In addition, the final restriction, that of linear reactivity, is relaxed, and the k_∞ versus burnup values from the assembly spectrum calculation (e.g., LEOPARD) are directly input as a table. An n^{th} order (specified by the user) Lagrangian interpolation is performed at each burnup step required in the computation. Table 4.3 summarizes the principal features of the code, and Fig. 4.9 displays a flow chart of the code. A further description of the code, a listing, and a sample problem can be found in Appendix E. The code calculates the burnups for each batch (starting with an internally generated initial estimate) and iterates until the EOC k_∞ values for batch I are equal to the BOC values of k_∞ for batch I + 1. This method is ideal for equilibrium cycle calculations. At EOC the power fractions are recalculated via the theta formula (Eq. 4-16) and the iteration is restarted until overall convergence is achieved.

TABLE 4.3 FEATURES OF THE ALARM CODE

Non-linear reactivity vs. burnup behavior can be accommodated	N^{th} order Lagrangian interpolation in a $\rho(B)$ table is employed
Power-weighted reactivity averaging is employed	$\rho_{sys} = \sum_{i=1}^{N} f_i \rho_i$
Batch fraction need not be kept constant	Number of assemblies in a batch and location (peripheral and/or interior) are input parameters
Peripheral leakage is estimated using a linear reactivity/power correlation	$\rho_L = \alpha + \beta f_{per}$ $f_{per} = \sum_{i=1}^{N} f_{i,per}$
Interior batch power is calculated using k^θ method	$f_{i,int} = \frac{\frac{M_{i,int}}{M_i} (k_i)^{\theta}_{int}}{\sum_{i=1}^{N} f_i}$
Peripheral batch power is calculated using a separate k^θ correlation, correcting k for leakage	$f_{i,per} = \frac{\frac{M_{i,per}}{M_i} (k_i PNL_i)^{\theta}_{per}}{\sum_{i=1}^{N} f_i}$

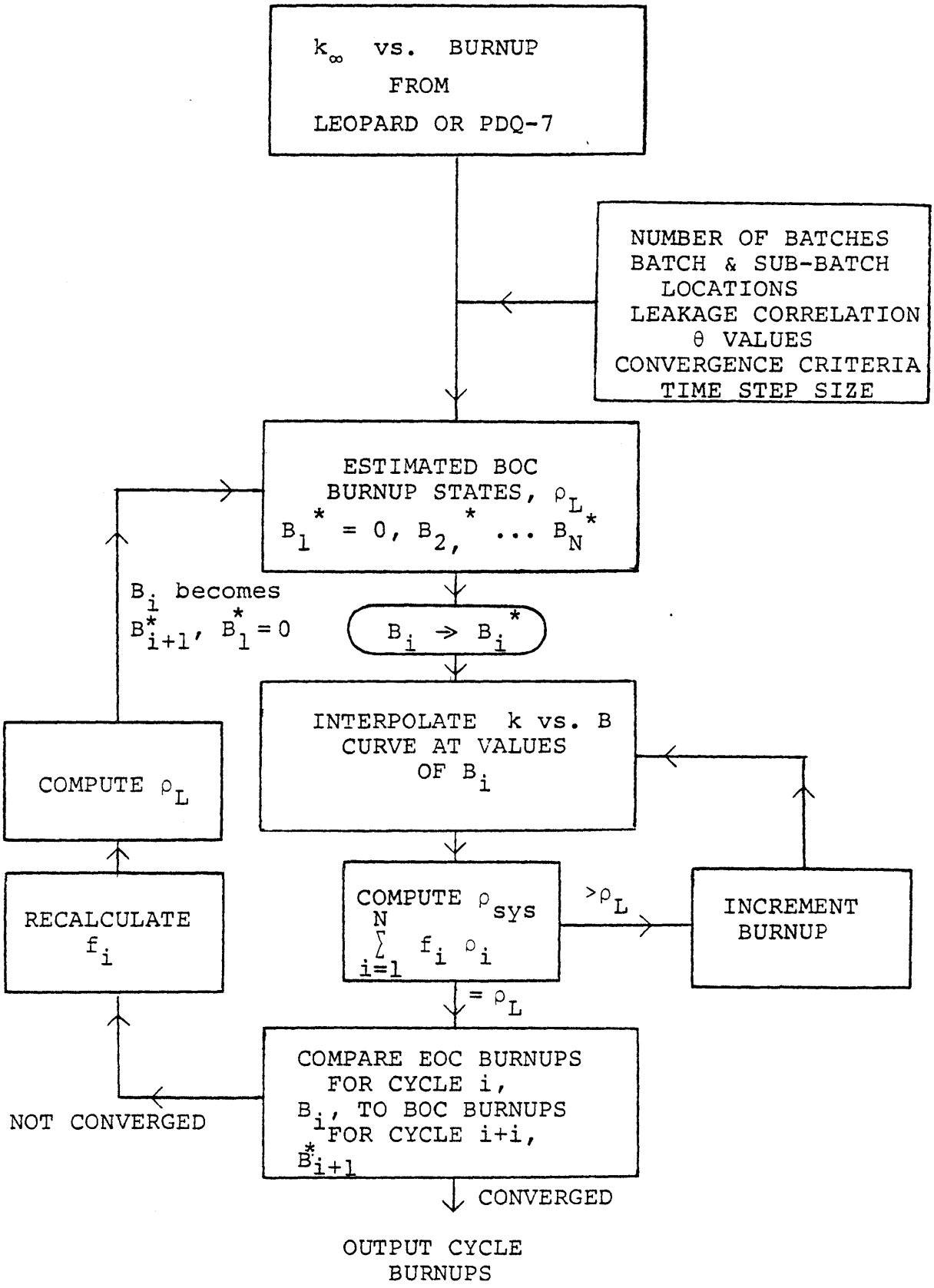

FIG. 4.9 FLOWCHART FOR ALARM CODE METHODOLOGY

If the k_∞ versus burnup data input to the code comes from an infinite medium spectrum calculation, the leakage correlation supplied to the code should have an axial leakage term incorporated in the first constant. If the k_∞ versus burnup data comes from a PDQ-7 bundle calculation, and includes the effect of axial leakage, only radial leakage effects are included in the correlation.

The code was applied to the low-leakage fuel management problem analyzed in Chapter 3. A leakage correlation was developed for application to equilibrium cases by fitting the (near-equilibrium) values of the peripheral assembly powers for both cases available (low-leakage and out-in) to their corresponding leakage reactivity values. The k_∞ versus burnup values for 4.30 and 4.44 w/o U-235. Maine Yankee assemblies, generated by LEOPARD, were input for the out-in and low-leakage cases, respectively. The values of θ_{per} and θ_{int} were both set equal to 2.0, and the non-leakage probability for peripheral batches was taken to be 0.77. A shim penalty of 0.5% $\Delta\rho$ was applied to the low-leakage case to allow for the use of burnable poison in suppressing the radial power peaking associated with this fuel arrangement. The ALARM code was then used to compute the steady-state burnup in both cases; from the burnup the uranium utilization was then estimated. The uranium savings of the low-leakage core relative to the out-in core was found to be 5.574% before adjustment for

the reload enrichment differences. After adjustment, a 2.1% U_3O_8 savings resulted. The detailed computer studies reported by CE (M-3) predict a 2.5% saving--a value which includes the effect of having 5.6% less fuel in the low-leakage assemblies, an effect not simulated here. However, the overall assembly-averaged spectrum becomes more thermal under this condition, which tends to compensate for the fuel removal. Thus, our simple first cut at this complex problem yields rather satisfactory agreement especially since no attempt was made at a posteriori fine tuning of any of the model's parameters such as θ and PNL. A proper analysis would involve the calculation of the k_∞ versus burnup curves for both types of lattices in a full PDQ-7 spatial assembly treatment with the boron rods explicitly included.

4.6 Chapter Summary

In this chapter, simple algorithms have been developed which enable the user to calculate the power splits among batches in a reactor core, and to determine the power in the peripheral zone of the reactor for input into a radial leakage correlation. The algorithms were assembled into a code, ALARM, which can be used to generate batch power histories: i.e., the program fulfills the function of a "poor man's" PDQ. ρ versus burnup curves of arbitrary shape can be input into the code, in which a "curve following" depletion computation is used to estimate cycle burnups. The application of these methods to fuel management problems will be documented further in Chapter 6.

CHAPTER 5

AXIAL FUEL MANAGEMENT

5.1 Introduction

Previous work at M.I.T. (K-1, F-1) and by many others elsewhere (M-3, C-5, R-2) indicated that improvements in "axial fuel management" could result in uranium savings in PWRs. In this chapter the basic fuel assembly design variables which comprise an axial fuel management strategy will be examined. Several different axial blanket fuel arrangements will be surveyed and the most promising options will be analyzed in detail.

5.2 Analytical Considerations

The goal of improved uranium utilization in PWRs can be achieved by maximizing the reactivity of a fuel bundle over life. Consider a fuel assembly divided into N axial regions (i=1,N); the reactivity of region i can be written as:

$$\rho_i = \rho_{o,i} - A_i \, B_{avg} \, g_i/(1/N) \qquad (5.1)$$

where $\rho_{o,i}$ is the initial reactivity of the fuel in region i, A_i is the slope of the reactivity vs. burnup curve for the fuel in the i^{th} region, B_{avg} is the average burnup of the assembly (MWD/MT), g_i is the cumulative fraction of the total assembly energy generated in the i^{th} region since the start of assembly irradiation, and 1/N is the average cumulative power generated in each region. Thus, the burnup

in region i can be written as:

$$B_i = B_{avg}\, N\, \frac{\int_0^t f_i(t)\, dt}{\int_0^t \sum_{i=1}^{N} f_i(t)\, dt} = B_{avg}\, N\, g_i \qquad (5.2)$$

Considering all N regions of the assembly, the set of local reactivity values can be written as:

$$\rho_1 = \rho_{o,1} - A_1\, B_{avg}\, N\, g_1$$

$$\rho_2 = \rho_{o,2} - A_2\, B_{avg}\, N\, g_2$$

$$\vdots$$

$$\rho_N = \rho_{o,N} - A_N\, B_{avg}\, N\, g_N \qquad (5.3)$$

Applying the equation for power-weighted reactivity; namely,

$$\rho_{sys} = \left[\sum_{i=1}^{N} f_i\, \rho_i\right] - \rho_L \qquad (5.4)$$

to Eq. 5.3 yields:

$$\rho_{sys} = \left[\sum_{i=1}^{N} f_i\, \rho_{o,i}\right] - \left[\sum_{i=1}^{N} A_i\, B_{avg}\, N g_i\, f_i\right] - \rho_L \qquad (5.5)$$

where f_i is the power fraction in region N at the time of evaluation. It is useful to consider the special case of a critical reactor ($\rho_{sys} = 0$) which operated with a time-invariant power profile ($f_i = g_i$) and a uniform fuel loading. For this limiting case:

$$\rho_{sys} = 0 = \rho_o - \left[\sum_{i=1}^{N} AB_{avg}\, N\, f_i^2\right] - \rho_L \qquad (5.6)$$

and the average assembly burnup is given by:

$$B_{avg} = \frac{\rho_o - \rho_L}{AN\left[\sum_{i=1}^{N} f_i^2\right]} \qquad (5.7)$$

Clearly, the average burnup can be maximized by minimizing the leakage reactivity, ρ_L, and by establishing as uniform a power profile (all f_i equal) as possible. Since the axial leakage reactivity can be correlated as

$$\rho_L = \alpha + \beta\, f_{per} \qquad (5.8)$$

the minimization of ρ_L involves the reduction of power in peripheral regions (i.e., achieving a low value of f_{per} within two or three migration lengths of the ends of the fuel assembly). Minimization of ρ_L conflicts with the minimization of the axial power profile index $\sum_{i=1}^{N} f_i^2$.

The equations become more complicated if more than one type of fuel is present in the assembly. Consider the case where axial regions 1 through M consist of fuel with reactivity ρ_o and slope A and regions M+1 through N consist of fuel with reactivity ρ'_o and slope A' . The reactivity equation can be written as:

$$\rho_1 = \rho_{o,1} - AB_{avg}\, N\, f_1$$

$$\rho_2 = \rho_{o,2} - AB_{avg}\, N\, f_2$$

.

.

.

$$\rho_M = \rho_{o,M} - AB_{avg}\, N\, f_M$$

$$\rho_{M+1} = \rho_{o,M+1} - A'B_{avg}\, N\, f_{M+1}$$

.

.

.

$$\rho_N = \rho'_{o,N} - A'B_{avg}\, N\, f_N \qquad (5.9)$$

In this case, the burnup at a given point in time can be written as

$$B_{avg} = \frac{\left[\sum_{i=1}^{M} f_i \rho_{o,i}\right] + \left[\sum_{i=M+1}^{N} f_i \rho'_{o,i}\right] - \rho_L}{N\left[A\left[\sum_{i=1}^{N} f_i^2\right] + A'\left[\sum_{i=M+1}^{N} f_i^2\right]\right]} \qquad (5.10)$$

The formulation embodied in Eq. 5.10 provides an approximate way to compare various strategies for fuel management under various assumptions about the power profile. However, there are several salient points which must be addressed regarding multi-zone fueling in the axial direction.

1) Substantial changes in the axial power shape typically occur during an assembly's first cycle of residence

in the reactor (i.e., 0-10000 MWD/MT). This weakens the assumption that $f_i = g_i$.

2) Lowering the power generated at the ends of the bundle generally involves reducing the enrichment of the fuel on the periphery. Thus, the neutron energy spectrum in these regions, where leakage is also high, may not be sufficiently close to the infinite medium spectrum assumed for the calculation of the ρ vs. burnup curves for these regions; and thermal-hydraulic feedback effects have been neglected.*

3) For end regions consisting of uranium oxide of less-than-natural uranium enrichments (<0.711 w/o U-235) the ρ vs. burnup curves can be highly non-linear.

4) From the thermal-hydraulic standpoint, both the peak and average powers and the detailed axial power shape are important because of the need to satisfy fuel centerline melt and DNBR constraints. Thus, one is not free to arbitrarily pick an axial power shape or fuel loading scheme that optimizes uranium utilization alone.

Because of these considerations, it was decided that only detailed PDQ-7-Harmony depletion analyses of the axial direction should be used for final determination of the uranium savings produced by these interacting effects. Nevertheless, the following general guidelines for axial fuel management strategy were deduced from the analytical model and used to select and screen the cases for the final evaluation:

*Uniform axial temperature distribution assumed

1) minimize power in the peripheral core regions

2) in non-peripheral regions the power profile should be as flat as possible.

In addition, since the axial leakage can be correlated as

$$\rho_L = \alpha + \beta f_{per} \tag{5.11}$$

it may be possible to employ materials (e.g., beryllium, zirconium) that lead to coefficients (α, β) which are smaller than the values typical of assemblies "reflected" by the mixture of stainless steel and water in the upper and lower assembly support structure, and which therefore lead to lower leakage reactivities for the same peripheral power.

5.3 Axial Blanket Results*

Since the uranium utilization calculations are particularly sensitive to the peripheral zone power, investigations have been centered around techniques designed to either reduce the power (and hence ρ_L) or to alter the structural material near the end of the assembly to reduce ρ_L at the same peripheral power. The standard Maine Yankee reactor assembly design described in Appendix A was used for the analysis. The five cases analyzed are shown in Fig. 5.1.

The reference case consisted of a 69 inch (half-core) fueled region containing 3.0 w/o U-235 and an unfueled region which consisted of 28 inches of stainless steel structure and water. The fuel cross-sections were homogenized using

* Uniform axial temperature distribution assumed.

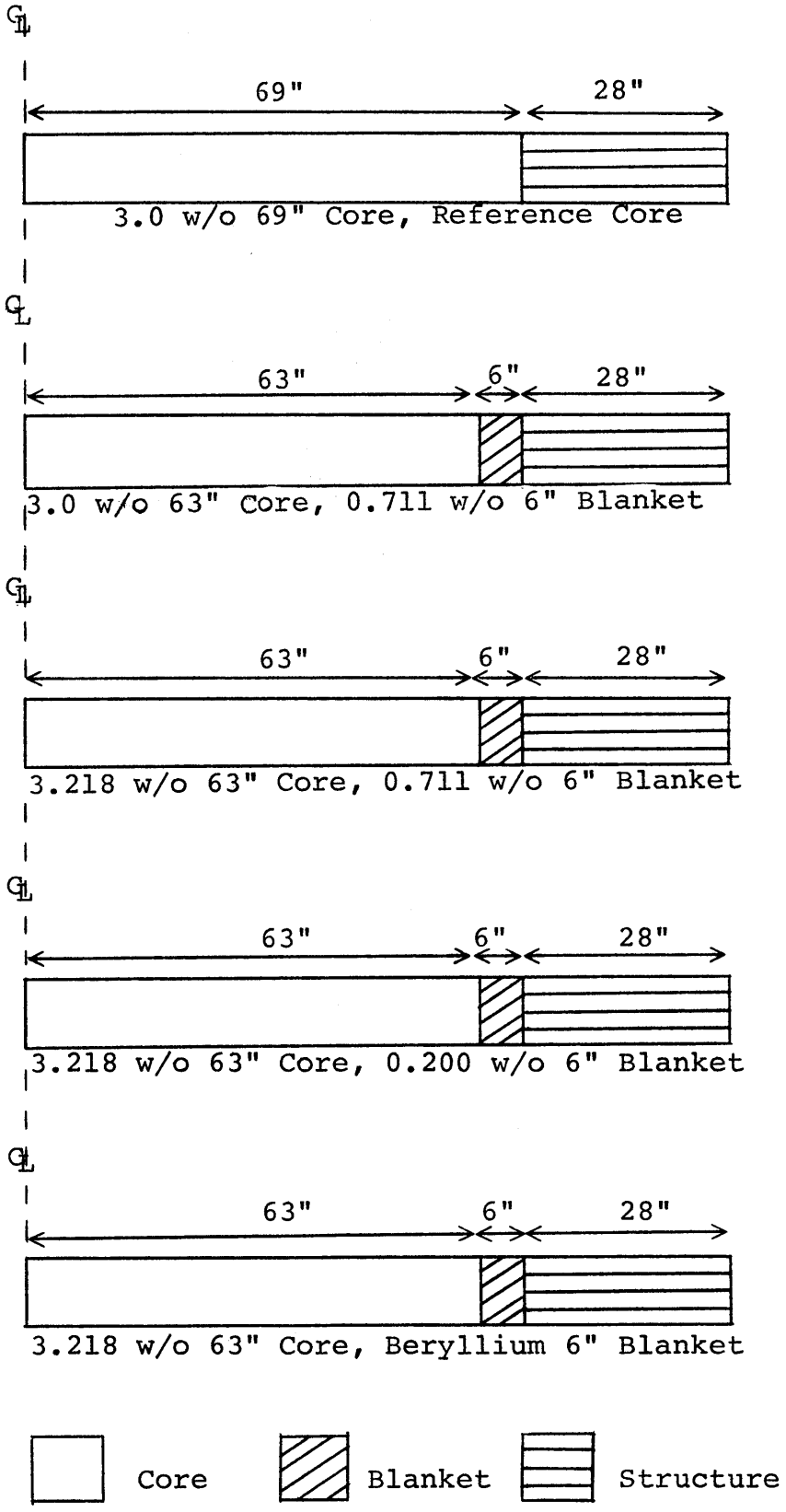

FIG. 5.1 CASES CONSIDERED FOR IMPROVING URANIUM UTILIZATION VIA AXIAL FUEL MANAGEMENT

a LEOPARD supercell geometry. For all cases, the total power level of the bundle was kept constant. Table 5.1 shows the values of ρ_{eff}, ρ_L, and the axial peak-to-average power ratio in the assembly as a function of time (in hours) at effective full power. The values of reactivity vs. burn-up for the reference case were submitted to the ALARM code under conditions of no radial leakage, equal radial power sharing among batches ($\theta_I = \theta_P = 0.0$), and three-batch fuel management. The results indicate that the spent fuel is discharged after 26,179 hours of irradiation at full power.

Two natural uranium blanket cases were examined. In case 2, 63 inches of 3.0 w/o U-235 occupied the central core region, while the last six inches of the core were replaced with natural uranium (0.711 w/o U-235). Case 3 is essentially the same except that the central core region consists of 3.218 w/o U-235 instead of 3.0 w/o U-235. Thus, Case 3 and the reference case have the same feed-to-product ratio (F/P). The values of ρ_{eff}, ρ_L and axial peak-to-average power for Cases 2 and 3 are listed in Tables 5.2 and 5.3 respectively. Both cases have nearly identical leakage reactivities and power profiles over their entire burnup history. The fuel assembly analyzed in case 2 is discharged at 24,860 hours, whereas the fuel assembly analyzed in Case 3 is discharged at 26,797 hours. The relative uranium requirement of these cases will be examined in the section which follows.

TABLE 5.1 REFERENCE CASE BURNUP RESULTS

Time (Hours at full power)	ρ_{eff}	ρ_L	Peak-to-Average Power Ratio
0	0.24778	0.00314	1.500
125	0.22033	0.00432	1.329
800	0.21048	0.00448	1.318
1500	0.20324	0.00508	1.230
3000	0.18678	0.00651	1.148
4500	0.16951	0.00739	1.128
6000	0.15180	0.00834	1.121
7500	0.13399	0.00902	1.107
9000	0.11575	0.00983	1.106
10500	0.09743	0.01037	1.091
12000	0.07865	0.01117	1.098
13500	0.05949	0.01217	1.087
15000	0.04005	0.01236	1.087
16500	0.01969	0.01316	1.094
18000	-0.00101	0.01365	1.083
19500	-0.02242	0.01447	1.093
21000	-0.04477	0.01514	1.090
22500	-0.06746	0.01570	1.081
24000	-0.09091	0.01643	1.083
25500	-0.11473	0.01689	1.072
27000	-0.13851	0.01735	1.064
28500	-0.16021	0.01669	1.056
30000	-0.18159	0.01724	1.031

TABLE 5.2 NATURAL URANIUM BLANKETED ASSEMBLY BURNUP RESULTS, 3.0 W/O CORE REGION

Time (Hours at full power)	ρ_{eff}	ρ_L	Peak-to-Average Power Ratio
0	0.24738	0.00147	1.590
125	0.21941	0.00197	1.431
800	0.20916	0.00209	1.402
1500	0.20141	0.00239	1.313
3000	0.18378	0.00315	1.215
4500	0.16536	0.00370	1.193
6000	0.14666	0.00426	1.182
7500	0.12777	0.00477	1.172
9000	0.10859	0.00524	1.161
10500	0.08930	0.00573	1.149
12000	0.06939	0.00629	1.155
13500	0.04926	0.00672	1.143
15000	0.02848	0.00733	1.151
16500	0.00709	0.00784	1.144
18000	-0.01469	0.00837	1.141
19500	-0.03740	0.00914	1.157
21000	-0.06105	0.00962	1.139
22500	-0.08501	0.01033	1.148
24000	-0.10949	0.01094	1.141
25500	-0.13401	0.01152	1.131
27000	-0.15663	0.01151	1.079
28500	-0.17850	0.01198	1.072
30000	-0.19992	0.01232	1.064

TABLE 5.3 NATURAL URANIUM BLANKETED ASSEMBLY BURNUP RESULTS
3.218 W/O CORE REGION

Time (Hours at full power)	ρ_{eff}	ρ_L	Peak-to-Average Power Ratio
0	0.25574	0.00143	1.591
125	0.22836	0.00193	1.426
800	0.21819	0.00205	1.402
1500	0.21076	0.00232	1.319
3000	0.19401	0.00303	1.216
4500	0.17649	0.00355	1.194
6000	0.15868	0.00408	1.183
7500	0.14069	0.00456	1.173
9000	0.12241	0.00503	1.164
10500	0.10400	0.00546	1.155
12000	0.08507	0.00597	1.156
13500	0.06592	0.00639	1.145
15000	0.04609	0.00695	1.154
16500	0.02564	0.00743	1.146
18000	0.00475	0.00795	1.146
19500	-0.01732	0.00865	1.160
20000	-0.03984	0.00912	1.144
22500	-0.06304	0.00980	1.153
24000	-0.08686	0.01037	1.147
25500	-0.11087	0.01095	1.140
27000	-0.13317	0.01099	1.086
28500	-0.15510	0.01146	1.084
30000	-0.17655	0.01179	1.070

In Case 4, the natural uranium blanket of Case 3 is replaced with a depleted uranium (0.2 W/O U-235) blanket. The reactivity history for this case is shown in Table 5.4. The peak to average power ratios are higher for this case than for Case 3 bacause the power in the last six inches is somewhat depressed. However, the leakage reactivity, ρ_L, is also reduced significantly, and this implies more efficient neutron utilization. The discharge time for Case 4 is computed by the ALARM code to be 26466 hours.

In the fifth and final case, the depleted uranium blanket fuel pellets of Case 4 are replaced by beryllium metal slugs. The cross sections for this region were generated using the HAMMER code since the available LEOPARD library did not include beryllium.

The beryllium region has a higher fast neutron albedo than stainless steel-containing regions, and as a result, more neutrons are returned to the core region. However, this causes the power to rise in the peripheral regions, which forms an offsetting increase in neutron leakage. The reactivities and peak-to-average power ratios for the beryllium blanket case are shown in Table 5.5.

The leakage reactivities for the beryllium blanket case are comparable to those of the reference case over life and even drop lower than those of the reference case near the end of life. Additional benefit comes from the remarkably flat power profile in the fueled region over life. A lower

TABLE 5.4 DEPLETED URANIUM BLANKETED ASSEMBLY BURNUP RESULTS 3.218 W/O CORE REGION

Time (Hours at full power)	ρ_{eff}	ρ_L	Peak-to-Average Power Ratio
0	0.25565	0.00091	1.612
125	0.22815	0.00122	1.450
800	0.21788	0.00132	1.424
1500	0.21033	0.00151	1.339
3000	0.19329	0.00202	1.234
4500	0.17548	0.00243	1.212
6000	0.15743	0.00286	1.199
7500	0.13916	0.00327	1.190
9000	0.12065	0.00368	1.180
10500	0.10198	0.00409	1.172
12000	0.08281	0.00454	1.171
13500	0.06342	0.00495	1.160
15000	0.04328	0.00549	1.172
16500	0.02259	0.00594	1.160
18000	0.00013	0.00649	1.166
19500	-0.0297	0.00711	1.175
21000	-0.04370	0.00764	1.163
22500	-0.06721	0.00831	1.164
24000	-0.09121	0.00889	1.162
25500	-0.11517	0.00948	1.153
27000	-0.13736	0.00956	1.095
28500	-0.15934	0.01018	1.099
30000	-0.18068	0.01055	1.081

5.5 BERYLLIUM METAL BLANKETED ASSEMBLY BURNUP RESULTS, 3.218 W/O CORE REGION

Time (Hours at Full Power)	ρ_{eff}	ρ_L	Peak-to-Average Power Ratio*
0	0.25583	0.00414	1.442
125	0.22849	0.00542	1.294
800	0.21832	0.00566	1.276
1500	0.21091	0.00632	1.201
3000	0.19414	0.00792	1.112
4500	0.17647	0.00889	1.095
6000	0.15842	0.00978	1.087
7500	0.14009	0.01048	1.090
9000	0.12138	0.01108	1.122
10500	0.10246	0.01158	1.139
12000	0.08292	0.01216	1.158
13500	0.06307	0.01251	1.152
15000	0.04233	0.01313	1.167
16500	0.02093	0.01346	1.150
18000	-0.01237	0.01393	1.144
19500	-0.02459	0.01441	1.135
21000	-0.04850	0.01463	1.105
22800	-0.07347	0.01506	1.090
24000	-0.09893	0.01519	1.053
25500	-0.12381	0.01502	1.032
27000	-0.14733	0.01476	1.047
28500	-0.17064	0.01486	1.040
30000	-0.19300	0.01471	1.049

* Since the fuel pellet is shorter, multiply results by 69/63 to compare active linear power to other cases.

peak-to-average power ratio permits better fuel utilization near the ends of the fueled region. However, the fuel stack length is shorter, and hence the peak-to-average power value must be multiplied by 69/63 to obtain linear power values which can be compared to the reference case on an absolute basis. The ALARM code calculates an irradiation time of 26096 hours for the beryllium-blanketed case. Fig. 5.2 shows the leakage reactivities for four cases as a function of time.

5.4 Uranium Utilization for Assemblies with Axial Blankets

The feed-to-product ratio for the cases analyzed in Section 5.3 can be written as

$$\frac{F}{P} = \frac{V_{core}}{V_{total}}\left\{\frac{\varepsilon_{core} - 0.2}{0.711 - 0.2}\right\} + \frac{V_{blanket}}{V_{total}}\left\{\frac{\varepsilon_{blanket} - 0.2}{0.711 - 0.2}\right\} \tag{5.12}$$

where V_{core} is the volume of the core region, $V_{blanket}$ is the volume of the blanket region, V_{total} is the sum of V_{core} and $V_{blanket}$, and ε_{core} and $\varepsilon_{blanket}$ are the core and blanket enrichments, respectively. The feed-to-product ratios for the five cases and the uranium (natural) usage are shown in Table 5.6.

Table 5.7 shows the relative hours at effective full power, the relative natural uranium feed and the relative uranium usage ($\frac{MTF}{MWD}$) for each case.

The natural uranium blanket case with the 3.0 w/o core falls short of the reference case discharge time by about

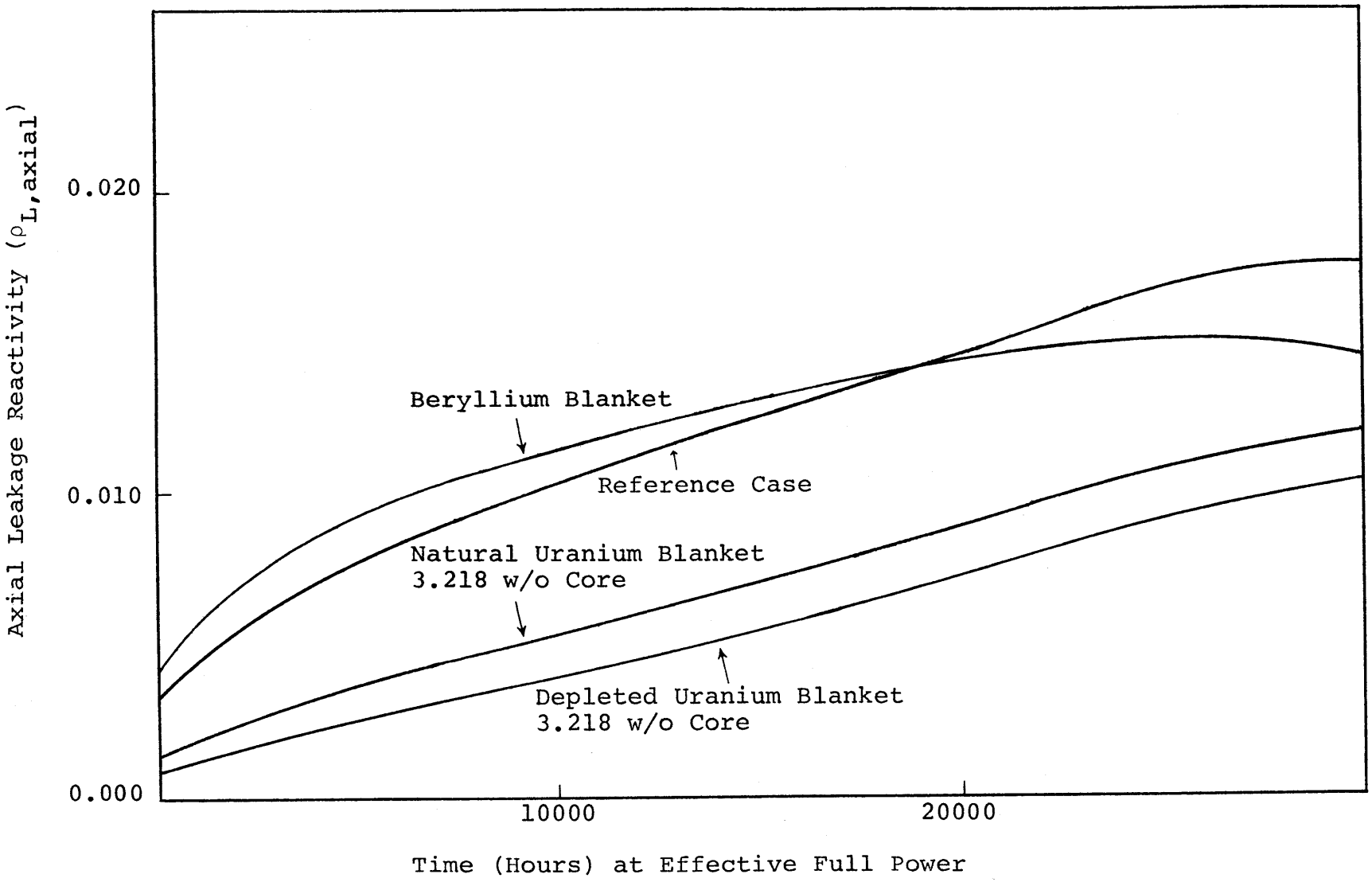

FIG. 5.2 AXIAL LEAKAGE REACTIVITY ($\rho_{L,axial}$) VS. TIME AT EFFECTIVE FULL POWER FOR REFERENCE AND BLANKET CASES

TABLE 5.6 FEED-TO-PRODUCT RATIOS AND RELATIVE NATURAL URANIUM USAGE FOR AXIAL FUEL MANAGEMENT CASES

Case	Type	F/P	Relative Natural Uranium Usage
1	3.0 W/O 69" Core Reference Core	5.47945	1.00000
2	3.0 W/O 63" Core 0.711 W/O 6" Blanket	5.08993	0.92891
3	3.218 W/O 63" Core 0.711 W/O 6" Blanket	5.47945	1.00000
4	3.218 W/O 63" Core 0.200 W/O 6" Blanket	5.39246	0.98413
5	3.218 W/O 63" Core Beryllium 6" Blanket	5.39246	0.98413

TABLE 5.7 RELATIVE URANIUM REQUIREMENTS FOR NORMALIZED POWER OUTPUT FOR VARIOUS BLANKET STRATEGIES

Case	Type	Relative Hours at Effective Full Power	Relative Natural Uranium Feed	Relative Uranium Requirements per Unit Energy Output
1	3.0 W/O 69" Core Reference Core	1.00000	1.00000	1.00000
2	3.0 W/O 63" Core 0.711 W/O 6" Blanket	0.94962	0.92891	0.97819
3	3.218 W/O 63" Core 0.711 W/O 6" Blanket	1.02361	1.00000	0.97693
4	3.218 W/O 63" Core 0.200 W/O 6" Core	1.01096	0.98413	0.97346
5	3.218 W/O 63" Core Beryllium 6" Blanket	0.99682	0.98413	0.98727

5.1%, but produces a uranium saving of 2.19%. The natural uranium blanket case with the 3.218 w/o core surpasses the reference case discharge time by 2.36% and produces a uranium saving of 2.31%. In order to match the cycle length of the reference case, the enrichment of the core should be adjusted to a value between 3.0 and 3.218 W/O U-235. For this case the uranium saving would lie between 2.19% and 2.31%.

The Case 4 configuration with the depleted uranium blanket extends the cycle length by about 1.01%, and thus would require a lower enrichment than the 3.218 w/o value used in the core zone. This would reduce the uranium saving from the 2.65% value quoted by perhaps as much as 0.05%. However, to first order, these effects are negligible.

Case 5 demonstrates that a 1.13% uranium saving is possible using a beryllium blanket. The saving results from the decrease in leakage reactivity attributable to the higher albedo of beryllium relative to stainless steel plus water. Additionally, the beryllium-blanketed core achieves flatter power profiles over life, which means that the fuel near the end of the core is more fully utilized. This decreases the axial profile index of Eq. 5.6.

Table 5.8 shows the maximum/average power ratio at BOL for the blanketed cases relative to the reference case. Clearly, all of the blanketed cases have higher axial peaking factors than the reference case at BOL.

TABLE 5.8 MAXIMUM/AVERAGE POWER AT BOL FOR BLANKETED CASES COMPARED TO THE REFERENCE CASE

Case	Type	Relative Maximum/ Average Power*
1	3.0 W/O 69" Core Reference Core	1.000
2	3.0 W/O 63" Core 0.711 W/O 6" Blanket	1.060
3	3.218 W/O 63" Core 0.711 W/O 6" Blanket	1.061
4	3.218 W/O 63" Core 0.200 W/O 6" Blanket	1.075
5	3.218 W/O 63" Core Beryllium 6" Blanket	1.053

* Maximum/Avg power divided by Maximum/Avg power for reference core.

This limitation at BOL can be compensated for by one or a combination of several strategies:

1) enrichment zoning of the core region to redistribute power
2) inclusion of burnable poison (e.g., gadolinium) in the oxide fuel in the regions where power peaks would otherwise occur
3) Use of annular fuel pellets over part of the core length to adjust the local fuel-to-moderator ratio

5.5 Chapter Summary

Improvement of uranium utilization in PWRs by use of axial fuel arrangement schemes ideally involves a concurrent reduction of axial leakage and a flattening of power in fueled zones to efficiently burn all segments of the fuel. The use of natural uranium blankets six inches in length can result in uranium savings of about 2.3%, whereas the use of depleted uranium blankets of the same length can result in ore savings of up to 2.7%.

Replacing the last six inches of fuel with beryllium metal slugs can yield a uranium saving of about 1.1%. These results should eventually be subjected to a more careful analysis using transport theory methods since diffusion theory (particularly in only two groups) may not be adequate to compute leakage near the material interfaces at the ends of the assembly. In addition, mitigation of the power

peaking which accompanies the use of blankets (by enrichment zoning, the use of zoned burnable poison, or zones of annular fuel pellets) should be examined since it is not clear that an optimum configuration has been reached at this point.

CHAPTER 6

RADIAL FUEL MANAGEMENT

6.1 Introduction

In this chapter, the advanced linear reactivity model is applied to problems relating to uranium utilization in extended cycle operation (i.e., 1.5 year cycles vs. 1.0 year cycles). The ALARM code is used to analyze the Maine Yankee reactor for extended cycle and low-leakage extended cycle operation relative to current operating conditions. Finally, the use of assemblies of natural uranium fuel on the core periphery is examined to determine if uranium savings are possible using this strategy.

6.2 Extended Cycle Length/Burnup

In recent years, utilities have been placing more emphasis on extended cycle lengths to improve overall power plant economics (S-3, S-8, F-2). However, the use of extended cycles in place of normal cycles (e.g., 18 month cycles vs. 12 months cycles) can cause a decrease in uranium utilization depending on the discharge burnup and the number of staggered fuel batches.

The discharge burnup of the fuel can be written as:

$$B_{dis} = \frac{\rho_o - \rho_L}{A\left\{\sum_{i=1}^{N}\sum_{j=i}^{N} f_i\, f_j\right\}} \qquad (6.1)$$

where ρ_L is the leakage reactivity and N is the number of in core batches (constrained at this point to integer values). If all assemblies in the reactor share power equally ($f_i = \frac{1}{N}$), the cycle schedule index in Eq. 6.1 is given by

$$CSI = \sum_{i=1}^{N} \sum_{j=i}^{N} f_i \, f_j = \frac{N + 1}{2N} \tag{6.2}$$

In this case, N = 1,2,...,∞.

For an integer number of batches, the cycle burnup is simply the discharge burnup divided by the number of batches. A utility operating with a fixed discharge burnup constraint may wish to vary the cycle burnup (and hence the time between refuelings). For a fixed enrichment this can only be accomplished by changing the reload fraction of the core. This will result in a non-integer number of batches in the core and ultimately it will affect the uranium utilization.

For a fixed reload enrichment, the number of reload assemblies, A_R, is related to the total number of assemblies in the core, A_T, by

$$A_R = A_T \frac{B_{cyc}}{B_{dis}} \tag{6.3}$$

where B_{cyc} is the average burnup of the fuel in one cycle and B_{dis} is the average discharge burnup of the fuel. If the discharge burnup is fixed, the cycle burnup can be adjusted by changing the number of reload assemblies.

The cycle schedule index can be derived for any combination of batches in a core (see Appendix F). If the power sharing among the assemblies is optimal, the cycle schedule index reduces to:

$$CSI \cong \frac{N + 1}{2N} \tag{6.4}$$

where N is now an integer or noninteger number given by:

$$N = \frac{A_T}{A_R} \tag{6.5}$$

Applying Eq. 6.3 gives the discharge burnup as:

$$B_{dis} = \frac{\rho_o - \rho_L}{A\left[\frac{B_{dis}}{B_{cyc}} + 1\right]} \Bigg/ 2\left[\frac{B_{dis}}{B_{cyc}}\right] \tag{6.6}$$

Maine Yankee reactor assembly burnup calculations have been analyzed using LEOPARD supercell geometry for enrichments ranging from 2.50 w/o U-235 to 5.00 w/o U-235. In this range, the initial extrapolated reactivity can be correlated as:

$$\rho_o = 0.0103556 + (0.0960171)\varepsilon - (0.0084899)\varepsilon^2 \tag{6.7}$$

and the slope of the reactivity vs. burnup curve, A, can be correlated as

$$A = 1.5617773 \times 10^{-5} - (0.2757294 \times 10^{-5})\varepsilon + (0.0184100 \times 10^{-5})\varepsilon^2 \left(\frac{MWD}{MT}\right)^{-1} \tag{6.8}$$

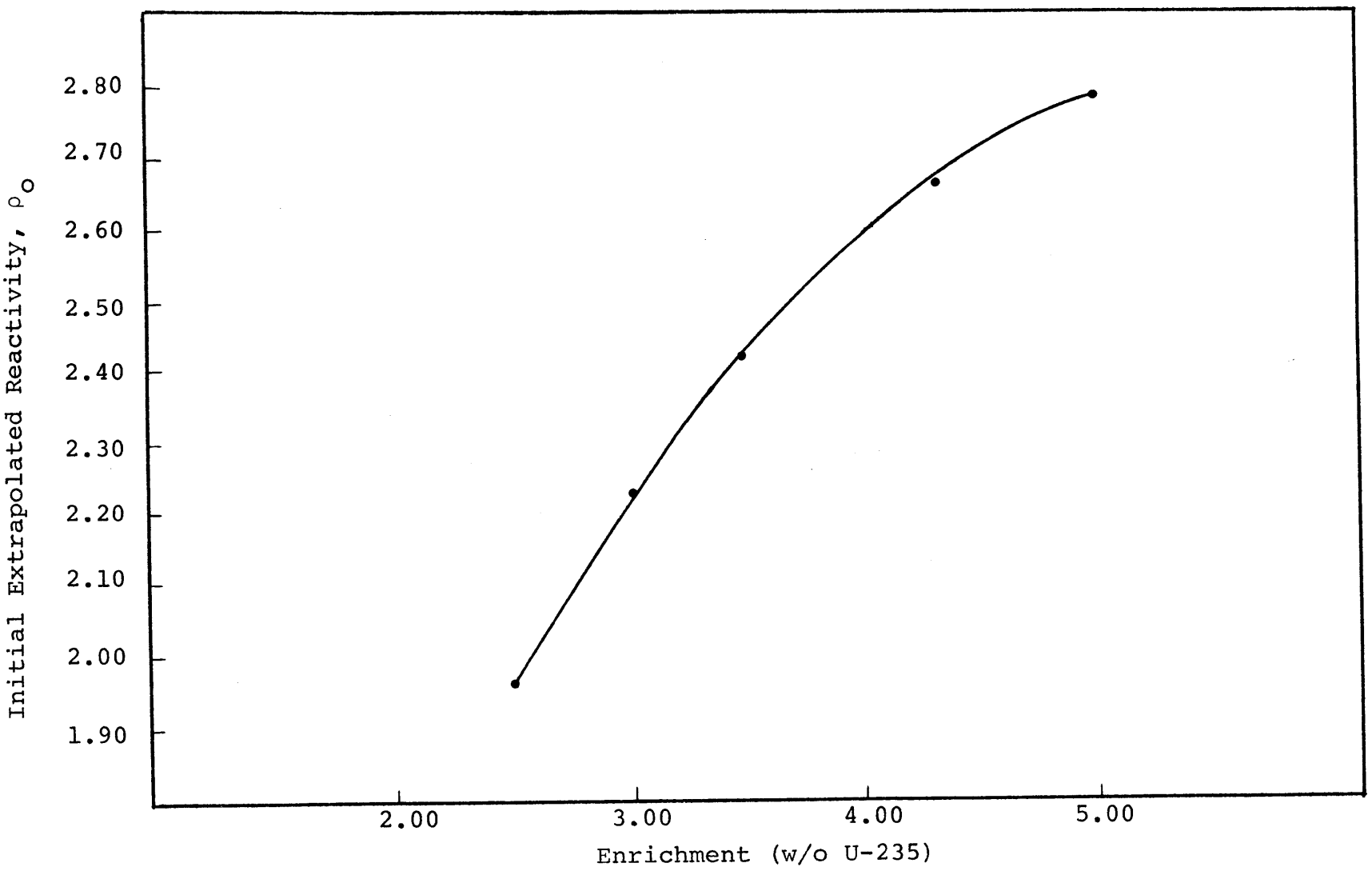

FIG. 6.1 REACTIVITY OF MAINE YANKEE REACTOR ASSEMBLIES FOR VARIOUS ENRICHMENTS

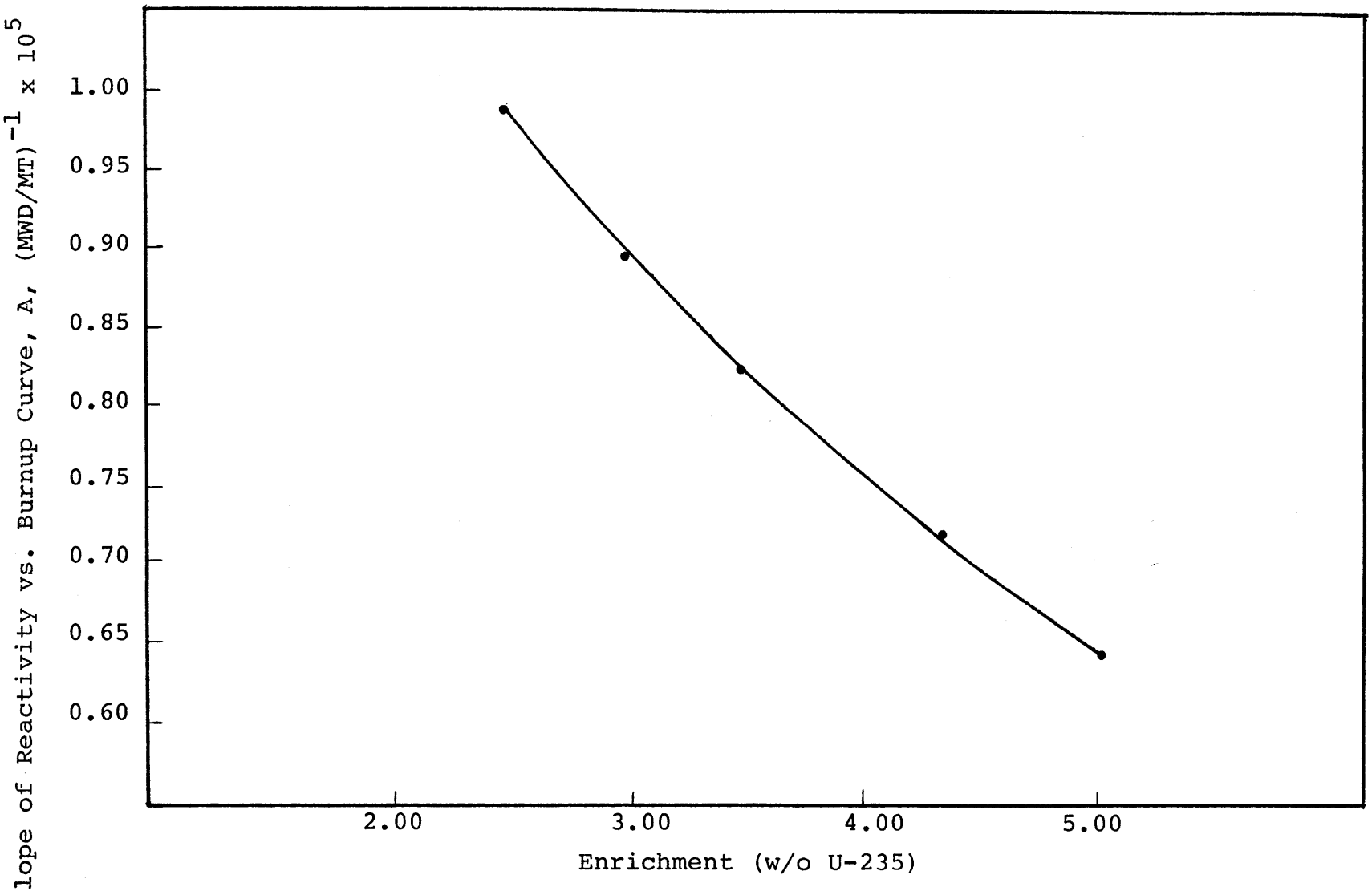

FIG. 6.2 SLOPE OF REACTIVITY VS. BURNUP CURVE FOR MAINE YANKEE REACTOR ASSEMBLIES FOR VARIOUS ENRICHMENTS

where ε is the enrichment of the feed in w/o U-235. The curves are plotted in Figs. 6.1 and 6.2.

Thus, Eq. 6.6 becomes:

$$\frac{B_{dis} + B_{cyc}}{2} = \frac{0.0103556 + (0.0960171)\varepsilon - (0.0084899)\varepsilon^2 - \rho_L}{\{1.561773 - (0.2757294)\varepsilon + (0.0184100)\varepsilon^2\}\times 10^{-5}} \tag{6.9}$$

The uranium utilization in MWD per Metric Ton of Feed $(\frac{MWD}{MTF})$ is given by

$$U = \frac{B_{dis}\ (\frac{MWD}{MTP})}{(\frac{F}{P})} = \frac{0.511\ B_{dis}}{(\varepsilon - 0.2)} \tag{6.10}$$

for an 0.2 w/o U-235 tails assay.

The cycle burnup can be related to the calendar time between startups by:

$$B_{cyc} = \frac{(P_{TH})(T-T_R)(CF)365}{(A_T)(M)} \tag{6.11}$$

where:

P_{TH} = Reactor thermal power rating (Mwth)

T = Time between startups (years)

T_R = Refueling downtime (years)

$T-T_R$ = Time the reactor is available to produce power

CF = Availability-based capacity factor

A_T = Total number of assemblies in reactor

M = Heavy metal loading per assembly (Metric Tons Uranium)

Eq. 6.7-6.11 were combined to estimate the uranium utilization of the Maine Yankee reactor for a variety of enrichments, discharge burnups, cycle times and batch numbers. The values for the reactor parameters of Eq. 6.13 are:

P_{th} = 2630 Mwth

T_R = 0.115068 years

C_F = 0.75

A_T = 217

M = 0.388 MT

In addition, a leakage reactivity of 0.042 was assumed and a tails assay of 0.2 w/o U-235 was used.

The results are shown in Fig. 6.3. The Maine Yankee reactor is currently entering cycle 4 of operation with a capacity factor of about 0.65. Nevertheless, if a current operating point could be defined for this figure it would be at ε= 3.04 and N = 3. This would correspond to a cycle time (startup to startup) of ~1.3 years, and a uranium utilization of 5500 MWD/MTF. Clearly, the graph demonstrates that substantial improvements in uranium utilization with cycle times acceptable to utilities (T > 1 year) can only be achieved by increasing the discharge burnup and the number of in-core batches. For example, a 5 batch core with a 1.3 year cycle would have a discharge burnup of about 53000 MWD/MTP and a uranium utilization of 6500 MWD/MTF. This represents an 18.2% improvement in uranium utilization, or

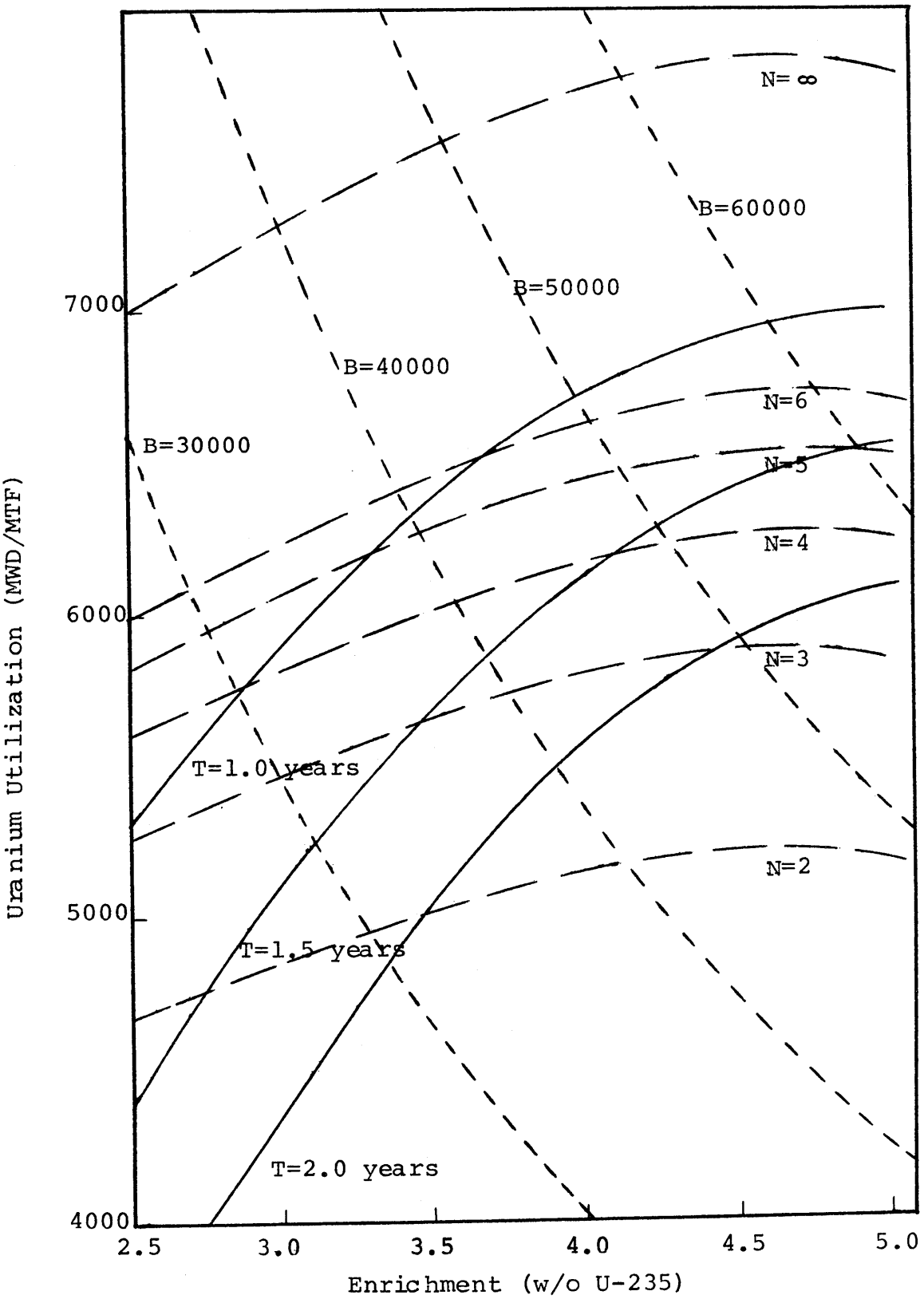

FIG. 6.3 URANIUM UTILIZATION VS. ENRICHMENT FOR THE MAINE YANKEE REACTOR

a 15.4% reduction in uranium requirements relative to current operating conditions.

6.3 Low-Leakage Extended Cycle Fuel Management

The ALARM code has been used to analyze the effects of extended cycle length and low-leakage fuel management on the uranium utilization of the Maine Yankee reactor. Three cases of practical interest were examined. The first case (the reference case) consisted of a reload of 72 assemblies of 3.0 w/o U-235 fuel operated in a normal out-in refueling mode. In the second and third cases, 72 assemblies of 3.4 w/o U-235 were used as the reload for out-in and low-leakage fuel management schemes. The radial leakage correlation for the Maine Yankee reactor developed in Chapter 4 was used, and a constant axial leakage reactivity allowance of 0.012 was included. The cycle burnups, discharge burnups, and uranium utilizations for the three cases are listed in Table 6.1. In the first two cases, the 44 peripheral assembly locations were loaded with fresh fuel, whereas in the low-leakage case, third cycle fuel was used for the peripheral locations. A deficit for burnable poison residual was not included in the extended cycle cases. The relative uranium requirements $(\frac{MTF}{MWD})$ for the three cases are listed in Table 6.2.

TABLE 6.1 COMPARISON OF EXTENDED CYCLE AND LOW-LEAKAGE EXTENDED CYCLE FUEL MANAGEMENT WITH CURRENT, THREE-BATCH, OUT-IN FUEL MANAGEMENT

Case	ε (W/O U-235)	Cycle Burnup (MWD/MTP)	Cycle Length (Years)	Discharge Burnup (MWD/MTP)	U (MWD/MTP)
Current Out-In	3.00	10304	1.32	30632	5590
1.5 year cycle Out-In	3.40	12028	1.522	35759	5710
1.5 year cycle Low-Leakage	3.40	12188	1.540	36734	5866

TABLE 6.2 RELATIVE URANIUM REQUIREMENTS FOR EXTENDED CYCLE, LOW-LEAKAGE EXTENDED CYCLE, AND REFERENCE CASE

Case	Uranium Requirement (MTF/MWD)	Relative Uranium Requirement
Reference 3.0 W/O Out-In	1.789×10^{-4}	1.000
Extended Cycle 3.4 W/O Out-In	1.751×10^{-4}	0.979
Extended Cycle 3.4 W/O Low-Leakage	1.705×10^{-4}	0.953

The use of extended cycle fuel management ($t_{cycle} \sim 1.5$ years) results in a 2.1% reduction in uranium requirements. Since extended cycle designs generally require more burnable poison than one year cycle designs, which implies larger end-of-cycle residuals, this gain must be considered optimistic. If the extended cycle design is operated in a low-leakage configuration a reduction of 4.7% in uranium requirements results, again neglecting the differential in burnable poison residual. Thus, the low-leakage configuration offers a possible 2.5% reduction in uranium requirements for extended cycle designs. However, the low-leakage extended cycle design may have larger poison residuals than the out-in scatter extended cycle design, thereby reducing the gains.

6.4 Natural Uranium Blankets

Investigations have been performed to determine the effectiveness of natural uranium blankets in improving the uranium utilization of pressurized water reactors. The reference design is the CE-System 80 reactor with five fuel batches and an initial enrichment of 4.34 W/O U-235. The reactivity equations for the reference design can be written as:

$$\rho_1 = \rho_o - AB_C N f_1$$
$$\rho_2 = \rho_o - AB_C N(f_1 + f_2)$$
$$\rho_3 = \rho_o - AB_C N(f_1 + f_2 + f_3)$$
$$\rho_4 = \rho_o - AB_C N(f_1 + f_2 + f_3 + f_4)$$

$$\rho_5 = \rho_o - AB_C N(f_1 + f_2 + f_3 + f_4 + f_5) \qquad (6.12)$$

The end-of-cycle reactivity condition is given by:

$$\sum_{i=1}^{5} f_i \rho_i = \rho_L \quad , \qquad (6.13)$$

where ρ_L is the radial leakage reactivity, which has been correlated for the system 80 design from published data (CEND-380) to be:

$$\rho_L = 0.01126 + 0.2214 f_{per} \quad , \qquad (6.14)$$

where f_{per} is the fraction of the total core power generated in the peripheral assembly locations. The equation for cycle burnup becomes:

$$B_C = \frac{\rho_o - 0.01126 - 0.2214 f_{per}}{5A \left\{ \sum_{i=1}^{N} \sum_{j=i}^{N} f_i f_j \right\}} \qquad (6.15)$$

If one-fifth of the core is replaced every cycle the feed to product ratio is given by:

$$\left(\frac{F}{P}\right) = \frac{\varepsilon - 0.2}{0.771 - 0.2} \qquad (6.16)$$

and the cycle burnup in MWD/MTF is given by:

$$B_C \left(\frac{MWD}{MTF}\right) = \frac{\rho_o - 0.01126 - 0.2214 f_{per}}{5A \left\{ \sum_{i=1}^{N} \sum_{j=i}^{N} f_i f_j \right\} \left\{ \frac{4.34 - 0.2}{0.511} \right\} \frac{1}{5}} \qquad (6.17)$$

The reactivity equations for the natural uranium blanket case can be written as:

$$\rho_1 = \rho_o - AB_C N\, f_1$$
$$\rho_2 = \rho_o - AB_C N(f_1 + f_2)$$
$$\rho_3 = \rho_o - AB_C N(f_1 + f_2 + f_3)$$
$$\rho_4 = \rho_o - AB_C N(f_1 + f_2 + f_3 + f_4)$$
$$\rho_5 = \rho_{o,unat} - A'\, B_C N\, f_5 \qquad (6.18)$$

When the EOC reactivity balance (Eq. 6.2) is applied, the cycle burnup is given by:

$$B_C = \frac{(1 - f_5)\rho_o + f_5\, \rho_{o,unat} - 0.01126 - 0.2214\, f_5}{5A \left\{ \sum_{i=1}^{4} \sum_{j=i}^{4} f_i\, f_j \right\} + 5A' \left\{ f_5^{\,2} \right\}} \qquad (6.19)$$

If one-fifth of the core is replaced with enriched fuel each cycle and the natural uranium zone is replaced every M cycles, the cycle burnup in MWD/MTF can be written as:

$$B_C\left(\frac{MWD}{MTF}\right) = \frac{(1-f_5)\rho_o - f_5\, \rho_{o,unat} - 0.01126 - 0.2214\, f_5}{\left[5A \left\{ \sum_{i=1}^{4} \sum_{j=i}^{4} f_i\, f_j \right\} + 5A' \left\{ f_5^{\,2} \right\}\right]\left[\left\{\frac{\varepsilon - 0.2}{0.711 - 0.2}\right\}\frac{1}{5} + \frac{1}{5M}\right]} \qquad (6.20)$$

The ratio of Eq. 6.20 and Eq. 6.17 gives the relative uranium feed use for the blanketed core with respect to the normal 5-cycle equilibrium core. In the normal five batch core, the peripheral assemblies are assumed to be fifth cycle fuel bundles and the remaining four batches share power equally. In the natural uranium blanket case, the four interior core batches also share power equally. Typical parameters for the lattices are:

ρ_o = 0.26614

A = 0.7154×10^{-5} $(MWD/MT)^{-1}$

$\rho_{o,unat}$ = -0.11934

A' = 0.48405×10^{-5} $(MWD/MT)^{-1}$

The use of $\rho_{o,unat}$ = -0.11934 throughout all cycles of the reactor is clearly optimistic, and is meant to give the natural uranium blanket case the maximum benefit of the doubt. In addition, the natural uranium blanket is optimistically assumed to have an in-core residence time of 10 years (M = 10) to minimize the feed requirements for the blanket case. The ratio of Eq. 6.9 to Eq. 6.6 is plotted as a function of the peripheral zone power fraction in Fig. 6.4.

Even under the best conditions, the natural uranium blanket case requires about 1% more ore than when an equivalent "spent fuel" blanket is used. Representative peripheral zone power fractions for fuel of this type range between 0.10 and 0.15. The advantage of the "spent fuel" over the UNAT blanket under these conditions ranges from 2% to 6%.

If power fractions are to be achieved in natural uranium blankets which are substantially lower than those that can be achieved by most representative 5-batch fuel arrangements, the attendant mid-core power peaking would probably lead to the use of more shim material, leaving residuals

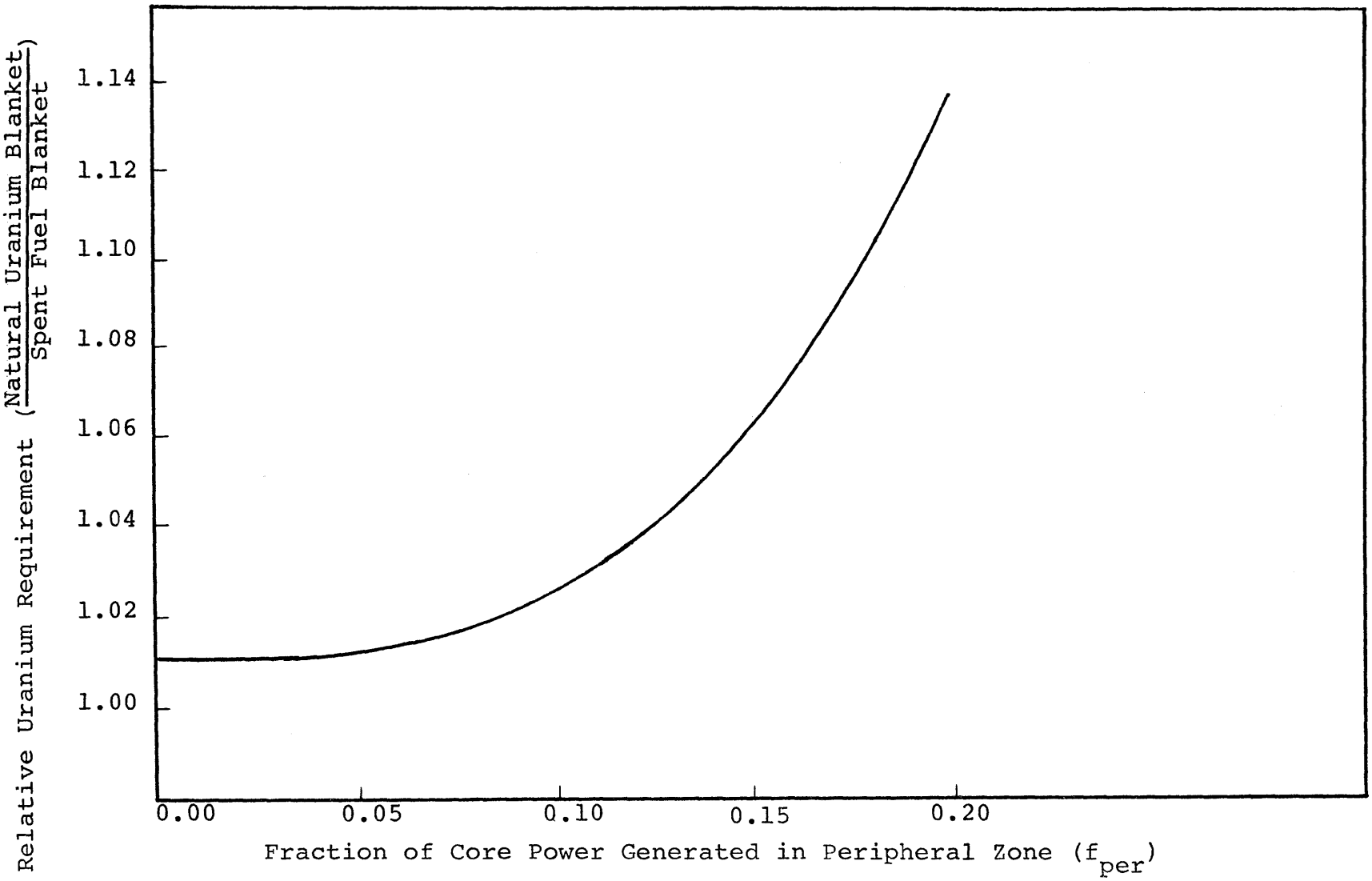

FIG. 6.4 RELATIVE WHOLE CORE URANIUM REQUIREMENT FOR NATURAL URANIUM BLANKET CASE RELATIVE TO SPENT FUEL BLANKET CASE

which would override any possible blanket-related advantage. The conclusion is that for a fixed core size, natural uranium blankets cannot compete with "spent fuel" blankets, i.e., an N-batch core with a natural uranium blanket cannot compete with an (N + 1) batch core which uses its oldest batch as a "blanket".

6.5 Chapter Summary

The uranium utilization for extended cycle fuel management schemes depends on the choice of discharge burnup, cycle burnup (hence number of fuel batches), reload enrichment and leakage reactivity. Only two of these first three parameters can be independently specified; usually the discharge burnup and the cycle burnup (and therefore the cycle length). The leakage reactivity can then be changed by decreasing the amount of fresh fuel on the core periphery.

The calculations of Fig. 6.3 show that the use of extended cycles will increase the uranium utilization $(\frac{MWD}{MTF})$ if the batch number, N, remains constant and the discharge burnup is increased. However, if the discharge burnup remains constant, the use of extended cycles will result in a decrease in uranium utilization and hence an increase in uranium requirements.

The ALARM code shows that the use of extended cycle (1.5 years vs. 1.32 years) out-in/scatter fuel management in the Maine Yankee Reactor will result in a reduction in

uranium requirements of 2.1% if the burnup is increased to approximately 36000 MWD/MT. Concurrent use of low-leakage fuel management in the extended cycle design, however, will result in a reduction of uranium requirements of 4.7% relative to the base case. Overall utility system economics may dictate the use of extended cycle operation. Assumptions about capacity factors and refueling downtime are necessary to compare cycle time and cycle burnup. For extended burnup core designs, the low-leakage scheme requires 2.6% less uranium than the out-in/scatter extended cycle design. If the burnup constraint can be increased to about 53000 MWD/MT, with a concurrent shift to 5 batch fuel management, a reduction of 15.4% in uranium requirements may be possible. Total uranium requirements for high burnup, low-leakage fuel management may (optimistically) approach values 18% lower than under current PWR operating conditions. An analysis which includes burnable poisons in the fuel to reduce peaking factors is necessary to determine burnable poison residuals, which may be high. Also, at higher burnups (~50000 MWD/MT) $\Delta\rho_L$ (ρ_L(out-in) - ρ_L(low-leakage)) is a smaller fraction of ρ_o, since ρ_o is higher for high enrichments. Thus, the advantages of a low-leakage design may be reduced.

Replacing peripheral assemblies with natural uranium blankets does not produce uranium savings even under very optimistic conditions. An N-batch core with a natural uranium blanket has a higher feed requirement than an N + 1

batch core with the oldest batch located on the core periphery.

The Hatch-2 (BWR) design calls for a peripheral row of natural uranium assemblies for the initial core, but switches to older fuel in later cycles. The discharged natural uranium bundles can be used in the first core of other BWRs (C-6). However, it does appear that the natural uranium assemblies cannot compete with spent fuel assemblies. The BWR bundles are only 6" in width, and this implies, but does not prove, that using split assemblies in a PWR, in which only the outer quadrants are natural uranium, would be at a similar disadvantage. Even so, the use of smaller assemblies in PWRs (1/4 the current assembly size) may enable lower peaking factors to be achieved in the core, and better low-leakage fuel management schemes to be developed--schemes that offer lower uranium requirements.

CHAPTER SEVEN

FUEL-TO-MODERATOR RATIO EFFECTS

7.1 Introduction

In this chapter, the effects of spectrum changes brought about by changes in the fuel-to-moderator ratio of the fuel lattice will be examined. The fuel-to-moderator ratio of the Maine Yankee Reactor is optimized with regard to uranium utilization by varying the lattice pitch, and at the optimized pitch, the effects of density changes in the fuel are analyzed. A brief discussion of resonance integrals and annular fuel is included to help clarify some recent contradictory results. Finally, the equations which describe "mechanical spectral shift" techniques are derived, and several cases of theoretical and practical interest are analyzed. By "mechanical spectral shift" we mean any process used to change lattice pitch and/or to displace coolant and thereby vary the fuel-to-moderator ratio. Detailed consideration is not given to the actual means used to implement spectral shift, except that the concepts evaluated correspond to pin pulling and bundle reconstitution. There have been as yet no suggestions of a practical scheme for accomplishing continuous mechanical spectral shift. This option was considered interesting, however, as a limiting hypothetical case. Moreover, the neutronic equivalence of pin pulling with bundle reconstitution and discontinuous mechanical shift (from the standpoint of uranium utilization) is demonstrated in Appendix G.

Similarly, we have not assessed the thermal/hydraulic consequences of these evaluations; in some cases the changes examined are so large as to lead one to expect serious difficulties. However, we are again interested in defining limiting cases.

7.2 Optimization of V_f/V_m for Fixed Lattice Designs

In any reactor design, there are several parameters which can influence the fuel-to-moderator ratio of the core; namely, fuel rod pitch, pellet diameter, fuel density, and the presence of voids in the pellet (annular pellets). The goal is to find the best H/U atom ratio for improving uranium utilization without exceeding the limitations imposed by the moderator temperature coefficient. Calculations by several investigators (B-1, M-1, R-1, M-5) indicate that optimizing the fuel-to-moderator ratio can improve uranium utilization by 1-5%. However, the results are reactor-specific--they depend on the current fuel-to-moderator ratio of the design analyzed. Some reactors may already be operating at or near the optimum conditions, while other lattices may leave considerable margin for improvement. Thus, case-specific uranium savings cannot necessarily be applied across the board to the entire reactor industry.

The fuel-to-moderator ratio of the Maine Yankee reactor (design parameters described in Appendix A) was varied by changing the lattice pitch at fixed fuel pin diameter for a fixed 3.0 w/o initial enrichment. The extrapolated reactivity,

ρ_o, as a function of the hydrogen-to-uranium atom ratio (H/U) is plotted in Fig. 7.1. Fig. 7.2 shows a plot of the slope of the reactivity vs. burnup curve as a function of the H/U atom ratio (i.e., A in $\rho = \rho_o - AB$).

For very wet lattices (H/U >5.0) the slope is much steeper than that at the current operating point (H/U = 4.38). The conversion ratio in this range is lower and thus less plutonium is produced and burned. Drying out the lattice raises the conversion ratio and produces more plutonium thereby increasing the net fissile inventory. The presence of the plutonium prevents the reactivity of the lattice from dropping as rapidly as it does in the wetter cases--the slope is less steep.

The conversion ratio continues to increase as the lattice is made drier. In this regime (H/U <2.5), however, the epithermal/thermal flux ratio is quite high and the effective η ($\nu\Sigma_f/\Sigma_a$) for both U-235 and Pu-239 is reduced. The slope of the reactivity vs. burnup curve ($\frac{d\rho}{dB}$) depends on $d\rho$, which is a function both of the amount of fissile material produced (hence, conversion ratio) and the reactivity worth of that fissile material. Thus, for these very dry lattices, the decreasing reactivity worth of Pu-239 and U-235 exceeds the benefit of increased Pu-239 production.

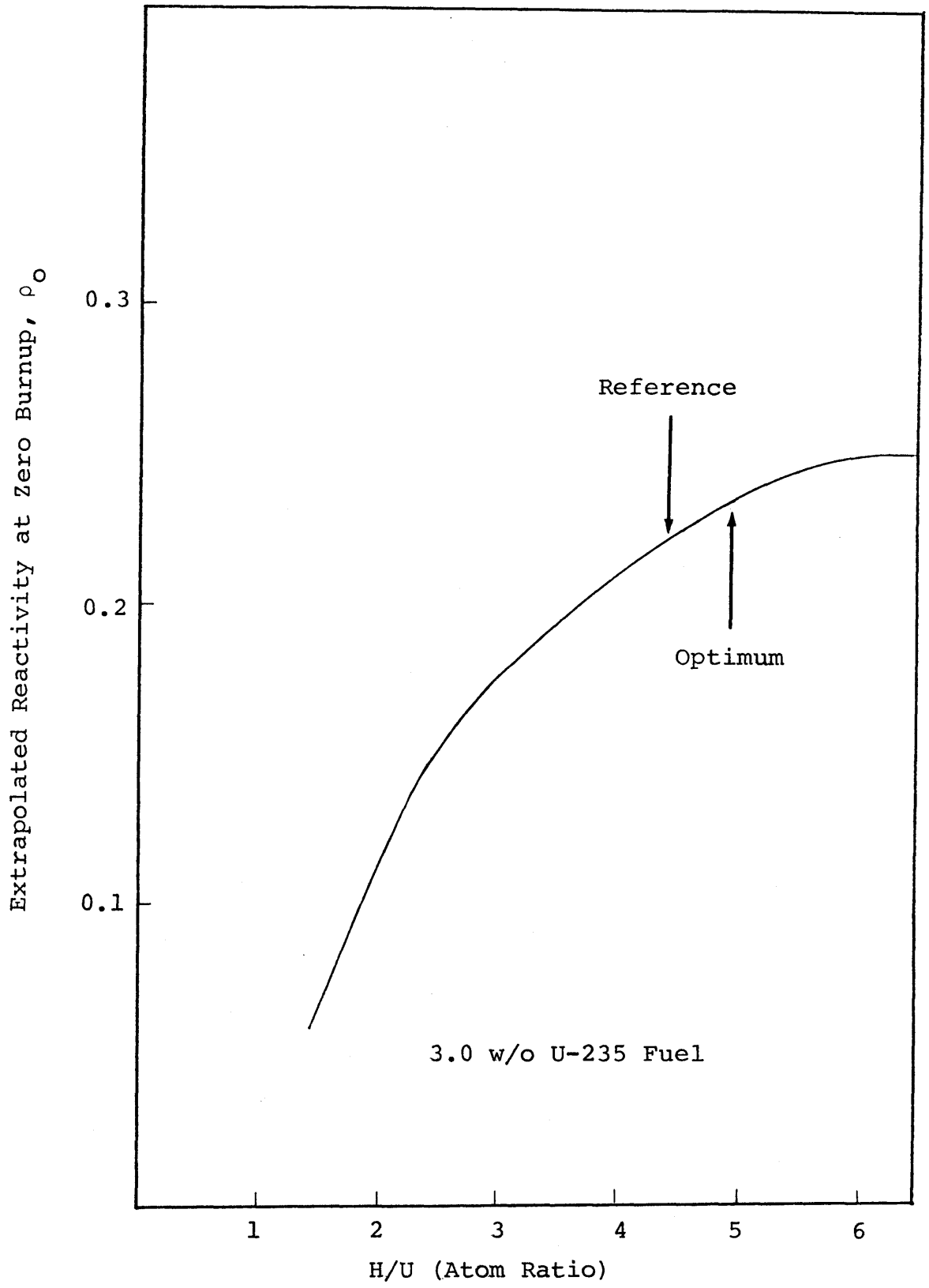

FIG. 7.1 INITIAL EXTRAPOLATED REACTIVITY FOR MAINE YANKEE ASSEMBLIES AS LATTICE PITCH IS VARIED (ε=3.0 w/o)

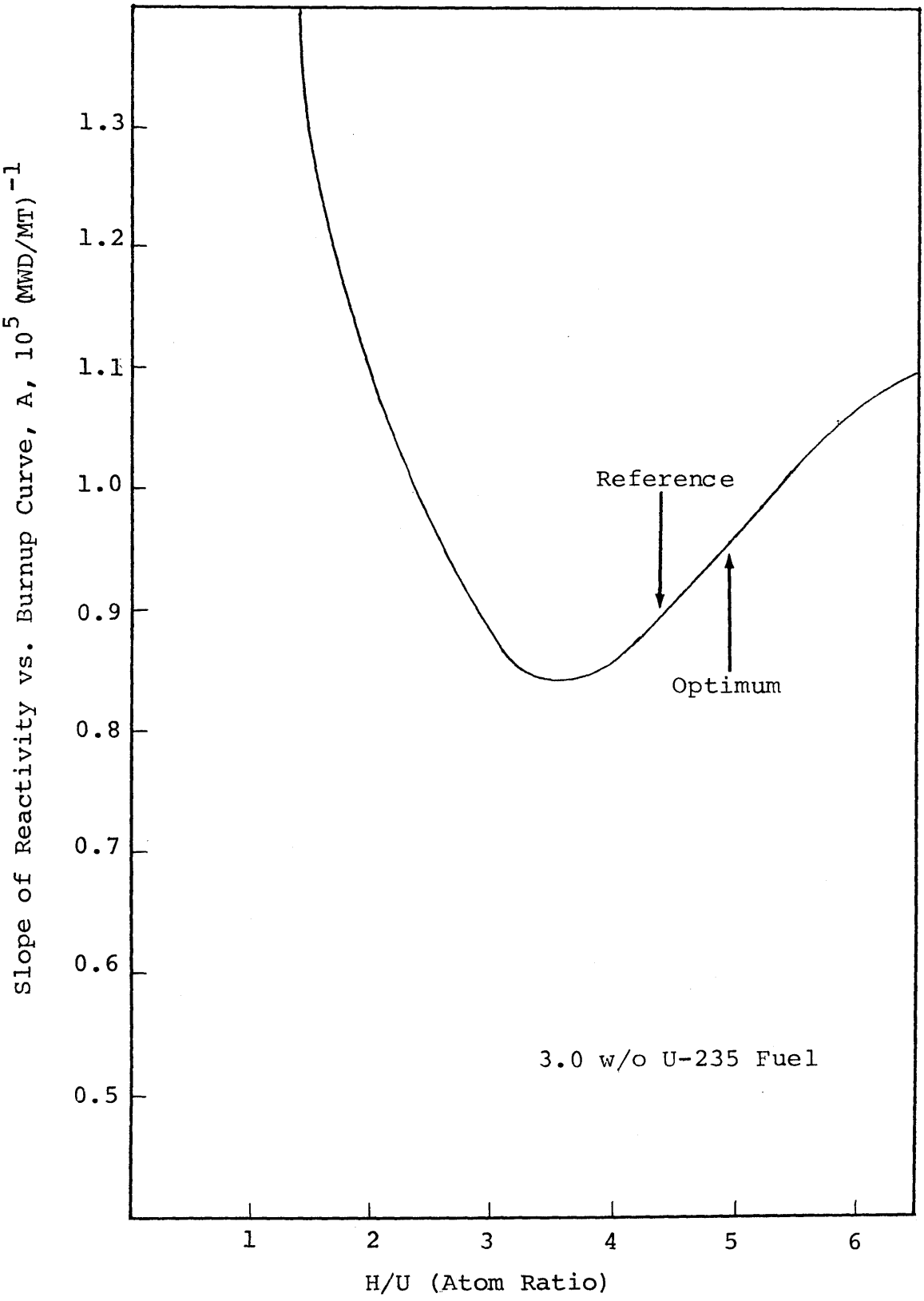

FIG. 7.2 SLOPE OF REACTIVITY VS. BURNUP CURVE FOR MAINE YANKEE ASSEMBLIES AS PITCH IS VARIED (ε=3.0 w/o)

The uranium utilization of the fuel can be written as

$$U\ \left(\frac{MWD}{MTF}\right) = \frac{B_{dis}}{(F/_p)} = \frac{(\rho_o - \rho_L)}{A\ \left(\frac{N+1}{2N}\right)\left(\frac{\varepsilon-0.2}{0.711-0.2}\right)} \qquad (7.1)$$

when equal power sharing among assemblies is assumed. Thus the ratio of ρ_o to A dominates the behavior of uranium utilization. The uranium utilization of the Maine Yankee reactor as a function of H/U is plotted in Fig. 7.3 for conditions of equal power sharing among assemblies, ρ_L = 0.042, and a tails assay of 0.2 w/o U-235. The peak in the uranium utilization curve occurs at 4.85, which is very close to the current assembly operating point (H/U = 4.38) for the Maine Yankee assemblies, and the uranium utilization is not significantly different within this range.

A similar optimization was performed for five batch high discharge burnup fuel (B_{dis} ~50,000 MWD/MT). The curves for extrapolated reactivity (ρ_o), slope (A), and uranium utilization (MWD/MTF) for the 4.34 w/o U-235 lattices as a function of H/U are shown in Figs. 7.4-7.6. The uranium utilization at the current operating point (H/U = 4.38) is 6445 MWD/MTF, whereas at the optimum point on Fig. 7.6 (H/U = ~5.0) the uranium utilization is ~6610 MWD/MTF. This represents a reduction in uranium requirements of about 2.5%, relative to a high burnup lattice operating at the current H/U atom ratio.

It should be noted that for five batch, high burnup cores it may be easier to develop acceptable moderator temperature

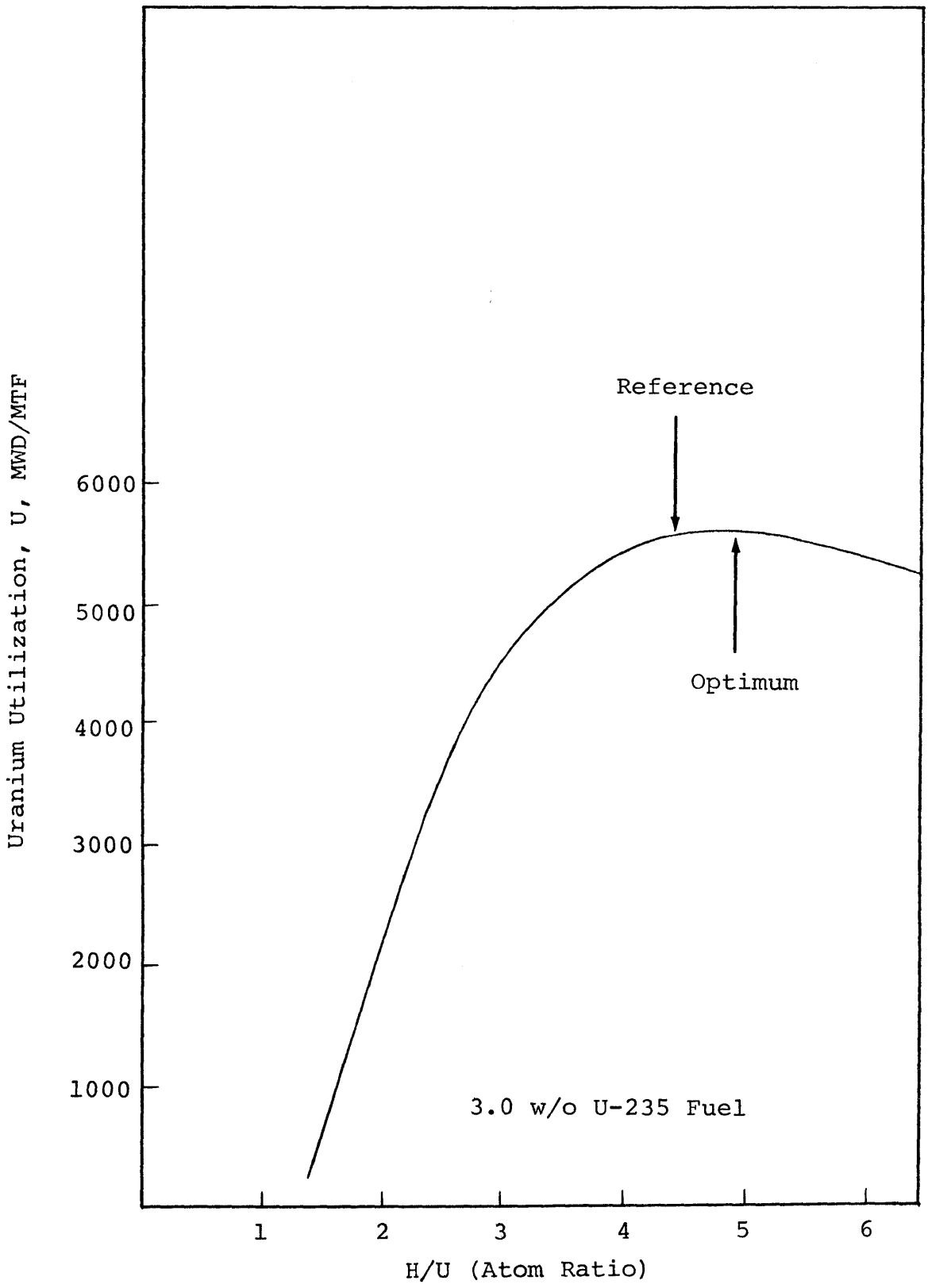

FIG. 7.3 URANIUM UTILIZATION VS. H/U ATOM RATIO FOR MAINE YANKEE ASSEMBLIES AS PITCH IS VARIED (ε=3.0 w/o)

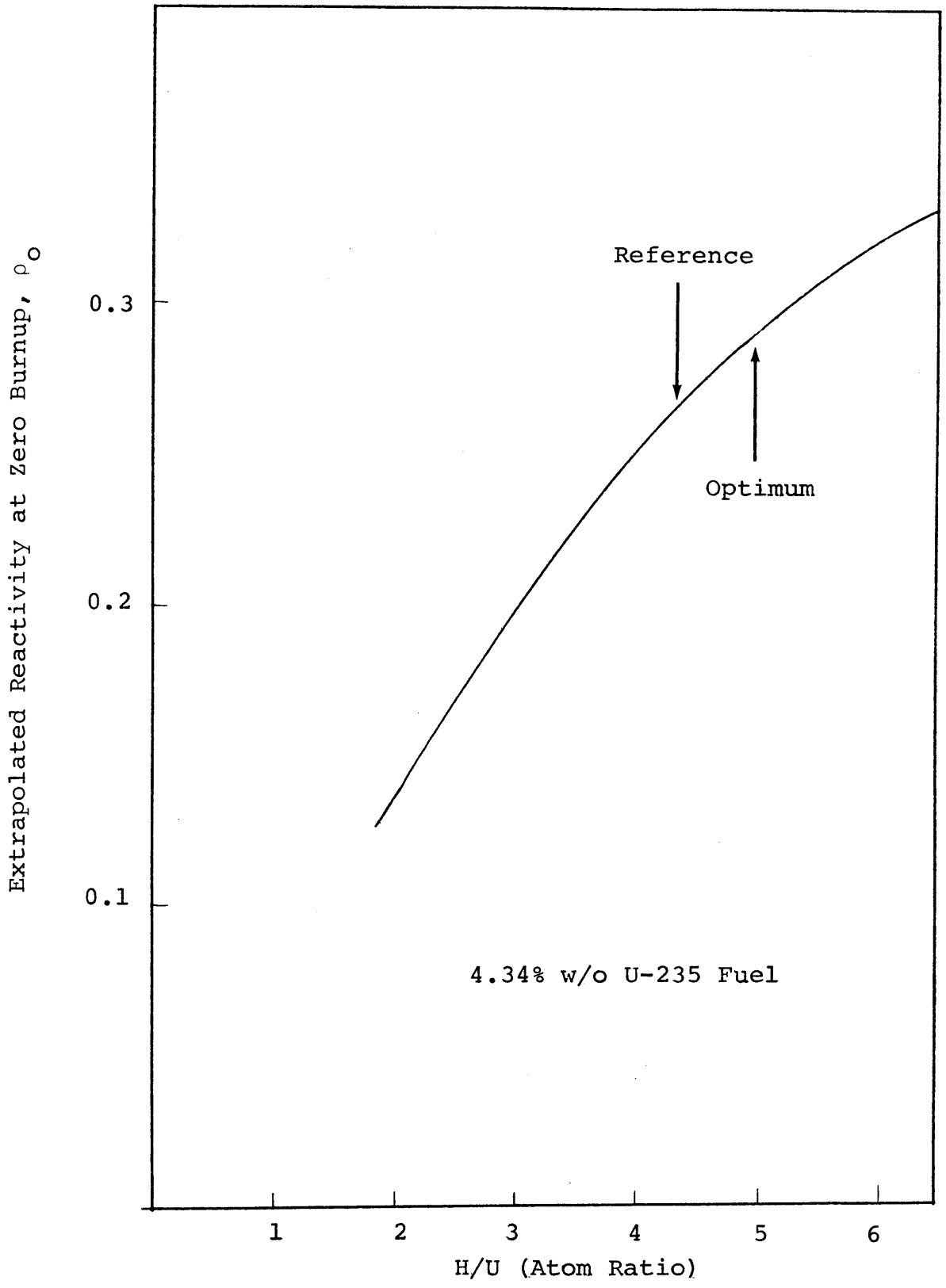

FIG. 7.4 INITIAL EXTRAPOLATED REACTIVITY FOR MAINE YANKEE ASSEMBLIES AS LATTICE PITCH IS VARIED (ε=4.34 w/o)

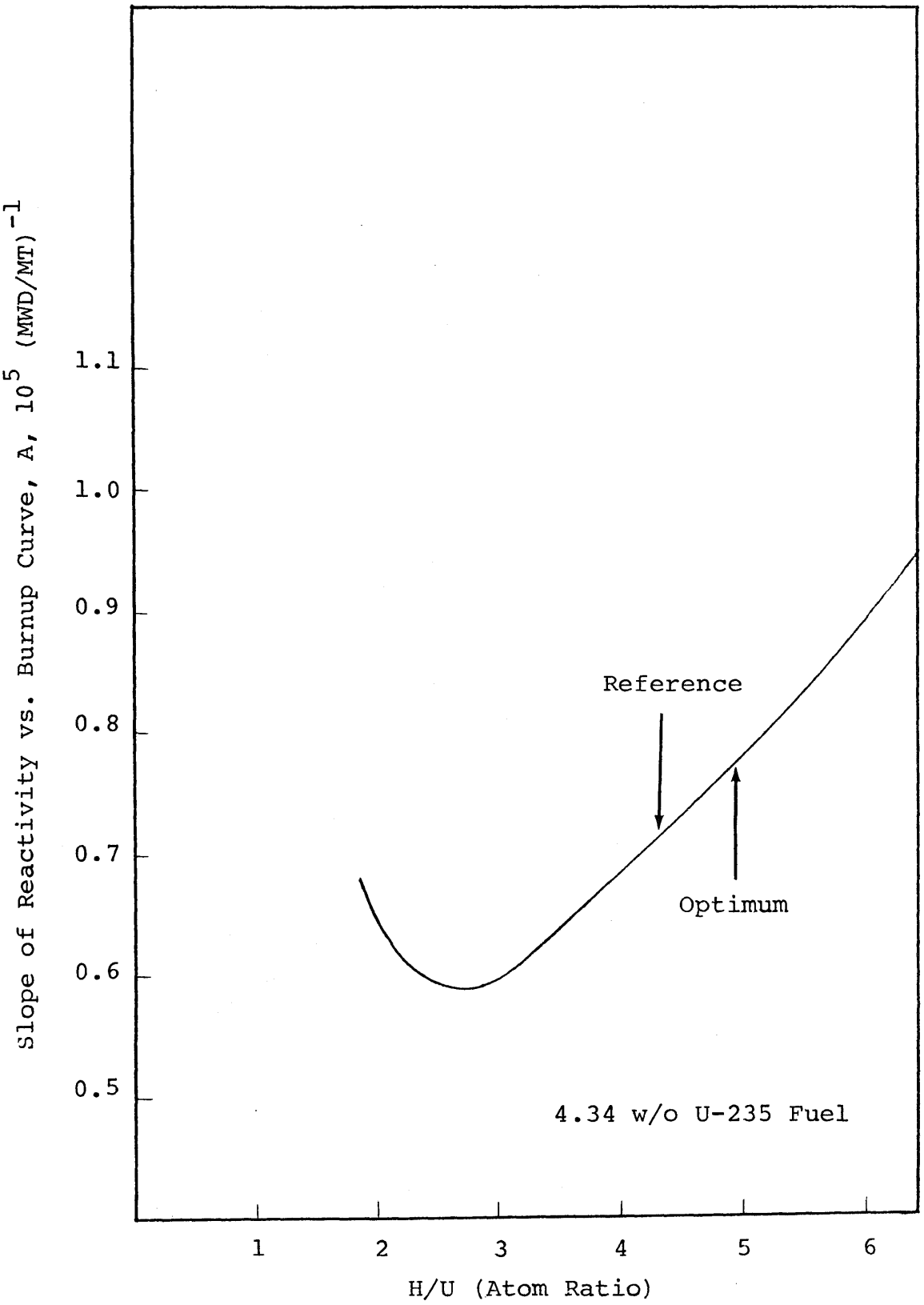

FIG. 7.5 SLOPE OF REACTIVITY VS. BURNUP CURVE FOR MAINE YANKEE ASSEMBLIES AS PITCH IS VARIED (ε=4.34 w/o)

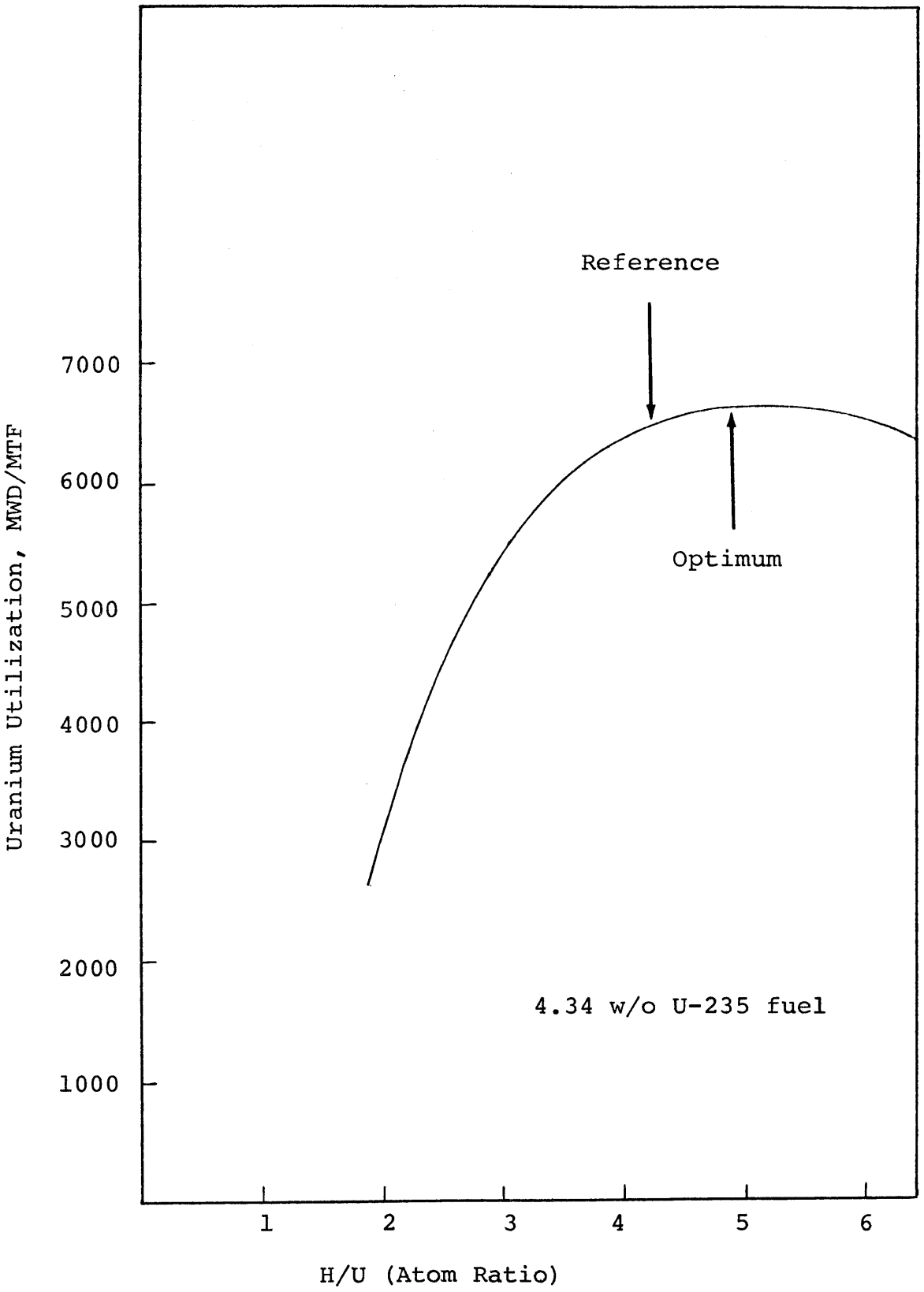

FIG. 7.6 URANIUM UTILIZATION FOR MAINE YANKEE ASSEMBLIES AS PITCH IS VARIED (ε=4.34 w/o)

coefficients (M-1) than for three-batch low burnup cases. Thus, the 2.5% reduction in uranium requirements may be achievable without compromising safety margins associated with the moderator temperature coefficient. These benefits can be achieved provided the H/U atom ratio change can be reached without changing lattice pitch or overall reactor size. It must be recognized that this optimization was performed at a fixed density (ρ = 10.04 g/cc) and fixed pellet radius (R=0.18225").

The resonance integral of the dominant fertile species (e.g., U-238) plays a key role in the optimization of a lattice with respect to uranium utilization. Isolated-pin effective resonance integrals can be correlated in the form (H-4):

$$RI^{28} = C_1 + C_2 \sqrt{S/M} \tag{7.2}$$

where C_1 and C_2 are constants (which vary slightly depending on the nature of the fuel: oxide, metal or carbide), S is the effective surface area of the fuel pellet and M is the mass of U-238 in the pellet. Since the surface area is proportional to $2\pi R_p$ and the mass of U-238 is proportional to $\pi R_p^2 \rho$, the condition for resonance integral equivalence becomes

$$R_p \rho = \text{constant} \tag{7.3}$$

In practice the situation is more complicated: for example, Dancoff shadowing reduces the effective pin diameter in a tightly-packed lattice. However changes from case to case in the range of practical interest are small. In other words, Eqs. 7.2 and 7.3 can only be used to find the approximate neighborhood of an equivalent set of lattices; the free parameters can then be perturbed until a better match is evidenced

in state-of-the-art computations. Fig. 7.7 shows the relative uranium utilization vs. H/U atom ratio for three cases:

ρ = 9.30 g/cc; R_p = 0.20323", ρ = 10.04 g/cc; R_p=0.18823",

ρ = 10.95 g/cc; R_p = 0.17261"

For these cases, $\sqrt{S/M}$ is a constant and, as can be seen from the figure the uranium utilization is, to first order, nearly identical. Differences are less than one percent in the range of interest before any fine tuning. Thus, it appears that a specification of H/U atom ratio and resonance integral is all that is required to determine uranium utilization, inasmuch as their specification determines the value of ρ_o and A.

It should be recognized, however, that the optimizations shown in Figs. 7.6 and 7.7 were H/U atom ratio optimizations at a fixed value of $\sqrt{S/M}$. A full scope optimization would require a determination of the uranium utilization as a function of both H/U atom ratio and $\sqrt{S/M}$ (for both low burnup and high burnup cases). It is possible that an overall maximum on this three-dimensional surface may occur at an H/U atom ratio and $\sqrt{S/M}$ value different from that shown in Fig. 7.17. If a maximum does exist (and can satisfy the conditions necessary for negative moderator coefficient operation at that point) it may provide additional improvements in uranium utilization.

7.3 Annular Fuel

The use of annular fuel has been proposed as a means to achieve improved uranium utilization, in that it would facilitate higher burnup by allowing more space for fission product gases, and by permitting the fuel to run cooler--thereby

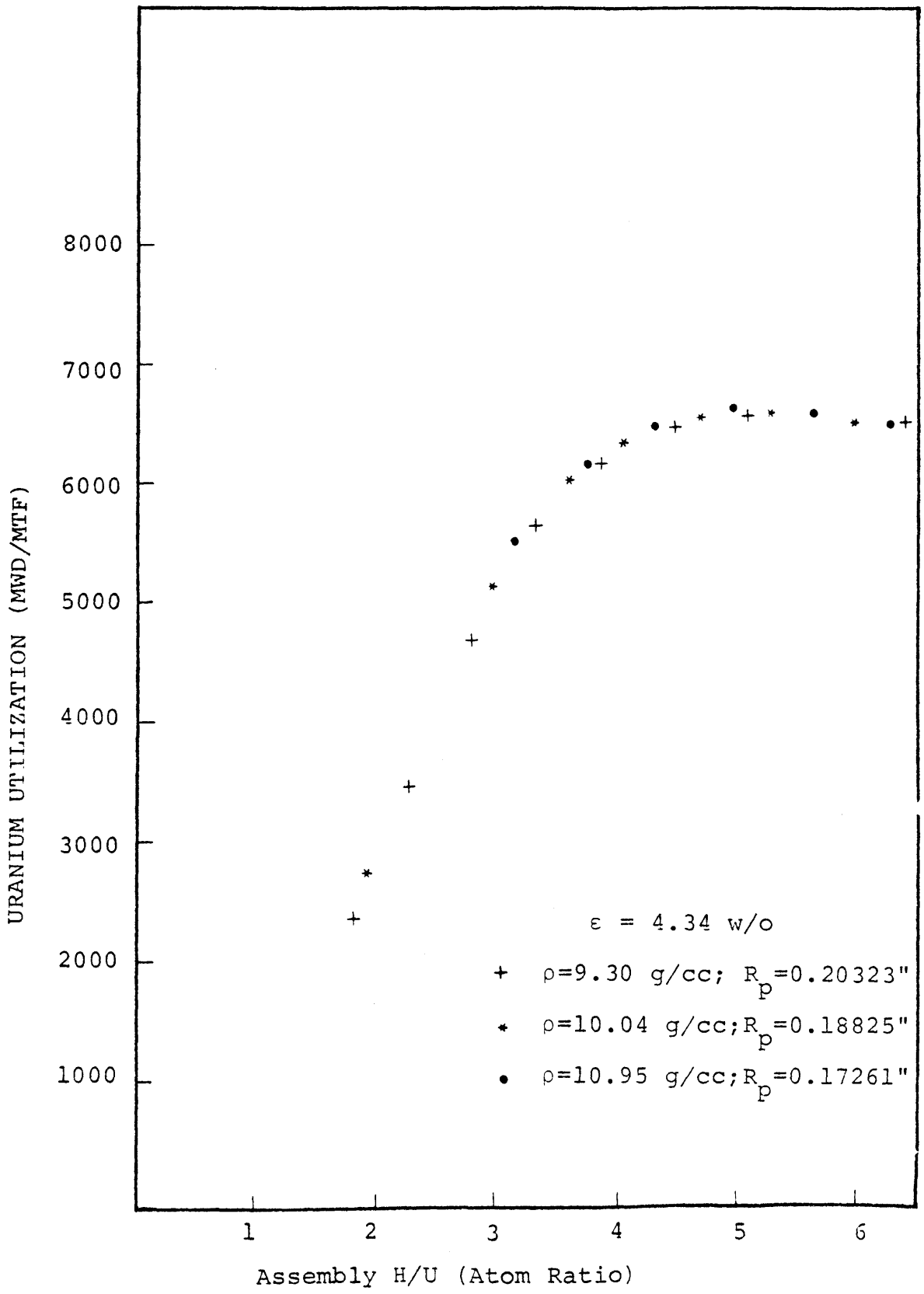

FIG. 7.7 URANIUM UTILIZATION VS. H/U ATOM RATIO FOR LATTICES WITH EQUIVALENT RESONANCE INTEGRALS

reducing fission product gas release from the UO_2 matrix. Whether or not this is accompanied by inherent physics advantages or disadvantages is still a matter of debate (B-1, M-4, M-5).

Monte Carlo calculations carried out at B&W (B-1) have indicated that at 12% annular voids the use of reduced, uniform pellet smear density to simulate the annular fuel is satisfactory (see Fig. 7.8). Fortunately this is close to the optimum performance point identified by B&W from both a thermal-mechanical and neutronic/economic standpoint. We have therefore used reduced homogeneous pellet smear density to evaluate the use of fuel having a 10% annular void. The most important finding is that the results are sensitive to where one starts and ends the optimization as regards the lattice H/U ratio. Table 7.1 summarizes the results for low burnup. As can be seen LEOPARD pin cell calculations show a slight advantage, while the wetter supercell calculations do not. Wetter pin cells than shown here also exhibited no advantage.

Table 7.2 shows the effects of density changes in uranium utilization for high burnup (ε=4.34 w/o) fuel. It can be seen from the table that a density change at a fixed pellet radius not only changes $\sqrt{\frac{S}{M}}$ but also changes the H/U atom ratio, moving it away from the local optimum defined in Section 7.2.

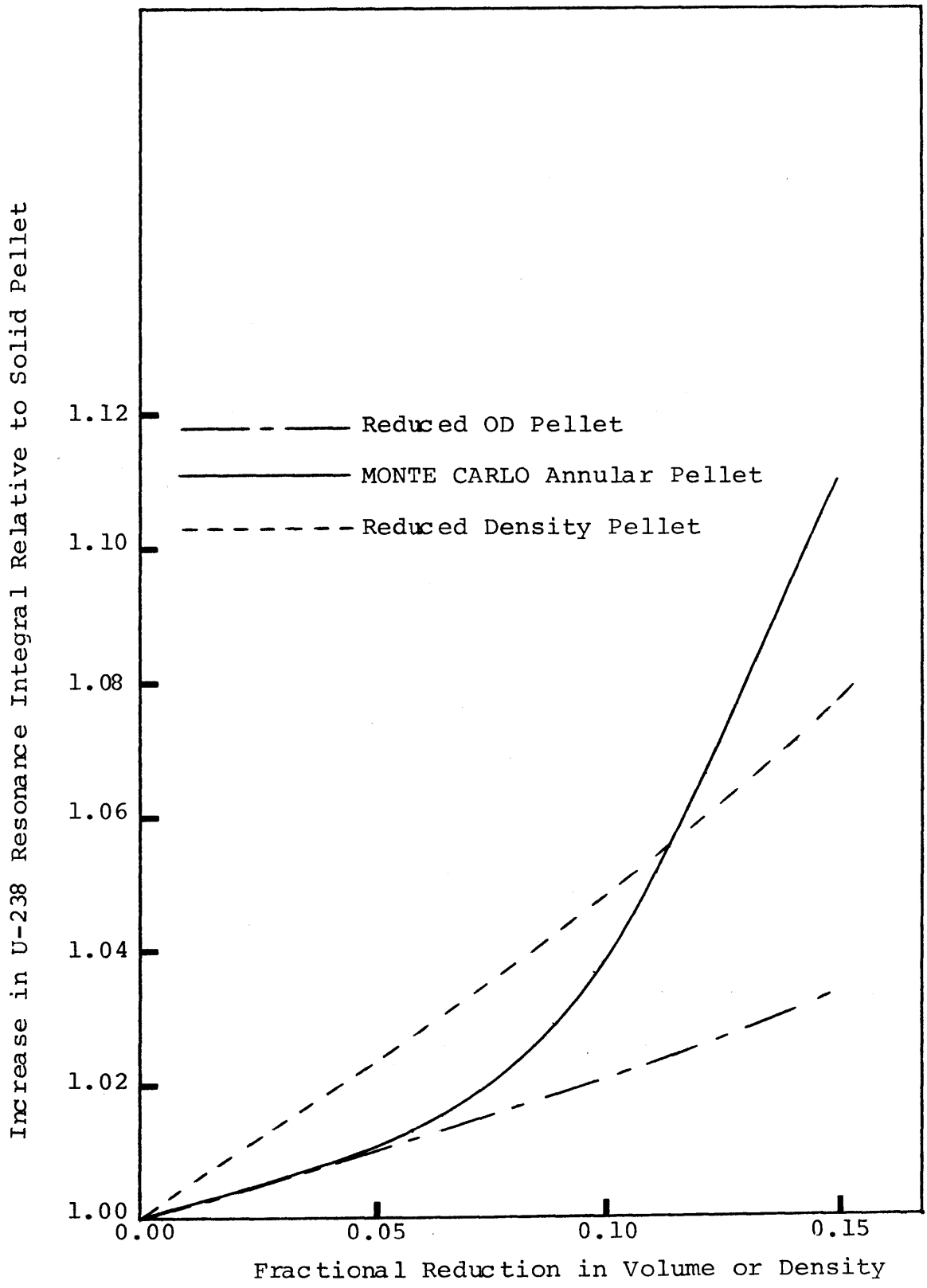

FIG. 7.8 CHANGE IN RESONANCE INTEGRAL AS A FUNCTION OF REDUCTION IN HEAVY METAL CONTENT (B-1)

TABLE 7.1 EVALUATION OF ANNULAR FUEL

Density (g/cc)	Enrichment (w/o U-235)	Core H/U Atom Ratio (HOT,BOL)	MWD MT NAT U FEED
Leopard Pin Cells			
10.43	2.89	3.448	5129
10.04	3.00	3.582	5217
9.40**	3.19	3.826	5347
9.18	3.30	3.918	5398
Leopard Super Cells			
10.43	2.89	4.166	5542
10.04*	3.00	4.381	5540
9.40**	3.19	4.622	5539
9.18	3.30	4.733	5549
Adjusted Super Cells			
10.43	2.89	4.310	5539
10.04	3.00	4.381	5540
9.40**	3.19	4.358	5539
9.18	3.30	4.356	5545

* Maine Yankee Reference Case

** Simulates fuel having a 10% annular void.

TABLE 7.2 EFFECTS OF FUEL DENSITY CHANGES ON URANIUM UTILIZATION FOR HIGH BURNUP FUEL (ϵ = 4.34 w/o U-235)

Density (g/cc)	$\sqrt{S/M}$ $(cm^2/g)^{1/2}$	H/U (atom ratio)	Uranium Utilization (MWD/MTF)
10.95	0.9850	4.49	6540
10.40	1.0107	4.72	6557
10.04	1.0287	4.89	6590
9.80	1.0412	5.01	6557
9.30	1.0688	5.28	6540

The effect of the decrease in the average pellet temperature associated with the use of annular fuel was estimated. To accentuate the effect, the effective resonance temperature was reduced from 1232°F to 700°F in a LEOPARD supercell case. The burnup results indicated a potential reduction in uranium requirements of 0.86% for this extreme temperature perturbation. A realistic reduction would be on the order of 20-50°F depending on design, and thus, the uranium savings would be about 0.03%-0.08% or about 0.00162 %/°F. To first order, this effect is clearly negligible, particularly since a small change in fuel density or radius can produce comparable effects in non-annular fuel. Thus, we conclude that annular fuel offers no inherent neutronic advantage per se: improvements should be attributed to the concurrent change in S/M and fuel-to-moderator ratio: changes which can also be implemented by other means.

The B&W results shown in Fig. 7.8 might be interpreted to imply that annular fuel enables one to operate at a given H/U ratio with a U-238 resonance integral not achievable by density reduction or fuel rod diameter changes. Fig. 7.9 shows the change in the relative U-238 resonance integral as a function of the fractional reduction in uranium content produced by changes in rod diameter, fuel density, and combinations of the two. It can be seen from the figure that between the bounding curve of fixed density-variable radius (ρ=10.04 g/cc) and fixed radius-variable density (R_p= 0.18824")

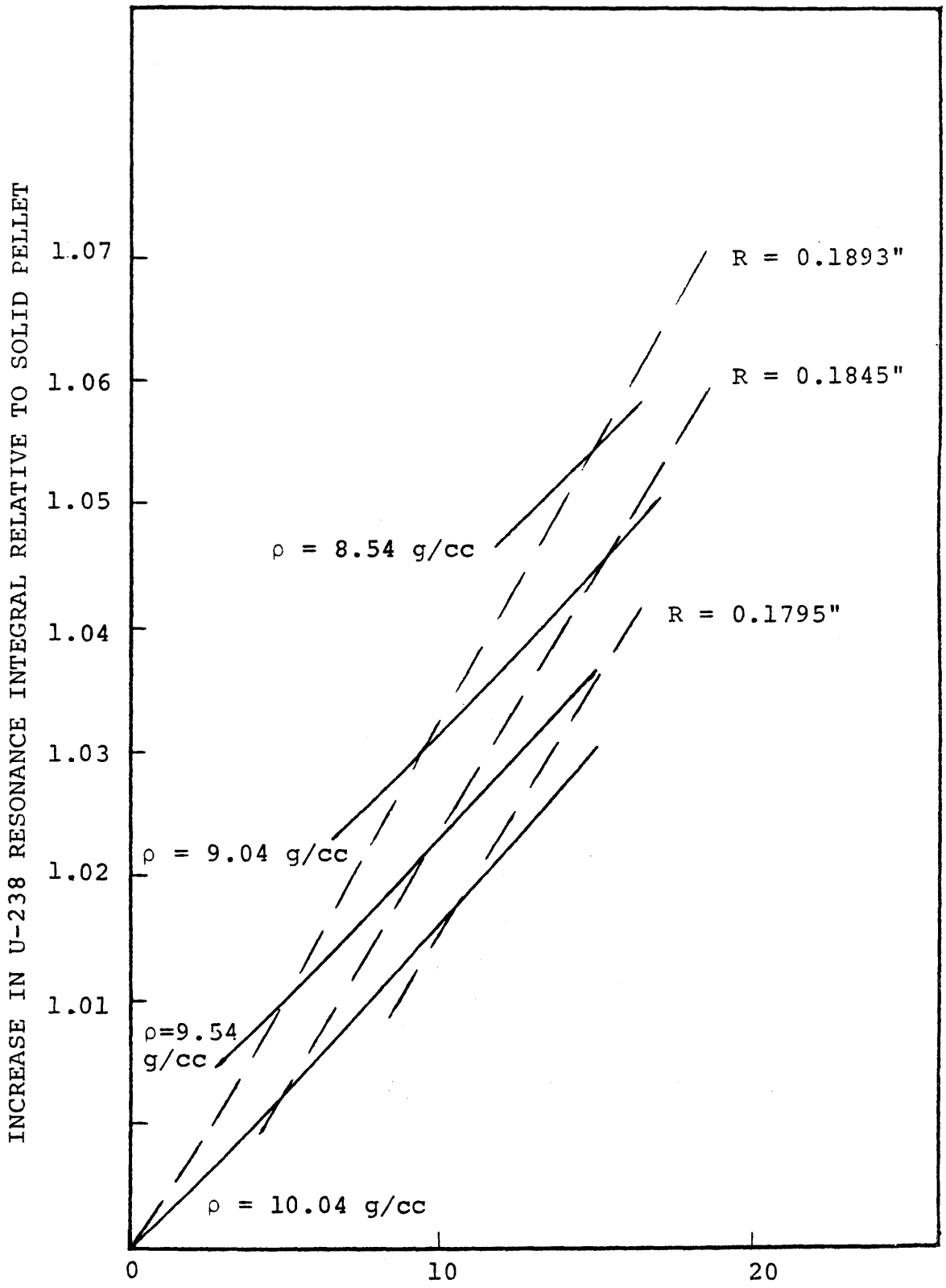

FIG. 7.9 RELATIVE U-238 RESONANCE INTEGRAL FOR VARIOUS CHANGES IN PIN DIAMETER AND FUEL DENSITY

any value of the resonance integral within the area can be produced by some combination of rod radius and fuel density (at a given H/U ratio); or, more simply, for any annular fuel design, at a given H/U atom ratio, it is possible to define a neutronically equivalent solid pellet, at the same H/U atom ratio, by manipulating the rod diameter and fuel density.

Despite this fact, there are several possible advantages to annular fuel:

1) The presence of the void offers a compliance volume for increased fission gas production at high burnups, and the cooler fuel releases less gas in the first place.

2) The use of annular fuel may offer a convenient method for reaching a specific H/U ratio without changing rod diameter or lattice pitch, an option which preserves the basic assembly thermal/hydraulic design, which can represent a substantial savings in redesign costs.

3) Annular fuel may be mechanically superior to solid fuel in terms of pellet-clad interactions.

4) There is less stored energy in the fuel and hence it becomes easier to satisfy the ECCS/LOCA (Appendix K) limits.

7.4 Variable Hydrogen/Uranium Atom Ratio

Current pressurized water reactors are designed and the fuel is managed to provide a certain amount of excess reactivity in the core at the beginning of a burnup cycle. This excess reactivity is compensated by soluble boron poison

dissolved in the H_2O moderator. All variable fuel-to-moderator ratio schemes, whether they involve using D_2O in variable amounts to change the H/U atom ratio, or a mechanical movement of the fuel to reduce the effective fuel-to-moderator (and thereby H/U) ratio, are designed to minimize the use of control poison.

At low H/U atom ratios, the fast-to-thermal flux ratio (ϕ_1/ϕ_2) is much higher than that encountered under current PWR operating conditions. As a result, the relative absorption in U-238 is much higher, and the fuel reactivity is decreased. In a sense, these "spectral shift" concepts really trade boron poison for U-238 "poison". The benefit in the spectral shift concept, however, is that the neutron is not lost--the neutron captured in U-238 forms Pu-239, which is fissile. The optimum H/U ratio for a plutonium lattice is even higher than that for a U-235 lattice so that a subsequent "softening" of the spectrum (by increasing the H/U ratio) as the fuel burnup increases, can improve the net uranium utilization of the fuel. The spectral shift concepts have higher conversion ratios (more Pu-239 produced) and potentially better utilization of that plutonium to sustain burnup reactivity lifetime.

Since spectral shift concepts involve eliminating boron control poison, it is useful to examine the maximum theoretical improvement possible if this were accomplished. Recall that the reactivity of a fuel assembly can be accurately

represented by the linear relation

$$\rho = \rho_o - AB \tag{7.4}$$

where ρ_o is the extrapolated initial reactivity, A is the slope of the reactivity vs. burnup curve $(\frac{MWD}{MT})^{-1}$, and B is the burnup of the assembly $(\frac{MWD}{MT})$. The slope of the reactivity vs. burnup curve is really the sum of two components:

1) a fission product component which accounts for the essentially linear increase in fission product content with burnup, and

2) a fissile burnup component which accounts for the net decrease in the fissile material inventory with burnup.

Thus, the reactivity of a fuel assembly can be written as:

$$\rho = \rho_o - A_{FP}\, B - A_{burn}\, B \tag{7.5}$$

where A_{FP} is the component of the slope caused by fission product buildup, A_{burn} is the component of the slope caused by fissile inventory decrease, and A_{burn} plus A_{FP} equals A. Results from LEOPARD supercell calculations run with full fission product inventories and with zero fission product inventories give:

$$\rho_o = 0.220804$$

$$A_{total} = 0.89242 \times 10^{-5}\ (\frac{MWD}{MT})^{-1}$$

$$A_{FP} = 0.55385 \times 10^{-5}\ (\frac{MWD}{MT})^{-1}$$

$$A_{burn} = 0.33857 \times 10^{-5}\ (\frac{MWD}{MT})^{-1}$$

for a 3.0 w/o U-235 initial enrichment. The discharge burnup of the fuel can now be written as:

$$B_{dis} = \frac{\rho_o - \rho_L}{A_{FP}\left(\frac{N+1}{2N}\right) + A_{burn}\left(\frac{N+1}{2N}\right)} \tag{7.6}$$

where N is the number of in-core batches, ρ_L is the leakage reactivity, and equal power sharing among assemblies has been assumed. For the case of on-line refueling ($N = \infty$) boron is not necessary because the excess reactivity of the freshest fuel is balanced by the reactivity deficit of the oldest fuel. Neutrons are shared internally among fuel assemblies and none are lost to boron. Such neutron sharing can be imitated by absorbing neutrons in U-238 to form Pu-239 and subsequently burning the Pu-239 later in life. The neutron is, in a sense, "stored" until it is needed. For N-batch cores ($N < \infty$) with optimal spectral shift (no boron absorptions) the discharge burnup can be estimated by taking the continuously renewed fuel burnup limit of Eq. 7.6:

$$B_{dis} = \frac{\rho_o - \rho_L}{A_{FP}\left(\frac{N+1}{2N}\right) + A_{burn}\left(\frac{\infty+1}{2\infty}\right)}$$

$$= \frac{\rho_o - \rho_L}{A_{FP}\left(\frac{N+1}{2N}\right) + \frac{1}{2}A_{burn}} \tag{7.7}$$

Table 7.3 lists the estimated discharge burnups for normal boron poison control and spectral shift control, and the uranium requirement benefit as a function of the number of in-core batches for a fixed radial and axial leakage of 0.042.

TABLE 7.3 ESTIMATED THEORETICAL BENEFITS OF OPTIMIZED SPECTRAL SHIFT CONTROL AS A FUNCTION OF THE NUMBER OF BATCHES

Number of Batches	Normal Burnup (MWD/MT)	Spectral Shift Burnup Fission Product N = N Fuel Burnup N = ∞ (MWD/MT)	Percent Decrease in Uranium Requirement
1	20044	29050	31.1
2	26726	33682	21.7
3	30067	35573	15.5
4	32071	36600	12.4
5	33407	37246	10.3
10	36444	38607	5.6
∞	40088	40088	0.0

The relative benefits of spectral shift control decrease as the number of staggered fuel reload batches increases. Boron control requirements are lower for an increased number of batches, thus, elimination of boron has a correspondingly reduced advantage.

The LEOPARD code contains an option which permits one to progressively vary the D_2O to H_2O ratio in a unit cell burnup calculation. A slight modification to the code was made to permit the inclusion of voids (instead of D_2O) in the H_2O moderator. Thus, mechanical spectral shift concepts could be evaluated without the complication of D_2O scattering and moderation. The case of single-batch fuel management, no leakage, and continuous mechanical spectral shift was considered. The void content input into LEOPARD was adjusted such that the unit cell was held just critical at all points. Eq. 7.5 (applied to the reference supercell) predicts a discharge burnup of 34473 MWD/MT (for zero leakage), whereas the LEOPARD results using the continuous spectral shift technique, show a discharge burnup (for zero leakage) of about 34270 MWD/MT for a return to the same (BOL) H/U ratio (4.38) as the reference supercell. Further increases in H/U atom ratio (H/U >4.38) will increase the reactivity of the lattice and extend the burnup of the single batch case by

(approximately) an additional 2500 MWD/MT. There are several points which must be noted regarding these results:

1) The optimum H/U atom ratio of the fuel is a burnup-dependent function which also depends on the time-dependent path that the lattice takes in H/U "phase space".

2) The fission products will, in general, have a different reactivity worth in the spectral shift cases relative to the fixed H/U designs. This raises some question as to the applicable value of A_{FP} in Eq. 7.5. Perhaps determination of A_{FP} at some cycle-average, or endpoint H/U atom ratio would be more appropriate.

3) A continuous spectral shift applied to high discharge burnup fuels (high initial enrichment) would produce more plutonium and may yield better uranium savings.

4) The accuracy of the LEOPARD results are open to question for very dry lattices (C-1).

Based on these considerations, the results of Table 7.3 should be considered to be at least slightly optimistic with respect to the predicted physics benefits. Engineering constraints present additional problems:

1) Accomplishing the single-batch spectral shift described via mechanical means would probably be impractical from a thermal/hydraulic standpoint in current reactor designs because of the attendant degradation in heat transfer conditions for the farthest off-design configurations.

2) Many concepts which might permit a continuously variable fuel-to-moderator ratio would probably introduce safety

problems because of the possibility of accidental reactivity insertions.

3) The more practicable mechanical spectral shift techniques would require extensive manual fuel assembly adjustments during refueling outages and would therefore be noncontinuous in nature. The introduction of such "discretization" would certainly reduce the maximum achievable benefits of spectral shift. Thus, Table 7.3 should be considered extremely optimistic with respect to thermal/hydraulic and mechanical considerations.

7.5 H/U Atom Ratio Changes During Refueling

Various schemes have been proposed for accomplishing mechanical spectral shift in PWRs; most involve pulling pins from assemblies to produce "wetter" lattices and the formation of new assemblies from the pins that were removed (R-1). Figure 7.10 shows one such scheme. Fresh fuel is loaded (53 assemblies with 264 pins/assembly) in a reactor with 193 assemblies. After cycle one, during the refueling interval, 64 pins are pulled from each fresh assembly and 17 additional fuel assemblies are manufactured. Thus, the cycle two fuel is "wetter" than the cycle one fuel, and there are more assemblies of type two fuel than there are of type one fuel. From a neutronic standpoint, the same type of "dry-wet" spectral shift can be accomplished by the scheme shown in Fig. 7.11. In this scheme, the cycle one fuel operates at the same H/U atom ratio as the cycle one fuel of the previous

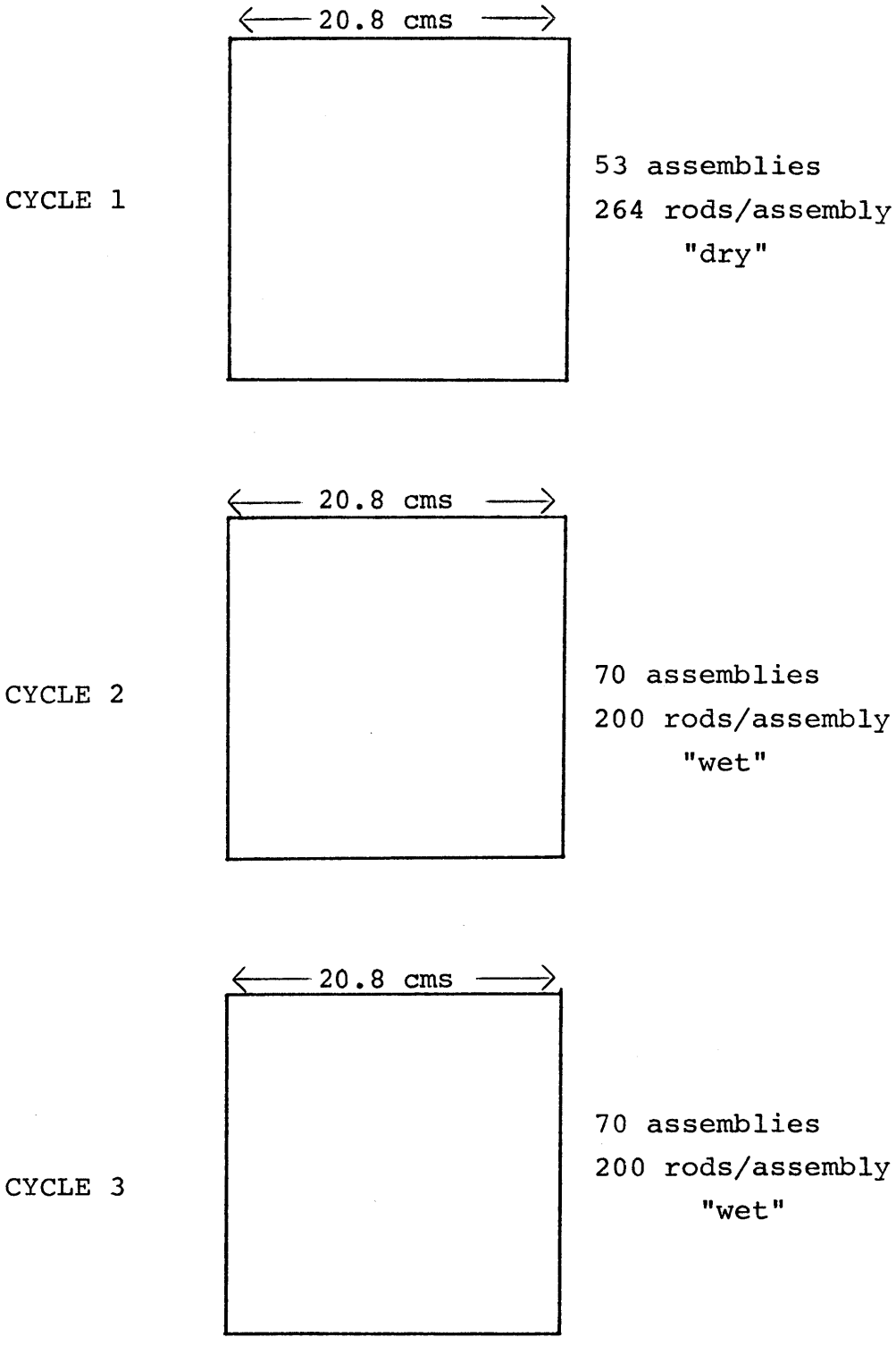

FIG. 7.10 LATTICE SPECTRAL SHIFT SCHEME USING PIN-PULLING AND BUNDLE RECONSTITUTION

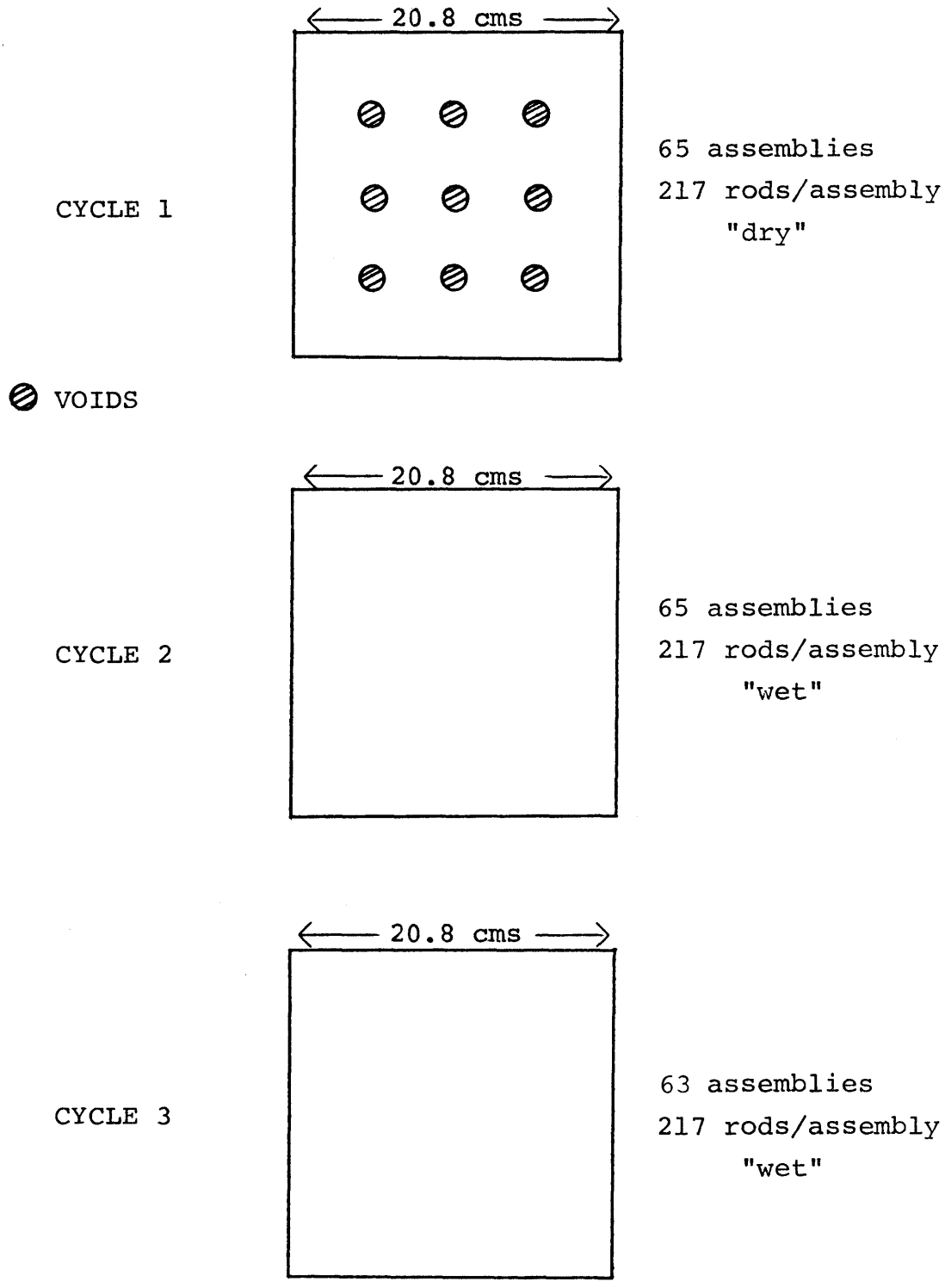

FIG. 7.11 LATTICE SPECTRAL SHIFT SCHEME USING "VOID" INCLUSION IN CYCLE ONE ASSEMBLIES

scheme, but the same H/U atom ratio is produced by introducing voids into the coolant (in some unspecified fashion). At the refueling interval, the voids are removed and the lattice is as wet as the type two fuel from the previous scheme. In this scheme, the number of pins per assembly and the number of assemblies per batch remains constant.

It is shown in Appendix G that in terms of the uranium utilization, these two schemes are absolutely equivalent. However, it is easier to calculate the optimum uranium savings for the scheme shown in Fig. 7.11 since the complications associated with feed adjustments and power sharing become more transparent for this evaluation. The unit cell calculations were made with LEOPARD, using the variable void option programmed into the code (as discussed in Appendix B). (It is not clear that such a variable void scheme could ever be practical). Lattice modifications must be made during refuelings and the time between refuelings must remain sufficiently long that the overall capacity factor is not adversely affected. The fact that the lattice modifications remain fixed during the cycle reduces the flexibility (and potential benefits) of this scheme. Two types of fuel management scenarios have been developed for mechanical spectral shift concepts (R-1). In Concept 1, the fresh fuel lattice is drier than the reference case at the beginning of a cycle and the reactor is run until it reaches criticality with no boron present. The oldest fuel batch is discharged, fresh fuel is loaded, and the lattice modifications are made to the once burned fuel.

In Concept 2, the fresh fuel is drier than the reference case at beginning-of-cycle and the reactor is run until it reaches criticality with no boron present. The reactor head is removed and lattice modifications are made to the freshest fuel (which inserts reactivity) without discharging the oldest fuel batch. The vessel is then closed and the reactor is restarted and run until the extra reactivity insertion is burned out.

The reactivity vs. burnup curves for the procedures of interest are diagrammed in Figs. 7.12-7.14. The first figure represents normal three batch fuel management. Batches 1-3 start irradiation at points A_1, A_2 and A_3, and complete irradiation at EOC at points B_1, B_2 and B_3. Concept 1 is illustrated in Fig. 7.13. The batches begin irradiation at points C_1, C_2, and C_3 and end irradiation at D_1, D_2 and D_3. During the refueling outage batch three is discharged and the lattice of batch one (which becomes batch two in the new cycle) is adjusted such that reactivity is inserted. The reactivity change ($\Delta\rho$) is given by

$$\Delta\rho = \rho(C_2) - \rho(D_1) \tag{7.8}$$

It is important to recognize that in normal (non-spectral shift, fixed lattice) fuel management the reactivity was considered a "state function" or "state vector function" of the burnup. However, for spectral shift designs the reactivity is now a path-dependent function, i.e. the reactivity at any point depends not only on the burnup but also on the path

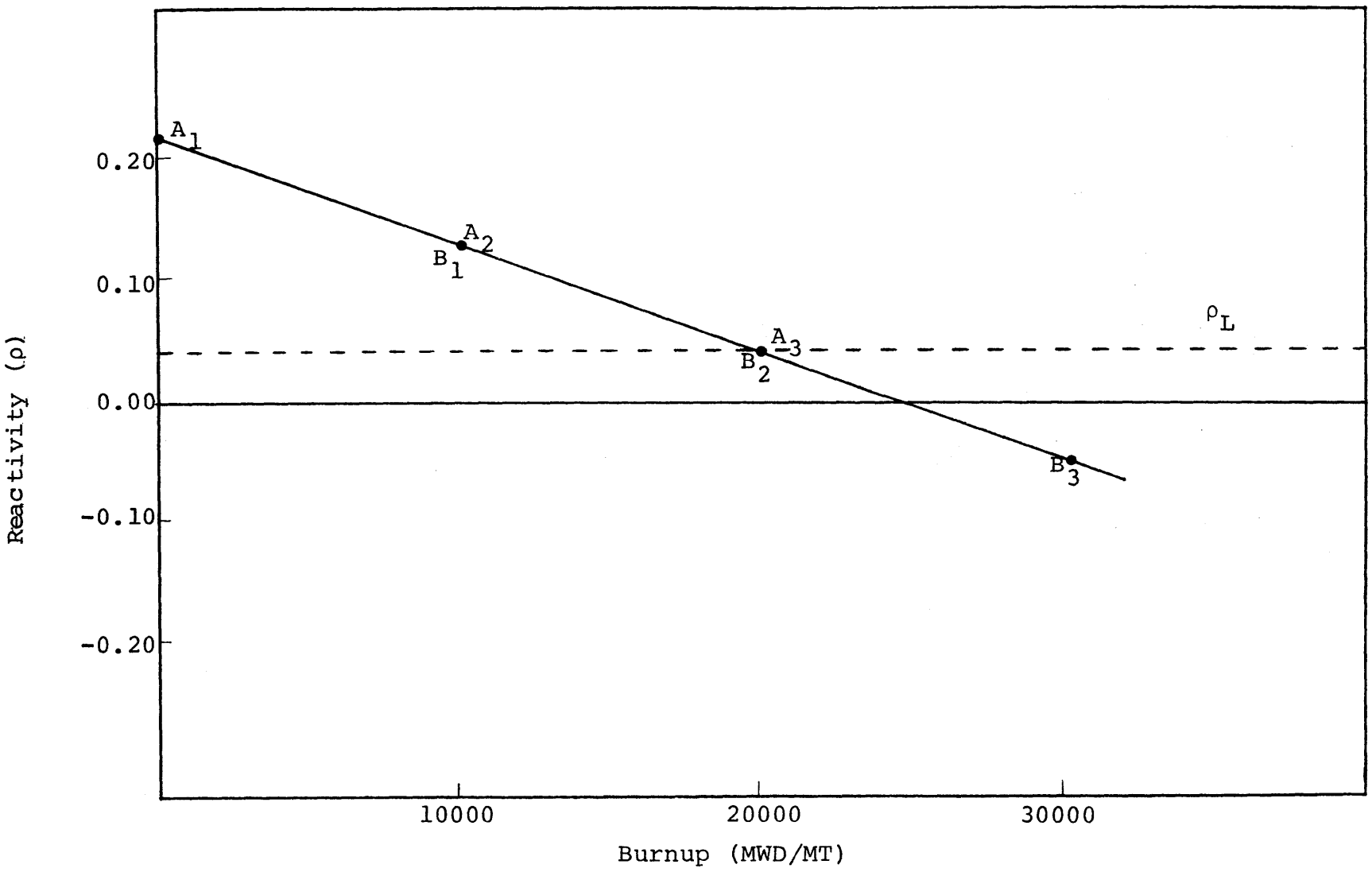

FIG. 7.12 REACTIVITY VS. BURNUP FOR CONVENTIONAL THREE BATCH FUEL MANAGEMENT

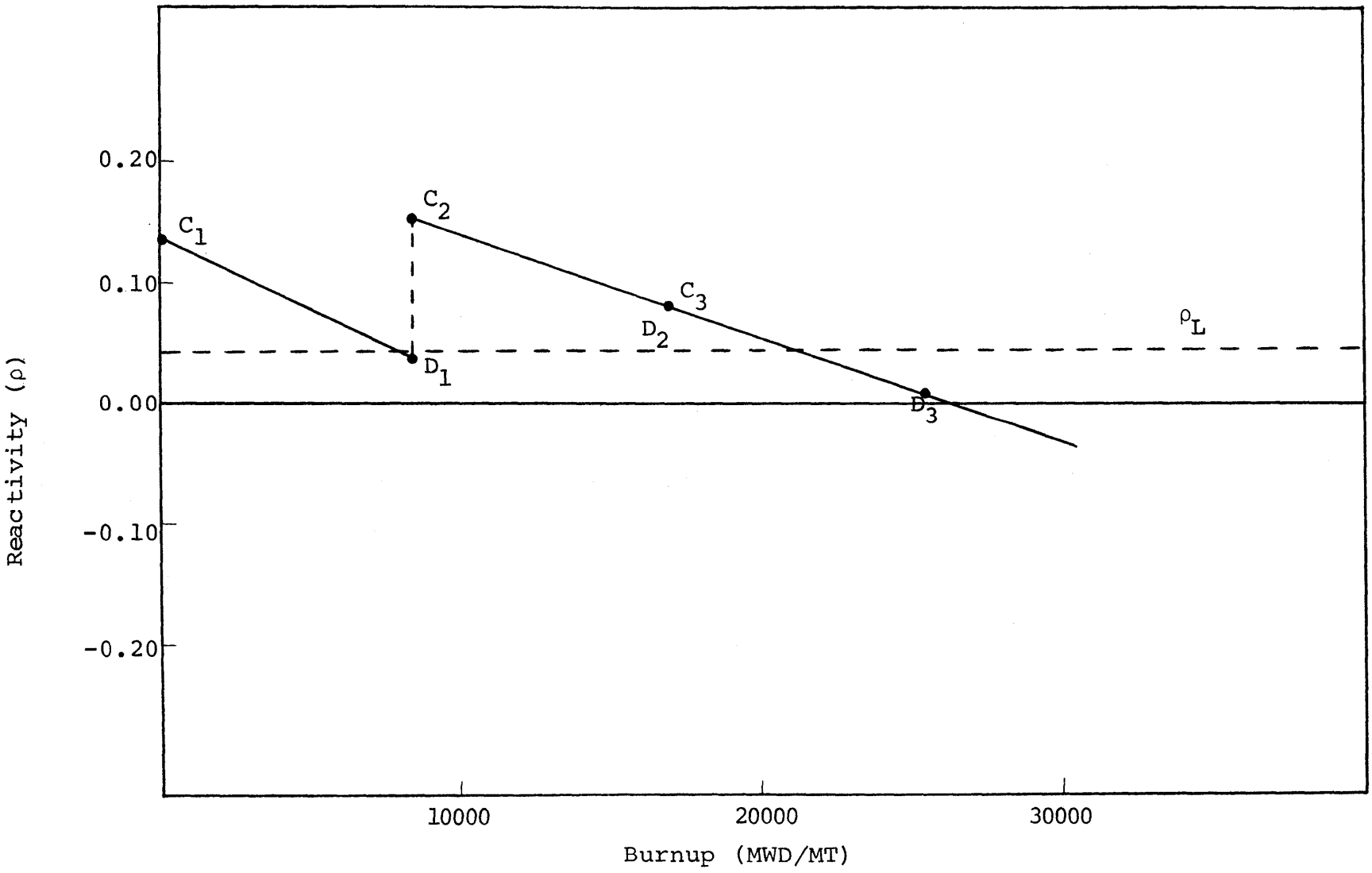

FIG. 7.13 REACTIVITY VS. BURNUP FOR CONCEPT 1 MECHANICAL SPECTRAL SHIFT

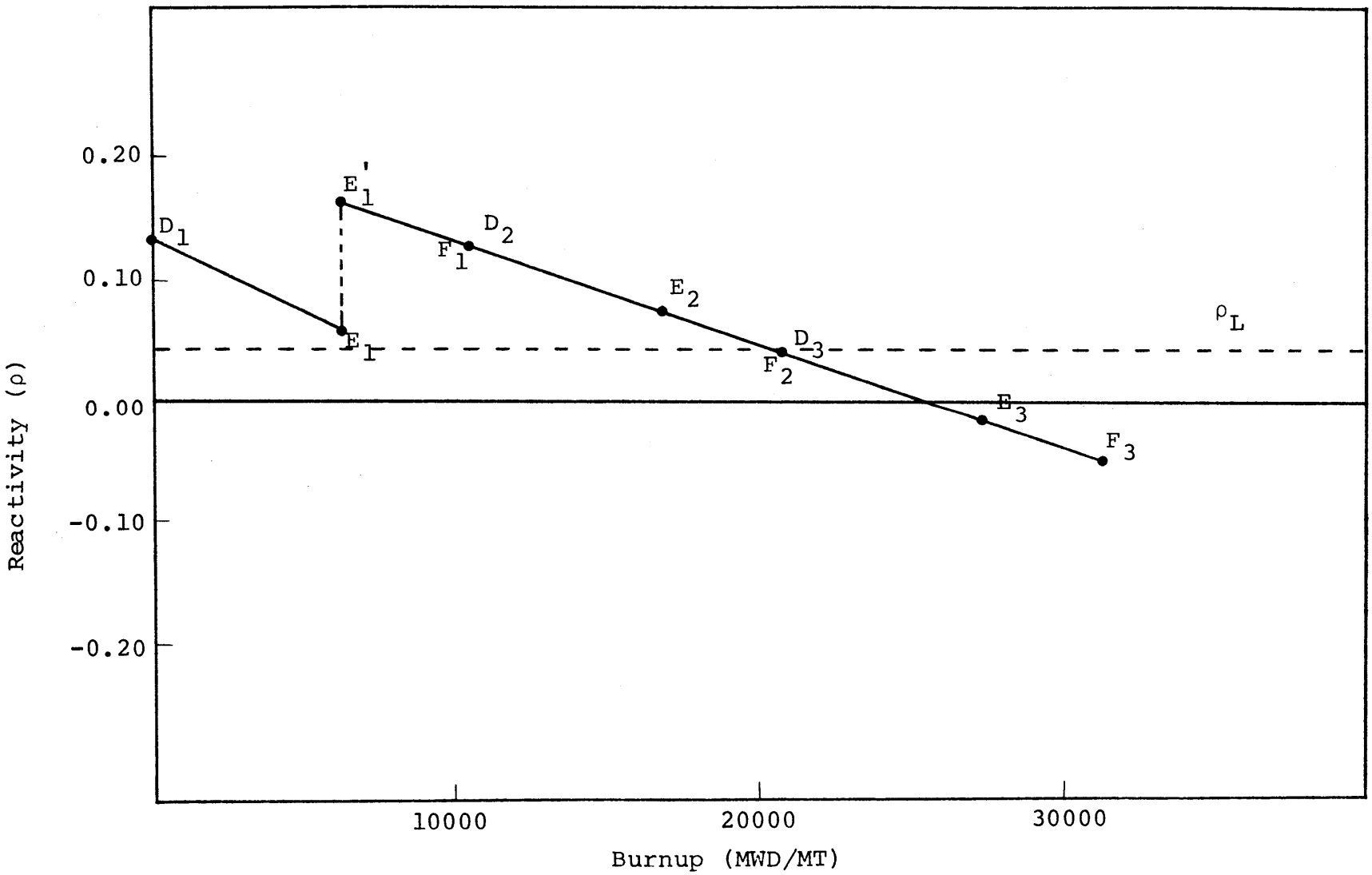

FIG. 7.14 REACTIVITY VS. BURNUP FOR CONCEPT 2 MECHANICAL SPECTRAL SHIFT

taken (in H/U phase space) to achieve that burnup. Thus, the points C_1, C_2, C_3, D_1, D_2 and D_3, and $\Delta\rho$ may vary significantly depending on the H/U ratios the assembly has encountered during burnup. It is critical to recognize that these points cannot be arbitrarily determined once the H/U atom ratio changes have been prescribed.

A possible reactivity vs. burnup curve for a Concept 2 design is shown in Fig. 7.14. The fuel batches begin the cycle at the points D_1, D_2 and D_3. Burnup continues until criticality is reached at points E_1, E_2 and E_3. The reactor head is removed and the lattice of batch 1 is adjusted to insert reactivity (point E_1'). The vessel is closed (without removing fuel assemblies) and the reactor is restarted and operated until the excess reactivity, $\Delta\rho(E_1' - E_1)$, is consumed. The oldest fuel is discharged at point F_3.

Variable lattice schemes can be generalized to any number of batches and/or reactivity insertions (lattice changes) at any of several points in the life of the fuel assembly. Although no attempt was made to find the optimal H/U (atom ratio) trajectory, a methodology based on the Advanced Linear Reactivity Model was developed, which is general enough to include any realistic combination of lattice changes and batch fractions, for the calculation of uranium utilization.

Recall that for ordinary three batch fuel management the reactivity equations of the batches can be written as:

$$\rho_1 = \rho_o - AB_{dis}\, f_1$$

$$\rho_2 = \rho_o - AB_{dis}\, (f_1 + f_2)$$

$$\rho_3 = \rho_o - AB_{dis}\, (f_1 + f_2 + f_3) \qquad (7.9)$$

and the condition for criticality is:

$$\rho_L = \sum_{i=1}^{3} f_i\, \rho_i \qquad (7.10)$$

which gives:

$$B_{dis} = \frac{\rho_o - \rho_L}{A\left\{\sum_{i=1}^{3}\sum_{j=i}^{3} f_i\, f_j\right\}} \qquad (7.11)$$

Consider the Concept 1 design shown in Fig. 7.13. The reactivity equations can be written as:

$$\rho_1' = \rho_o' - A'B_{dis}\, f_1$$

$$\rho_2' = \rho_o' - A'B_{dis}\, f_1 + \Delta\rho - A''B_{dis}\, f_2$$

$$\rho_3' = \rho_o' - A'B_{dis}\, f_1 + \Delta\rho - A''B_{dis}\, (f_2 + f_2) \qquad (7.12)$$

In this set of equations ρ_o' is the initial extrapolated reactivity of the lattice corresponding to point C_1, A' is the slope of the reactivity vs. burnup curve during the first cycle, $\Delta\rho$ is the reactivity insertion from lattice changes $(\rho(C_2) - \rho(D_1))$, and A" is the slope of the reactivity vs. burnup curve after the lattice change. Applying the criticality condition of Eq. 7.10 gives:

$$B_{dis} = \frac{\rho_o' - \rho_L + (f_2 + f_3)\ \Delta\rho}{A'\left[f_1^2 + f_1 f_2 + f_1 f_3\right] + A''\left[f_2^2 + f_2 f_3 + f_3^2\right]} \tag{7.13}$$

For a fuel rod with a specific value of $\sqrt{S/M}$, ρ_o' and A' are functions of the initial H/U atom ratio, A" depends on the final H/U atom ratio, and $\Delta\rho$ depends on the transition ("dry-wet") burnup B_{tran}. Eq. 7.13 must be optimized with respect to power split (f_1, f_2, f_3). Eq. 7.13 can be rewritten as:

$$B_c = \frac{\rho_o' - \rho_L + (1-f_1)\ \Delta\rho}{3A'f_1 + 3A''\left[f_2^2 + f_2 f_3 + f_3^2\right]} \tag{7.14}$$

The denominator is optimized (minimized) when $f_2 = f_3$ hence:

$$B_c = \frac{\rho_o' - \rho_L + (1-f_1)\ \Delta\rho}{3A'f_1 + 3A''\ \ 3\left(\frac{1-f_1}{2}\right)^2} \tag{7.15}$$

Since the lattice modification is made at the refueling, $3B_c\ f_1 = B_{tran}$ and hence:

$$B_{tran} = \frac{f_1\ \rho_o' - \rho_L + (1-f_1)\Delta\rho}{A'\ f_1 + A''\ \ 3\left(\frac{1-f_1}{2}\right)^2} \tag{7.16}$$

Thus, for Concept 1 fuel schemes, the choice of transition burnup, initial H/U atom ratio and final H/U atom ratio specifies the discharge burnup, i.e., Eq. 7.16 specifies f_1 absolutely. Concept 2 schemes are somewhat more difficult to analyze because they involve an extension of cycle using the same fuel. If the cycle length between points D_i and E_i in Fig. 7.14 (i = 1,2,3) is designated as B_c and the span from points E_i to F_i (i = 1,2,3) designated as ΔB_c, then the

reactivity equations can be written for B_c as:

$$\rho_1' = \rho_o' - A'B_c N f_1$$

$$\rho_2' = \rho_o' - A' B_c N f_1 + \Delta\rho - A''\Delta B_c N f_1^* - A'' B_c N f_2$$

$$\rho_3' = \rho_o' - A'B_c N f_1 + \Delta\rho - A'' \Delta B_c N f_1^* - A'' B_c N f_2 - A'' \Delta B_c N f_2^* - A''B_c N f_3 \quad (7.17)$$

and the equations for ΔB_c can be written as:

$$\rho_1' = \rho_o' - A'B_c Nf_1 + \Delta\rho - A''\Delta B_c N f_1^*$$

$$\rho_2' = \rho_o' - A'B_c N f_1 + \Delta\rho - A''\Delta B_c N f_1^* - A''B_c N f_2 - A''\Delta B_c N f_3^*$$

$$\rho_3' = \rho_o' - A' B_c N f_1 + \Delta\rho - A''\Delta B_c N f_1^* - A'' B_c N f_2 - A''\Delta B_c N f_2^* - A'' B_c N f_3 - A'' \Delta B_c N f_3^* \quad (7.18)$$

where ρ_o' is the reactivity at point D_1, $\Delta\rho$ is the reactivity change $(\rho(E_1') - \rho(E_1))$, A' is the slope of the reactivity vs. burnup curve before lattice modification, A" is the slope of the reactivity vs. burnup curve after lattice modification, N is the number of batches, B_c is the cycle length during irradiation between points D_i and E_i, ΔB_c is the cycle length for irradiation between points E_i and F_i, f_i is the power fraction in batch i at the end of B_c and f_i^* is the power fraction in batch i at the end of ΔB_c. The criticality

condition for Eq. 7.17 is:

$$\rho_L = \sum_{i=1}^{3} f_i \rho_i \tag{7.19}$$

whereas the criticality condition for Eq. 7.18 is:

$$\rho_L = \sum_{i=1}^{3} f_i^* \rho_i \tag{7.20}$$

Equations 7.17 to 7.20 can be combined to yield

$$B_c = \frac{\rho_o' - \rho_L + \Delta\rho(f_2+f_3) - \dfrac{f_1 \Delta\rho \left\{f_1^* f_2 + f_1^* f_3 + f_2^* f_3\right\}}{\left\{\sum_{i=1}^{3}\sum_{j=i}^{3} f_i^* f_j^*\right\} - (f_1^* f_2 + f_1^* f_3 + f_2^* f_3)}}{A'Nf_1 + A''N\left[(f_2^2 + f_2 f_3 + f_3^2) + \dfrac{(f_1^* f_2 + f_1^* f_3 + f_2^* f_3)(f_2^* f_2 + f_2^* f_3 + f_3^* f_3 - f_2^2 - f_2 f_3 - f_3^2)}{\left\{\sum_{i=1}^{3}\sum_{j=i}^{3} f_i^* f_i^*\right\} - f_1^* f_2 - f_1^* f_3 - f_2^* f_3}\right]} \tag{7.21}$$

and:

$$\Delta B_c = \frac{f_1 \Delta\rho - A'' B_c N\left[f_2 f_2^* + f_2 f_3^* + f_2 f_3^* - f_2^2 - f_2 f_3 - f_3^2\right]}{A''N\left[\left\{\sum_{i=1}^{3}\sum_{j=i}^{3} f_i^* f_j^*\right\} - f_1^* f_2 - f_1^* f_3 - f_2^* f_3\right]} \tag{7.22}$$

These two equations must be solved for B_c and ΔB_c. There are, however, six additional unknowns, the f_i and f_i^*. The additional equations required are:

$$f_1 + f_2 + f_3 = 1 \tag{7.23}$$

$$f_1^* + f_2^* + f_3^* = 1 \tag{7.24}$$

$$B_c N f_1 = B_{tran} \tag{7.25}$$

The power fractions can be estimated by

$$f_1 = C_1 f_1^* \tag{7.26}$$

$$f_2 = C_2 f_3 \tag{7.27}$$

$$f_2 = C_3 f_3^* \tag{7.28}$$

where C_1, C_2 and C_3 are constants (~1.0). The solution of Eqs. 7.21 and 7.22 using the conditions of Eqs. 7.26-7.28 gives the discharge burnup for a Concept 2 fuel management scheme which involves a lattice change from a specific initial H/U atom ratio to a final H/U atom ratio at a given transition burnup, B_{tran}. To determine the discharge burnup for more realistic power schedules, the conditions of Eqs. 7.26-7.28 must be adjusted. The optimum burnup schedule can be calculated by setting $C_2 = C_3 = 1.0$ and by iteratively solving for C_1 until $B_c + \Delta B_c$ is a maximum.

In realistic cases, the power split among assemblies should be determined by the k^Θ method developed previously and hence, the optimum burnup may not be achievable in a practical case.

Table 7.4 shows the results of a preliminary optimization of the Maine Yankee reactor assembly design for the Concept 1 fuel management scheme for a 3.0 w/o U-235 enrichment. None of the cases analyzed show any decrease in uranium requirements.

Table 7.5 shows the results for the same LEOPARD cases using the Concept 2 fuel management scheme. The conditions used were $f_2 = f_3 = f_2^* = f_3^*$ and $f_1 = f_1^*$. The values of f_1 in the converged solution are shown for each case. The optimum point occurs at an H/U atom ratio shift from 2.936 to 4.894.

The value of cycle burnup for this "best" lattice change corresponds to a choice of $C_1 = 1.0$ or $f_1 = f_1^*$. The value of C_1 was varied to determine if further benefits could be realized. At a value of $C_1 = 0.8919$ corresponding to $f_1 = 0.4126$, $f_1^* = 0.4626$, $B_c + \Delta B_c$ was 11089 MWD/MTP. This power history/power map is somewhat unrealistic; however, if it could be achieved a 9% reduction in uranium requirements would be realized.

Tables 7.4 and 7.5 do not represent a complete optimization of the Maine Yankee design. It may be possible that at other rod diameters or pellet densities (different $\sqrt{S/M}$) H/U atom ratio shifts may exist which would give improvements for both Concept 1 and Concept 2 schemes. Since the power split among assemblies is governed by the value of k and Θ (as shown in Chapter 4) a thorough optimization would include

TABLE 7.4 RELATIVE URANIUM FEED REQUIREMENTS FOR VARIOUS CONCEPT 1 STRATEGIES (B_{tran} = 8500 MWD/MTP)

Initial H/U (HOT, BOL)	FINAL H/U (HOT, Relative to U at BOL)	B_c	Relative Feed Requirement
4.381*	4.381	10085	1.000
2.551	3.644	8585	1.175
2.190	4.381	8651	1.166
2.629	4.381	9214	1.095
3.067	4.381	9523	1.059
3.505	4.381	9686	1.041
3.943	4.381	9770	1.032
2.447	4.894	9214	1.095
2.936	4.894	9539	1.057
3.426	4.894	9736	1.036
3.915	4.894	9872	1.022
2.780	5.560	9444	1.078
3.336	5.560	9605	1.050
3.892	5.560	9815	1.028

*Reference case.

TABLE 7.5 RELATIVE URANIUM FEED REQUIREMENTS FOR VARIOUS CONCEPT 2 STRATEGIES (B_{tran} = 8500 MWD/MTP)

INITIAL H/U (HOT, BOL)	FINAL H/U (HOT, Relative to U at BOL)	$B_c+\Delta B_c$	f_1	REL. FEED
4.381	4.381	10085	0.33	1.000
2.551	3.844	9917	0.46	0.983
2.629	4.381	10786	0.42	0.935
3.067	4.381	10535	0.34	0.957
3.505	4.381	10350	0.32	0.974
3.943	4.381	10067	0.30	1.002
2.447	4.894	10509	0.59	0.950
2.936	4.894	10979	0.38	0.919
3.426	4.894	10640	0.33	0.948
3.915	4.894	10340	0.30	0.975
2.780	5.560	10728	0.34	0.940
3.336	5.560	10468	0.31	0.963
3.892	5.560	10289	0.30	0.980

these effects in the calculation of initial H/U, final H/U, $\sqrt{S/M}$, and transition burnup B_{tran}. To first order, it appears that Concept 1 offers no uranium savings (and perhaps even some losses) and Concept 2 (when well-optimized) may provide uranium savings on the order of 10%. A complete optimization would be required to maximize Concept 2 savings. However, the results of such an optimization may suggest lattice changes that would violate thermal-hydraulic margins in the reactor and thus, these reductions in uranium requirements may not be achievable in actual practice.

7.6 Chapter Summary

Optimization of the Maine Yankee reactor design for H/U atom ratio suggests that at current discharge burnups (<36000 MWD/MT) there is no benefit to changing the current lattice design. On the other hand, at higher discharge burnups (~50000 MWD/MT) a potential 2.5% reduction in uranium requirements relative to the current H/U atom ratio can be achieved by a slight wettening of the lattice.

The use of annular fuel does not appear to offer any uranium savings per se, but annular fuel may facilitate operation, in a mode (wetter, higher burnup) which does improve uranium utilization. LEOPARD results indicate that for any annular fuel it is possible to find a solid pellet at an appropriate rod diameter and fuel density that is neutronically equivalent.

A methodology using the Advanced Linear Reactivity Model has been developed which can evaluate mechanical spectral shift concepts on a self-consistent basis. Mechanical spectral shift techniques based on the Concept 1 scheme (dry assemblies cycle 1, wet assemblies for cycles 2 and 3) do not appear to offer any uranium savings. It must be noted, however, that a thorough optimization was not performed. Nevertheless, all the cases analyzed using this scheme failed to break even with the reference case uranium utilization.

The Concept 2 scheme (dry-wet spectral shift during cycle 1), on the other hand, did produce uranium savings in some cases. The best case identified produced a reduction in uranium requirements of ~9%. Again, it must be noted that a thorough optimization may produce larger uranium savings.

For Concept 2 cases, however, the number of refueling shutdowns is doubled and this will adversely affect overall reactor capacity factors.

It must be conceded, however, that if a viable scheme could be devised for continuously varying lattice water content during normal operation, substantial improvements in uranium utilization could be realized (~18% for three-batch cores; ~10% for five-batch cores). So far, however, no one has come forth with an acceptable (economic, fail-safe) means to attain this goal other than the often considered (and rejected) H_2O/D_2O spectral shift concept.

CHAPTER 8

SUMMARY, CONCLUSIONS, AND RECOMMENDATIONS

8.1 INTRODUCTION

Over the past several years both political and economic considerations have precluded the commercial reprocessing of nuclear fuels in the United States. In the absence of reprocessing and breeder reactors it is desirable to extend uranium resources by optimizing current generation LWRs to use uranium on the once-through fuel cycle as efficiently as possible. Since the majority (nearly 2/3) of LWRs in the United States are pressurized water reactors, the research reported here has focused on the improvement of uranium utilization in current generation PWRs operating in the once-through mode. In addition, the emphasis has been on changes which can be readily backfit into existing reactors.

An important part of the present work has been the concern with the formulation of simple, but accurate models which can be used to separate out the concurrent contributions of simultaneous changes in several controlling variables (e.g. power history/power map and some design change of interest). Thus every effort is made to avoid obscuring the effect of concern, and making comparisons on an "all else being equal" basis.

8.2 BACKGROUND AND RESEARCH OBJECTIVES

The work described in this report was undertaken under the LWR Technology Program for Improved Uranium Utilization sponsored by the United States Department of Energy. Many investigators, both at MIT and elsewhere, have provided input along the same general lines to the Nonproliferation Alternative Systems Assessment Program (NASAP) (N-1), which in turn, provided input to the International Nuclear Fuel Cycle Evaluation (INFCE) (I-1). These investigators identified a variety of uranium-saving techniques which deserved further scrutiny

Consequently the general goal of the present work has been to develop, test, and apply self-consistent, methods for evaluating improvements in core design and fuel management strategy which would increase uranium utilization in PWRs.

8.3 Methodology Development

In order to analyze complex fuel management strategies the "Advanced Linear Reactivity Model" was developed. It was recognized that in the current range of interest with respect to fuel lattice parameters, reactivity, ρ , as a function of burnup, B $(\frac{MWD}{MT})$, was extremely linear, in fact, substantially more linear than the multiplication factor, k, as a function of burnup (See Fig. 8.1). Further analysis showed that the preferred

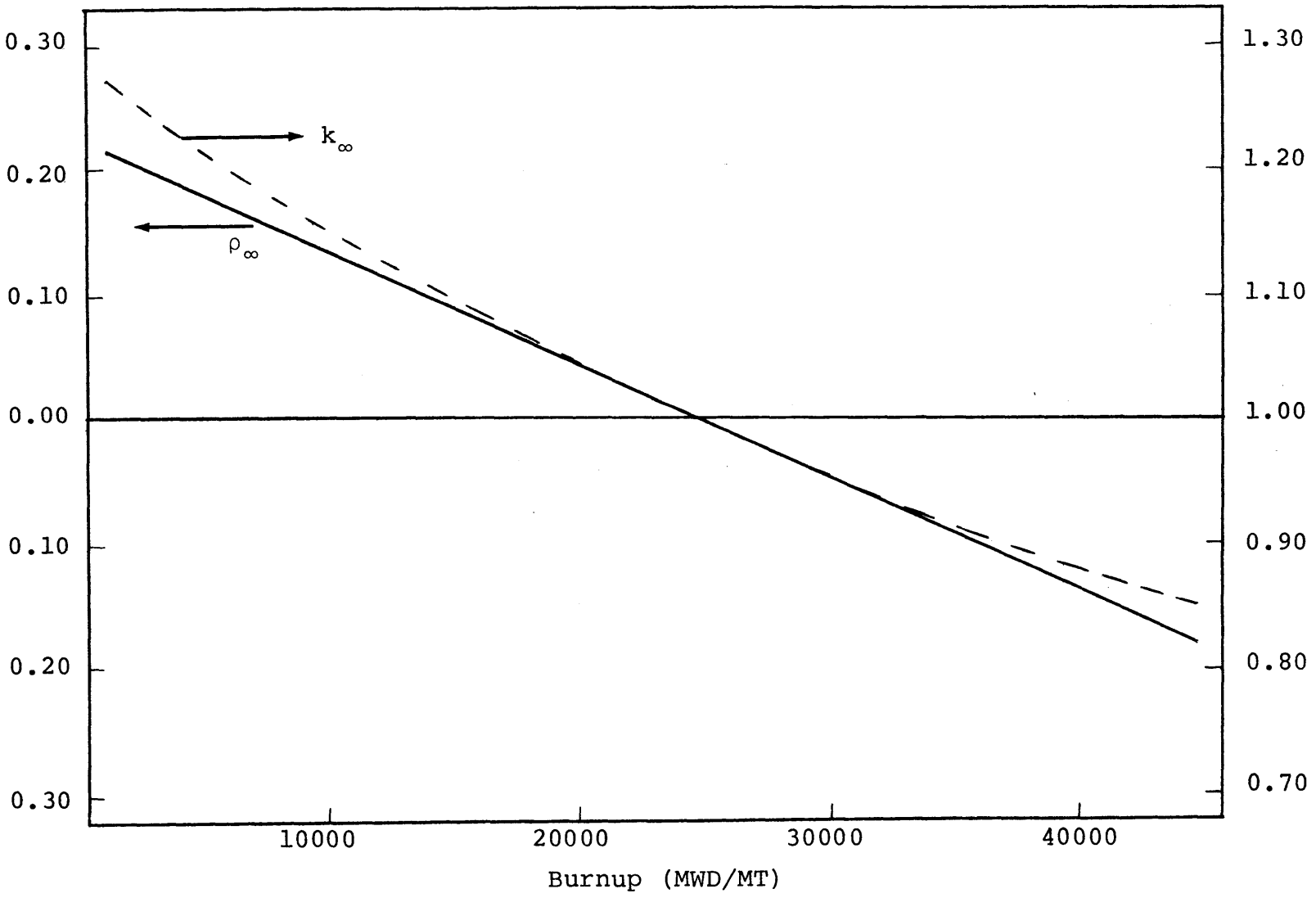

FIG. 8.1 k_∞ and ρ_∞ AS A FUNCTION OF BURNUP FOR A 3.0 W/O U-235 MAINE YANKEE SUPERCELL

scheme for the calculation of the reactivity of combinations of assemblies in a PWR was power fraction weighting; namely,

$$\rho_{sys} = \sum_{i=1}^{N} f_i \rho_i \qquad (8.1)$$

This formulation was verified (maximum error <0.4%) using PDQ-7. It was next shown that the effects of neutron leakage from the core could be incorporated as a decrement to system reactivity:

$$\rho_L = \frac{A_{ex\text{-}core}}{A_{total}\, k_{sys}} = \frac{A_{ex\text{-}core}}{F_{total}} \qquad (8.2)$$

where ρ_L is the leakage reactivity, $A_{ex\text{-}core}$ is the total absorption in non-core material (i.e. shroud, barrel, ex-core H_2O), A_{total} is the total absorption in the reactor (core + non-core material), k_{sys} is the system multiplication factor and F_{total} is the total neutron production in the reactor. Hence, the criticality condition in a reactor becomes:

$$\rho_L = \sum_{i=1}^{N} f_i \rho_i \qquad (8.3)$$

For an N-batch core, the reactivity vs. burnup equations can be written as:

$$\rho_1 = \rho_o - AB_cNf_1$$

$$\rho_2 = \rho_o - AB_cNf_1 - AB_cNf_2$$

$$\vdots$$

$$\rho_N = \rho_o - AB_cNf_1 - AB_cNf_2 - \ldots AB_cNf_N \qquad (8.4)$$

and when the criticality condition is applied:

$$B_{DIS} = \frac{\rho_o - \rho_L}{A\left\{\sum_{i=1}^{N}\sum_{j=i}^{N} f_i f_j\right\}} \qquad (8.5)$$

The leakage reactivity was found to depend only on the power generated within a few migration lengths of the core periphery. Very good linear correlations were found which permit representation of the leakage reactivity by relations of the form:

$$\rho_L = \alpha + \beta\, f_{per} \qquad (8.6)$$

where α and β are constants and f_{per} is the fraction of the total core power generated in the peripheral assemblies (See Fig. 8.2). Hence the discharge burnup becomes:

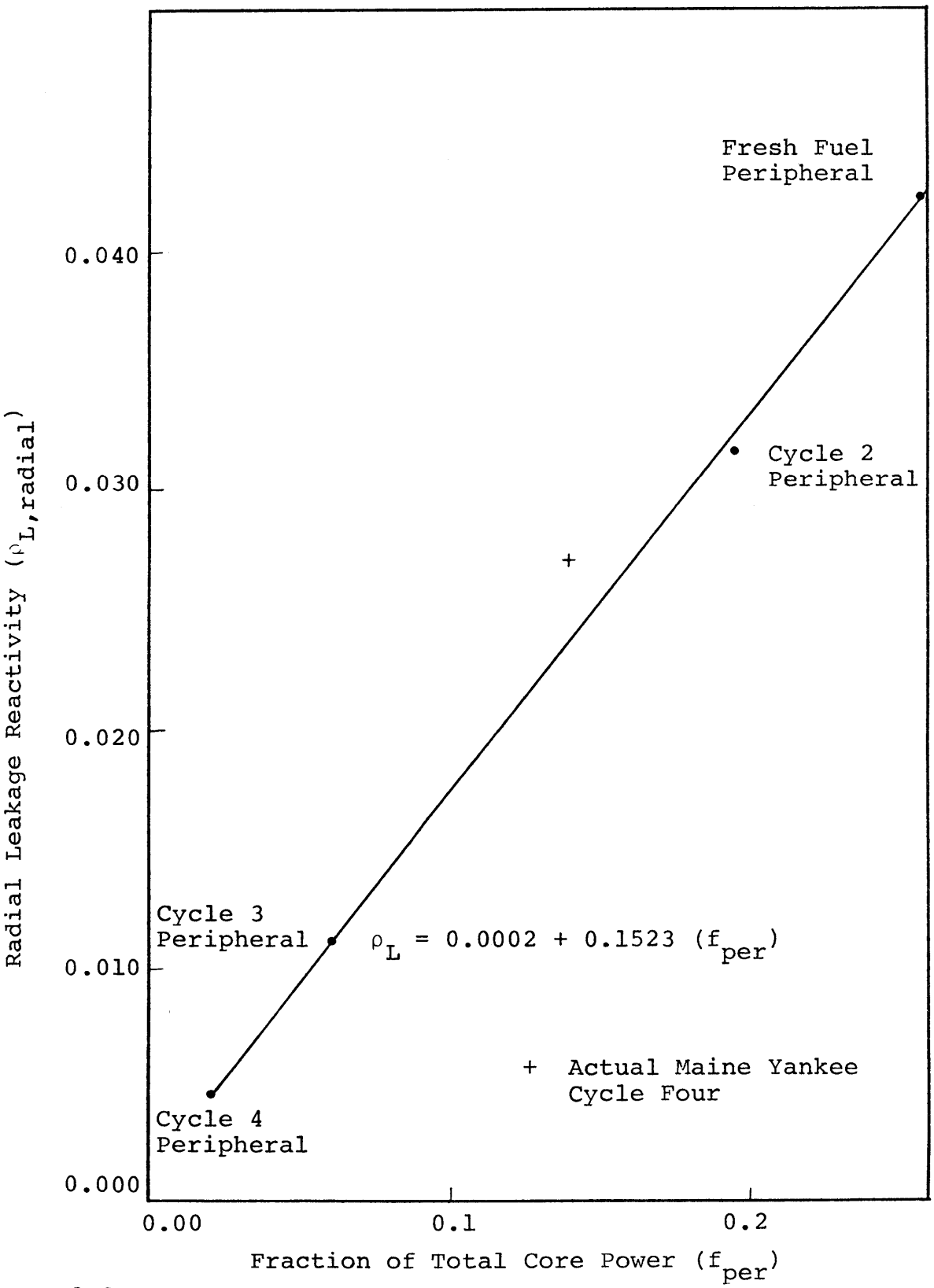

FIG. 8.2 RADIAL LEAKAGE REACTIVITY FOR M.Y. REACTOR VS. FRACTION OF CORE POWER GENERATED IN PERIPHERAL ASSEMBLIES

$$B_{dis} = \frac{\rho_o - (\alpha + \beta f_{per})}{A\left\{\sum_{i=1}^{N} \sum_{j=i}^{N} f_i f_j\right\}} \tag{8.7}$$

The cycle schedule index, CSI, given by

$$CSI = \sum_{i=1}^{N} \sum_{j=i}^{N} f_i f_j \tag{8.8}$$

quantifies the effects of burnup schedule on uranium utilization, whereas the leakage reactivity, ρ_L, accounts for the leakage effects. If the f_i and the values of f_{per}, α and β are known (for a given assembly type characterized by ρ_o and A), the uranium utilization can be determined by:

$$U\ (\frac{MWD}{MTF}) = \frac{B_{dis}\ (\frac{MWD}{MTP})}{F/P} \tag{8.9}$$

where F/P is the feed-to-product ratio given by:

$$\frac{F}{P} = \frac{\varepsilon - 0.2}{0.711 - 0.2} \tag{8.10}$$

for an 0.2 w/o tails assay and reload assembly enrichment ε.

The values of α and β depend on the specific reactor design studied, and can easily be extracted from

previous PDQ-7 calculations.

Extensive analytical and numerical studies, too tedious to repeat here, showed that power sharing among batches in a PWR is adequately characterized by the empirical relations

$$f_{i,int} = \frac{\frac{M_{i,int}}{M_i} (k_i)^{\theta}_{int}}{\sum_{i=1}^{N} f_i} \qquad (8.11)$$

for the interior assemblies of batch i and:

$$f_{i,per} = \frac{\frac{M_{i,\,per}}{M_i} (PNL_i k_i)^{\theta}_{per}}{\sum_{i=1}^{N} f_i} \qquad (8.12)$$

for the peripheral assemblies of batch i, where $M_{i,int}$ is the number of interior assemblies in batch i, $M_{i,per}$ is the number of peripheral assemblies in batch i, $M_i = M_{i,int} + M_{i,per}$, k_i is the assembly multiplication factor, PNL_i is the non-leakage probability for peripheral assemblies ($\sim$0.77), and θ_{int} ($\sim$1-2) and θ_{per} ($\sim$2) are the values of θ for interior and peripheral asemblies, respectively. The values of θ are design-specific and can be inferred by analysis of representative core maps. Fortunately, fuel discharge burnup values are not particularly sensitive to small changes in θ.

The restriction of linear reactivity was relaxed and the foregoing equations were incorporated into the ALARM (A-Linear Advanced Reactivity Model) computer code. Reactivity vs. burnup curves of arbitrary shape can be input to this program; an Nth order Lagrangian interpolation is performed to determine the reactivity of each batch at different burnups. Equations 8.1 - 8.12 are extremely versatile and with little or no modifications can be used to self-consistently analyze such design options as low-leakage fuel management, seed-blanket cores, variable fuel-to-moderator ratio designs, coastdown, and non-integer batch fractions. Furthermore, the equations can be reformulated for use on axial fuel management problems.

The remainder of the research effort was devoted to application of the preceding methods to the evaluation of a number of suggested improvements in core design and fuel management tactics. The work generally proceeded in three stages: an analytic treatment using the linear reactivity model to determine general trends and identify parameter sensitivity; a numerical evaluation using the ALARM code to obtain quantitative results; and, finally, for certain cases, verification using state-of-the-art physics methods (LEOPARD, PDQ-7).

In the sections which follow, the major areas investigated, and the principal findings in each area, are briefly summarized.

8.4 Axial Blankets*

The use of 6 inch thick blankets of natural uranium or depleted uranium (displacing enriched fuel) were found to provide 2.3% and 2.7% uranium savings, respectively. The use instead of 6 inches of beryllium metal slugs in an axial blanket were found to yield a uranium savings of 1.1%. However, axial power peaking factors are higher than normal for all three cases (by factors of 1.06, 1.075, and 1.053, respectively) and some means (enrichment, poison, or fuel-to-moderator ratio zoning) must be found to reduce these peaking factors before further optimization of axial blanket designs can be pursued.

8.5 Radial Blankets

It was found that assembly-sized natural uranium blankets do not yield any uranium savings for steady-state cores. An N-batch core with a natural uranium blanket can always be surpassed by an N + 1 batch core in which the oldest batch is loaded on the core periphery as a "spent fuel" blanket.

---

* All results using PDQ-7

8.6 Low-Leakage Fuel Management

It was found that low-leakage fuel management schemes for both low and high burnup cores (three batch and five batch fuel management) offer uranium savings of between 2% and 3%. The results are extremely sensitive to the amount of residual burnable poison present in the core. A reduction in this poison residual would increase the savings by an additional 1-2 percent.

8.7 Higher Burnups

Calculations for the Maine Yankee Reactor show that if the discharge burnup could be increased from the current 30,000 MWD/MT to 53,000 MWD/MT with a concurrent shift from 3 batch to 5 batch fuel management, a 15.4% reduction in uranium requirements is possible.

8.8 Optimization of the H/U Atom Ratio

The current Maine Yankee Reactor assembly is near optimum (H/U = 4.38, HOT, BOL) for low burnup operation. For high burnup operation ($\sim$53,000 $\frac{\text{MWD}}{\text{MTP}}$) the assembly should be made a bit wetter: H/U $\sim$5.0 (HOT, BOL). This will give a 2.5% reduction in uranium requirements relative to a high burnup, unoptimized (H/U = 4.38) case with the same enrichment.

8.9 Annular Fuel

Annular fuel offers no intrinsic uranium savings per se; savings should be attributed to the concomitant change in the H/U atom ratio and resonance integral. For any annular fuel design a solid pellet design can be found which will have the same uranium utilization. However, annular fuel may provide a convenient way of achieving the uranium savings without significantly altering the assembly design properties.

8.10 Mechanical Spectral Shift

For a current three batch PWR, continuous mechanical spectral shift applied to each batch can provide a theoretical maximum reduction in uranium requirements of 15.5%. Such a scheme, however, may well not be acceptable in light of current thermal/hydraulic and mechanical/operational constraints. Moreover, no one has yet proposed a practical way to continuously vary the H/U ratio in a PWR.

For a mechanical spectral shift scheme of the Concept-1 type (cycle one fuel "dry", cycle two and cycle three fuel "wet") no uranium savings were found and, in fact, uranium losses of a few percent appear to occur, although an all-inclusive optimization over all design space was not performed. For the mechanical spectral shift scheme designated Concept 2 (fresh fuel

starts its first cycle "dry" -- is modified during a short mid-cycle refueling shutdown and finishes the first cycle "wet") it appears that uranium savings on the order of 10% are possible; although, again, an extensive optimization was not performed. Despite these large savings, Concept 2 may be difficult to implement because of thermal/hydraulic considerations, and the decrease in overall capacity factor caused by the additional shutdown required for lattice adjustments. It was also discovered that pin-pulling and bundle reconstitution is mathematically equivalent to coolant void spectral shift (provided the power fractions in the pins are properly calculated).

8.11 Recommendations

Table 8.1 summarizes the potential uranium savings available from design and fuel management changes in current-generation PWRs. The savings should not be considered additive, since only a composite core analysis can determine possible synergisms among the individual changes. This table can serve as the basis for a series of recommendations for follow-on work, for which the need became evident during the course of the investigation which permitted compilation of the subject results.

It is clear from our work and that by other DOE contractors that the use of axial blankets (with an

TABLE 8.1 POTENTIAL URANIUM SAVINGS FROM DESIGN AND FUEL MANAGEMENT CHANGES IN CURRENT PWR CORES

CHANGE	REDUCTION IN URANIUM REQUIREMENT	COMMENT
Axial Blankets	0-3%; probably 2%	Savings depend on ability to satisfy axial power peaking constraints via enrichment zoning or burnable poison zoning.
Low-Leakage Fuel Management	2-3%; possibly 5%	Savings depend on ability to meet radial power peaking constraints with "low-residual" burnable poisons. Reduced assembly width may be useful.
Higher Burnup	∿15.4%	For increase in enrichment from 3.0 w/o U-235 to 4.34 w/o U-235, and concomitant switch from 3 batch to 5 batch fuel management. Same radial leakage reactivity loss assumed.
Natural Uranium Blankets (Assembly-sized)	Negative (relative to low leakage scheme)	Spent fuel is always a better blanket material than natural uranium.

TABLE 8.1 (Continued)

CHANGE	REDUCTION IN URANIUM REQUIREMENT	COMMENT
Optimized H/U Atom Ratio	Negligible at low burnup	Although the Maine Yankee reactor is currently optimized at a fixed rod diameter for H/U atom ratio; other reactors may not be, hence, reductions are reactor specific.
	∿2.5% at high burnup	Again, optimization is a reactor design specific result.
Mechanical Spectral Shift (Continuous)	15.5% - three batch (36,000 MWD/MT) 10.3% - five batch (37,000 MWD/MT)	Impractical in current reactor designs.
Mechanical Spectral Shift (Concept 1: end-of-cycle adjustment)	Negative (relative to current practice)	Detailed optimization may yet produce some small savings but lattice adjustments are tedious for such small savings.
Mechanical Spectral Shift (Concept 2: mid-cycle adjustment)	∿10% (3 batch core)	Thermal/Hydraulic considerations may be limiting. The extra refueling shutdown decreases the overall reactor capacity factor.

enrichment less than that of the core fuel) will save uranium provided one can satisfy axial peaking constraints. Further work should be done to pursue this concept to its ultimate embodiment. The models developed in this work provide an indication of the general approach to be followed, namely, reducing peripheral zone power while flattening interior core power. This can be accomplished by one or a combination of the following:

1) Enrichment-zoning the core interior, optimizing the zone lengths and enrichments, and simultaneously optimizing the blanket length and enrichment.
2) As above, but using zoned burnable poison to suppress core mid-zone power;
3) as above but using a zoned H/U ratio (by varying the diameter of the central void in annular fuel).

The use of beryllium metal as a reflector material should also be investigated further. In addition, multigroup S_N calculations should be performed to verify fast group albedos in all blanket concepts studied, since the use of diffusion theory and one fast group (as in PDQ-7) may not provide a sufficiently accurate description of neutron behavior in the high-leakage core/blanket and blanket/reflector interface zones.

There appears to be a growing interest among utilities in low leakage fuel arrangements in which the radial leakage is reduced by using older fuel assemblies (twice-burned, thrice-burned, etc.) on the core periphery. Peaking factors in the core interior are increased, however, particularly if a concurrent trend to higher burnup is envisioned, requiring increased use of burnable poison to flatten power. This in turn can result in larger poison residuals at EOC. Hence, more work needs to be done to optimize the cycle schedule index for low leakage fuel management, including the optimum use of burnable poison, evaluation of the use of assemblies which can be split into quarter-assemblies and reconstituted (to emulate the BWR with its smaller assemblies), and the use of more than one reload enrichment per reload batch (as in the Russian WWER (VVER), which employs two).

Mechanical spectral shift schemes of the Concept-2 type may provide substantial uranium savings if some practical way could be found to implement them without exceeding thermal-hydraulic safety limits and without decreasing overall reactor capacity factors. One approach which should be evaluated is the incorporation of floodable tubes into the assembly lattice grid.

Finally, it would be of some interest to determine the extent to which the improvments investigated

in this research would also prove beneficial for cores operated in the recycle mode. Low leakage fuel management and the use of axial blankets/axial power shaping would appear directly applicable with comparable savings, for example.

APPENDIX A*

DESIGN PARAMETERS FOR MAINE YANKEE REACTOR**

* See Reference S-1.

** See disclaimer in Acknowledgements.

MECHANICAL DESIGN FEATURES OF CYCLE 4 FUEL

	E and F	G, H, and I
Fuel Assembly		
Overall length	156.718**	156.718
Spacer grid size (max. square)	8.115	8.115
Retention grid	0	0
No. Zircaloy grids	8	8
No. Inconel grids	1	1
Fuel rod growth clearance	1.021	1.021
Fuel Rod		
Active fuel length	136.7	136.7
Plenum length	8.575	8.575
Clad OD	0.440	0.440
Clad ID	0.384	0.384
Clad wall thickness	0.026	0.028
Pellet OD	0.3765	0.3765
Pellet length	0.450	0.450
Dish depth	0.023	0.021
Clad material	Zr-4	Zr-4
Pellet density initial	95%	94.75%
Initial pressure	(*) psig	(*) psig
Poison Rods		
Overall rod length	146.513	146.322
Clad OD	0.440	0.440
Clad ID	0.388	0.388
Clad wall thickness	0.026	0.026
Pellet OD	0.376	0.376
Clad material	Zr-4	Zr-4

* YAEC 1099P. (Ref. B-6)
** All length dimensions are in inches.

MAIN YANKEE CYCLES 3 AND 4
NUCLEAR CHARACTERISTICS

Core Characteristics	Units	Cycle 3	Cycle 4
Core Average Exposure at BOC	MWD/MT	7,000	10,000
Expected Cycle Length at Full Power	MWD/MT	10,000	9,900
Initial U-235 Enrichment of Fuel Types			
Type RF 65 Cycle 3 assemblies	w/o	1.93	--
Type E 12 Cycle 3, 61 Cycle 4 assemblies	w/o	2.52	2.52
Type F 68 Cycle 3, 12 Cycle 4 assemblies	w/o	2.90	2.90
Type G 32 Cycle 3 and 4 assemblies	w/o	2.73	2.73
Type H 40 Cycle 3 and 4 assemblies	w/o	3.03	3.03
Type I 72 Cycle 4 assemblies	w/o	--	3.03
Control Characteristics			
Number of Control Element Assemblies (CEA's)			
Full Length		77	77
Part Length (not used)		8	*
Total CEA Worth			
HFP, BOC	%Δρ	9.18	8.30
HFP, EOC	%Δρ	9.56	9.30
Burnable Poison Rods			
Number (B_4C in Al_2O_3/Borosilicate glass)		756/0	160/16
Worth at HFP, BOC	%Δρ	1.4	0.5
Critical Soluble Boron (ARO) at BOC			
HZP, No Xe, Pk Sm	ppm	1075	1097
HFP, No Xe, Pk Sm	ppm	995	1013
HFP, Equilibrium Xe	ppm	782	797
Reactivity Coefficients (ARO)			
Moderator Temperature Coefficient			
HFP, BOC	$10^{-4}\Delta\rho/^{o}F$	-0.34**	-0.28
HFP, EOC	$10^{-4}\Delta\rho/^{o}F$	-1.98	-2.31

Maine Yankee Cycles 3 and 4
Nuclear Characteristics
(Cont.)

	Units	Cycle 3	Cycle 4
Fuel Temperature Component of Power Coeff.			
HZP, BOC	$10\text{-}5\Delta\rho/^{o}F$	-1.00	-1.53
HFP, BOC	$10\text{-}5\Delta\rho/^{o}F$	-1.00	-1.18
HZP, EOC	$10\text{-}5\Delta\rho/^{o}F$	-1.80	-1.76
HFP, EOC	$10\text{-}5\Delta\rho/^{o}F$	-1.37	-1.37
Total Delayed Neutron Fraction (β_{eff})			
BOC		0.00611	0.00597
EOC		0.00517	0.00525
Prompt Neutron Generation Time			
BOC	10^{-6} sec	29.3	29.6
EOC	10^{-6} sec	32.3	31.7
Inverse Boron Worth			
HZP, BOC	ppm/%$\Delta\rho$	84	87
HFP, BOC	ppm/%$\Delta\rho$	89	93
HZP, EOC	ppm/%$\Delta\rho$	74	76
HFP, EOC	ppm/%$\Delta\rho$	79	81

* Part length CEA's removed for Cycle 4
** Conditions of 2100 psia.

MAINE YANKEE CYCLE 4
GENERAL SYSTEM PARAMETERS

Quality	Value Cycle 3	Cycle 4
Reactor power level (102% of Nominal) (MWT)	2683	2683
Average linear heat rate (102% of Nominal) (kw/ft)	6.29	(6.35)*
Peak linear heat generation rate (PLHGR) (kw/ft)	16.5***	(15.7)[1]
Gap conductance at PLHGR (Btu/hr-ft^2-^{o}F)	2000***	(1949)[1] (2000)[2]
Fuel centerline temperature at PLHGR (^{o}F)	3788.1***	(3613.5)[1] (3782.2)[2]
Fuel average temperature at PLHGR(^{o}F)	2304.12***	(2212.9)[1]
Hot rod gas pressure (psi)	1221.4***	(1240.5)[1]
Moderator temperature coefficient at initial density ($\Delta\rho/^o$F)	0.0	0.0
System flow rate (lbm/hr)	134.57×10^6	124.57×10^6
Core flow rate (lbm/hr)	130.94×10^6	130.94×10^6
Initial system pressure (psia)	2250	2250
Core inlet temperature (^{o}F)	554	554
Core outlet temperature (^{o}F)	606.1	606.1
Active core height (feet)	11.39	11.39
Fuel rod OD (inches)	0.440	0.440
Number of cold legs	3	3
Number of hot legs	3	3
Cold leg diameter (inches)	33.5	33.5
Hot leg diameter (inches)	33.5	33.5
Safety injection tank pressure (psia)	219.7	219.7
Safety injection tank gas/water volume (cu. ft.)	2069.7/ 1430.3	2069.7/ 1430.3
Hot rod burnup (MWD/MTU) at the most limiting time for PCT	683*	(3391)[1] (1385)[2]

* Parentheses used to denote change in value from previous Cycle 3 reload analysis.
** Cycle 3 used low density fuel from Core IA which was blowdown limited. Cycle 4 does not include any low density fuel so these parameters have been omitted.
*** For most limiting high density fuel (batch F) in Cycle 3.
1 For batch H fuel, Cycle 4.
2 For batch I fuel, Cycle 4.

MAINE YANKEE CYCLE 4

THERMAL HYDRAULIC PARAMETERS AT FULL POWER

General Characteristics		Cycle 3	Cycle 4
Total Heat Output	10^6 MWT 10^6 Btu/hr	2630 8976	2630 8976
Fraction of Heat Generated in Fuel Rod		0.975	0.975
Nominal	psig	2235	2235(2085)†
Minimum in Steady State	psig	2185	2185(2035)
Maximum in Steady State		2285	2285(2135)
Design Inlet Temperature (steady state)	^oF	554	554(546)
Total Reactor Coolant Flow (design)	10^6 lb/hr	134.5	134.6(136.0)
Coolant Flow Through Core (design)	10^6 lb/hr	130.7	130.7(132.1)
Hydraulic Diameter (nominal channel)		0.044	0.044
Average Mass Velocity	10^6 lb/hr-ft^2	2.444	2.444(2.47)
Pressure Drop Across Cross (design flow)	psi	9.7	9.7(9.9)
Total Pressure Drop Across Vessel (based on nominal dimensions & design flow)	psi	32.4	32.4(33.1)
Core Average Heat Flux	Btu/hr-ft^2	178,740*	180,575*
Total Heat Transfer Area	ft^2	48,978*	48,480*
Film Coefficient at Average Conditions	Btu/hr-ft^2-^oF	5640	5636
Maximum Clad Surface Temp.	^oF	656	656
Average Film Temperature Difference	^oF	31.7	32
Avg. Linear Heat Rate of Rod	kw/ft	6.03*	6.09*
Average Core Enthalpy Rise	Btu/lb		68.7
Calculational Factors			
Engineering Heat Flux Factor		1.03	1.03
Engineering Factor on Hot Channel Heat Input		1.03	1.07
Flow Factors			
Inlet Plenum Nonuniform Distribution		1.05	1.05
End Pitch, Bowing and Clad Diameter		1.065	1.065

* Allows 0.3 percent axial shrinkage due to fuel densification.

† Numbers in parentheses are provided for conditions at a nominal pressure of 2,085 psig and a design inlet temperature of 546^oF.

APPENDIX B

SPECIAL USES AND MODIFICATIONS OF THE LEOPARD PROGRAM

At end-of-cycle most PWRs have essentially no soluble boron remaining in the coolant. Hence, LEOPARD results corresponding to the EOC burnup of each fuel batch should have no boron present. However, because the power fractions in each batch are different, the average burnup logged by each fuel batch (newest through oldest) will be different, and, hence, the correct boron coastdown endpoints are difficult to estimate.

The presence of boron in the fuel assembly forces an increase in the fast/thermal flux ratio to keep the thermal power output constant. Hence, the fast flux is increased and more Pu-239 is produced. It was found, however, that the use of the cycle-average boron concentration was adequate to match the isotopic concentrations produced by using the more exact boron coastdown treatment. In essence, the correct "average" spectrum is used. In order to obtain zero boron EOC k_∞ estimates, however, the following methodology was developed:

1) LEOPARD supercell calculations are run with the correct cycle-average boron concentration and the usual depletion time step sizes.

2) After every depletion time step (usually about 2500 MWD/MT) the boron concentration is set to zero and a very short (<1 MWD/MT) time step is used to find the k_∞ value

with no boron present. (If it is desirable to re-equilibrate xenon, then these time steps should be ~24 MWD/MT; this effect was found to be negligible in the present instance).

3) The cycle average boron is restored to the supercell and the next long depletion time step is run.

4) This procedure is continued until the projected discharge burnup is reached (or exceeded).

In this manner, the k_∞ values with no boron present can be determined and used for the EOC criticality calculation, but they will have been produced with the correct (boron present) spectrum.

For high burnup cases, a LEOPARD supercell which has been computed with no boron in the coolant can have a discharge burnup as much as 3% lower than the same supercell run with the method just described.

Note, however, that the key to estimating relative uranium savings is to compare cases on a consistent basis. Hence, if two cases are run without boron and the same two cases are run using the above boron removal technique, the relative advantage of one case over the other will be the same.

The LEOPARD code contains the option to vary the D_2O/H_2O molecule ratio as a function of burnup. For example, an input of -1.000 on the 101 poison control card gives a lattice with 50% H_2O and 50% D_2O. In order to input voids as a percentage of coolant volume (void fraction in coolant), the following modifications were made in two LEOPARD subroutines:

In subroutine INPUT change:

```
      PUREN(31,L)=WATER/(1.0+DENIMIC(I))                                  213
      PUREN(2,L)=PUREN(2,L)+PUREN(31,L)+PUREN(32,L)+2.*(PUREN(28.L)+      227
     1 PUREN(29,L)+PUREN(30,L))                                           228
915   PUREN(20,L)=PUREN(20,L)+2.*PUREN(32,L)                              243
```

to:

```
      PUREN(31,L)=WATER*(1.0-DENIMIC(I))                                  213
      PUREN(2,L)=PUREN(2,L)+PUREN(31,L)+2.*(PUREN(28,L)+                  227
     1 PUREN(29,L)+PUREN(30,L)                                            228
915   PUREN(20,L)=PUREN(20,L)                                             243
```

and in subroutine BURN change:

```
135   PUREN(31,J)=WATER/1.0-POISON(NOSTEP+1))                             155
      PUREN(20,J)=2.0*PUREN(32,J)                                         158
```

to:

```
135   PUREN(31,J)=WATER*(1.0+POISON(NOSTEP+1)                             155
      PUREN(20,J)=0.0                                                     158
```

Hence, entering -0.5 on the 101 poison entry card will give a lattice with 50% voids and 50% H_2O. The poison values on the depletion timestep cards are similarly specified.

APPENDIX C

OPTIMIZATION OF CYCLE SCHEDULE INDEX

The general equation for the discharge burnup of an N-batch core is:

$$B_{dis} = \frac{\rho_o - \rho_L}{A\left\{\sum_{i=1}^{N}\sum_{j=i}^{N} f_i\, f_j\right\}} \tag{C.1}$$

where ρ_o is the initial extrapolated reactivity, ρ_L is the leakage reactivity, A is the slope of the reactivity vs. burnup curve, and f_i is the power fraction in batch i. Selection of a set of power fractions to produce the maximum discharge burnup involves the cycle schedule index and the leakage reactivity, ρ_L, since the leakage reactivity can be written as:

$$\rho_L = \alpha + \beta\, f_{per} \tag{C.2}$$

It is useful, however, to consider the zero-leakage limit, which requires minimization of the cycle schedule index, CSI. The equation for the CSI is:

$$CSI = \sum_{i=1}^{N}\sum_{j=i}^{N} f_i\, f_j \tag{C.3}$$

subject to the constraint

$$\sum_{i=1}^{N} f_i = 1.0 \tag{C.4}$$

The equation for CSI really represents an equation for

ellipses (or elliptical solids depending on the value of N). In two dimensions (N=2) the CSI is written

$$CSI = f_1^2 + f_1 f_2 + f_2^2 \qquad (C.5)$$

In a graphical representation, different values of the CSI trace out concentric ellipses having their minor radius along a line at a 45^o angle to the f_1 axis. Since the CSI is proportional to the length of the minor radius, minimization of the CSI means finding the smallest minor radius which will satisfy the constraint equation (see Fig. C.1). This occurs when the ellipse is first tangent to the constraint line, or $f_1 = f_2$.

The result can be generalized to higher dimensions (N>2). For instance, for N=3 the CSI describes an elliptical solid, and the constraint equation ($f_1 + f_2 + f_3 = 1$) describes a plane. The smallest elliptical solid (minimum CSI) which will satisfy the constraint is the elliptical solid just tangent to the surface, hence $f_1 = f_2 = f_3$. Hence in the absence of peripheral leakage a flat power profile/uniform power history maximizes reactivity limited burnup.

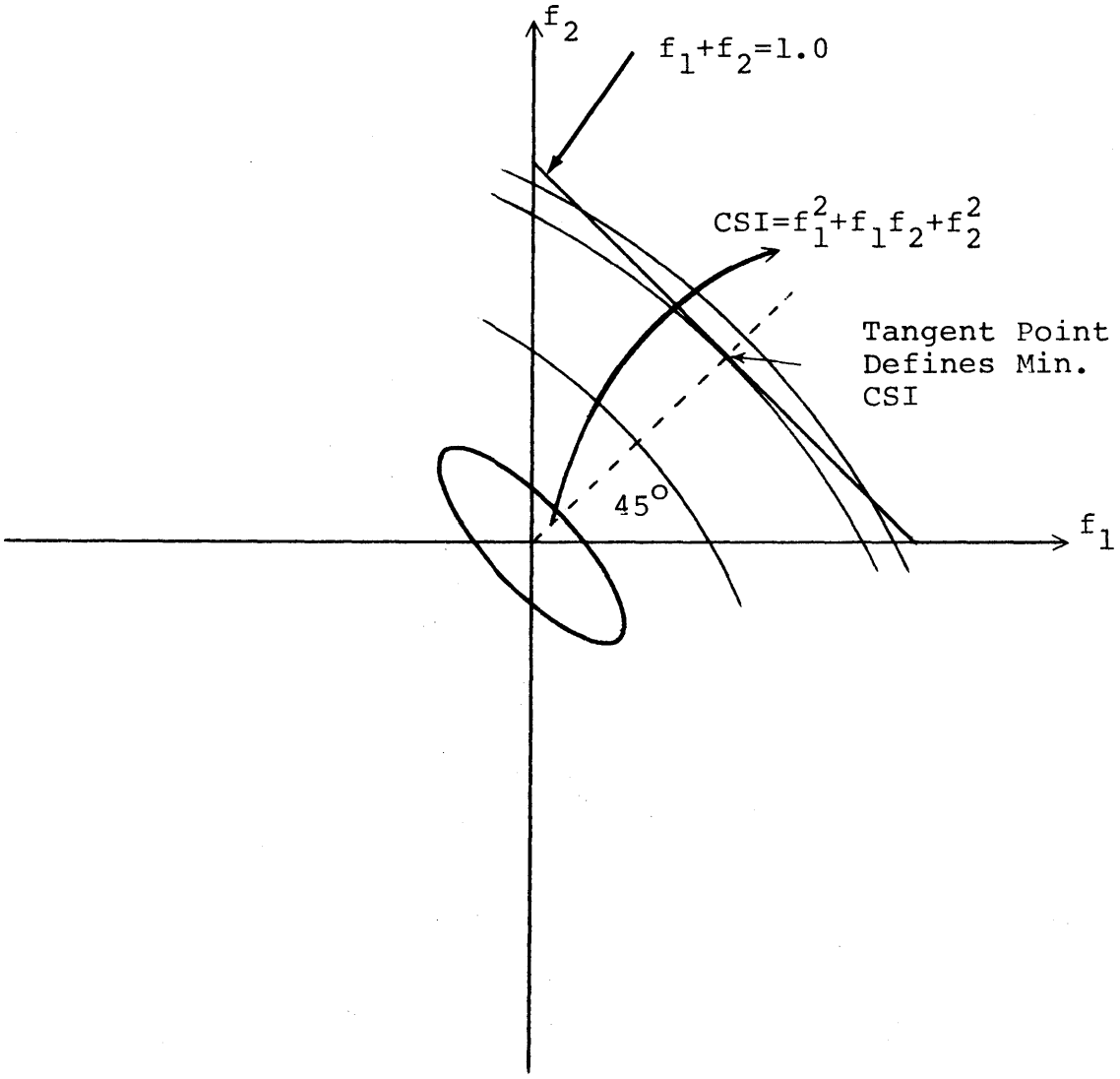

FIG. C.1 BEHAVIOR OF CSI RELATIVE TO THE CONSTRAINT EQUATION ($f_1+f_2=1.0$) FOR N=2.

APPENDIX D

DEVELOPMENT OF THE θ FORMULATION

Consider the two-bundle, zero-current boundary condition problem of Fig. 3.4. Using group-and-one-half theory it is possible to write the power in bundle one as

$$q_1 = C_1 \, k_1 \, \phi_{11} \tag{A.1}$$

where q_1 is the bundle power (relative to that of the average bundle), C_1 is a constant, k_1 is the infinite medium multiplication factor of region one, and ϕ_{11} is the fast group flux in region one. We can, by fiat, lump $C_1\phi_{11}$ into one term and say:

$$C_1 \, \phi_{11} = k_1^{N-1} \tag{A.2}$$

This is a definition, not an assumption; and hence:

$$q_1 = k_1^{N} \tag{A.3}$$

The same thing can be done for bundle two to give

$$q_2 = k_2^{M} \tag{A.4}$$

For the zero-current boundary condition problem

$$\frac{1}{k_{sys}} = \frac{f_1}{k_1} + \frac{f_2}{k_2} \tag{A.5}$$

where:

$$f_1 = \frac{q_1}{q_1 + q_2} \; ; \; f_2 = \frac{q_2}{q_1 + q_2} \tag{A.6}$$

Thus, combining terms gives

$$k_{sys} = \frac{k_1^N + k_2^M}{k_1^{N-1} + k_2^{M-1}} \tag{A.7}$$

We can arbitrarily define:

$$N = \theta + \Delta N$$
$$M = \theta + \Delta M \tag{A.8}$$

where θ is an unknown, to give:

$$k_{sys} = \frac{k_1^{\theta} k_1^{\Delta N} + k_2^{\theta} k_2^{\Delta M}}{k_1^{\theta-1} k_1^{\Delta N} + k_2^{\theta-1} k_2^{\Delta M}} \tag{A.9}$$

But it is always possible to find a ΔN and a ΔM such that

$$\frac{k_1^{\Delta N}}{k_2^{\Delta M}} = 1.0 \tag{A.10}$$

Thus, multiplying the numerator and denominator of Eq. A.9 by $k_2^{\Delta M}$ gives:

$$k_{sys} = \frac{k_1^{\theta} + k_2^{\theta}}{k_1^{\theta-1} + k_2^{\theta-1}} \tag{A.11}$$

It is important to recognize that no inherent assumptions are contained in this derivation--only definitions are used, i.e., $q_1 = k_1^N$ is completely arbitrary since given a q_1 and a k_1, N is defined. The importance of this formula (Eq. A.11) for system reactivity and power split calculations lies in the

fortunate result (see Fig. 4.2) that θ does not change significantly for a wide range of k_1 and k_2 combinations produced by a large variety of lattice adjustments. The value of theta does depend on problem size (i.e. the width of the separate regions (k_1,k_2) inside the zero-current boundary condition perimeter.

APPENDIX E

ALARM CODE INPUT SPECIFICATIONS, LISTING, AND SAMPLE PROBLEM

E.1 Code Description

The ALARM (A-Linear Advanced Reactivity Model) code is the equivalent of a poor man's PDQ-7. It enables one to calculate the average discharge burnup of a fuel batch including batch power sharing and radial and axial leakage effects. These effects are calculated using the methodology shown in Table 4.3 and Fig. 4.9. The format for input preparation is shown in Table E.1. The code is written in FORTRAN (Table E.2) but can easily be adapted to BASIC for use with minicomputers.

The sample problem uses LEOPARD results for a 4.34 w/o U-235 Maine Yankee (C-E design) assembly in a C-E SYSTEM 80^{TM} core. The leakage correlation is based on the "near-equilibrium" data points of Fig. 3.8 with a reactivity decrement of $0.005\Delta\rho$ added for the addition of burnable poison. A low-leakage loading pattern is used based on the data in Ref. M-3. The card images for the input are shown in Table E.3. Table E.4 is a listing of the code output.

TABLE E.1 INPUT INSTRUCTIONS

Card Set 1 (one card)

J: number of batches

IDEG: order of Lagrangian interpolation

TSTEP: time-step size (MWD/MT)

CONVRG: convergence criteria (MWD/MT)

FORMAT (8X, I2, 8X, I2, 2F10.4)

Card Set 2 (one or more cards)

PNL(I): batch non-leakage probabilities; J entries

FORMAT (8F10.3)

Card Set 3 (one or more cards)

AINT(I): number of internal assemblies in batch I; J entries

FORMAT (8F10.1)

Card Set 4 (one or more cards)

APER(I): number of peripheral assemblies in batch I; J entries

FORMAT (8F10.1)

Card Set 5 (one card)

ALPHA
BETA } leakage coefficients for $\rho_L = \alpha + \beta f_{per}$

FORMAT (2F10.4)

Card Set 6 (one card)

THETAI: interior assembly θ value

THETAP: peripheral assembly θ value

FORMAT (2F10.2)

Card Set 7 (one card)

N: number of (k, BURNUP) pairs entered

FORMAT (2X, I3)

Card Set 8 (one or more cards)

X(I): burnup values (MWD/MT); N entries

FORMAT (8F10.4)

Card Set 9 (one or more cards)

Y(I): value of k_∞ at each burnup; N entries

FORMAT (8F10.4)

Card Set 10

Termination Card: enter 99; FORMAT (2X, I3)

TABLE E.2 ALARM CODE LISTING

```
0001                IMPLICIT  REAL*8(A-H, O-Z) , REAL*8(K)
0002                DIMENSION X(100), Y(100)
0003                DIMENSION DONE(20), B(20), F(20), K(20), PNL(20)
0004                DIMENSION AINT(20), APER(20), PINT(20), PPER(20),ATOT(20)
                C
0005              20  READ(5,1020) J,IDEG,TSTEP,CONVRG
0006                  READ (5,1040) (PNL(I), I=1,J)
0007                  READ (5,1050) (AINT(I), I=1,J)
0008                  READ (5,1050) (APER(I), I=1,J)
0009                  READ (5,1060) ALPHA, BETA
0010                  READ (5,1030) THETAI,THETAP
                C
0011                  STORE = TSTEP
                C     ...READ N XANDY VALUES AND PRINT
0012                11  READ(5,1000) N
0013                  IF (N.EQ.99) STOP
0014                  READ(5,1010)(X(I),I=1,N)
0015                  READ (5,1010) (Y(I), I=1,N)
0016                  TSTEP = STORE
0017                  NUMB = 0
0018                  ATOTAL = 0.0
0019                  DO 122 I=1,J
0020                  ATOTAL = ATOTAL + APER(I) + AINT(I)
0021                  ATOT(I) = APER(I) + AINT(I)
0022                122   CONTINUE
                C
0023                  WRITE(6,3000)
0024                  WRITE(6,3010) J,ATOTAL,IDEG,TSTEP,CONVRG,THETAI,THETAP,ALPHA,BETA
0025                  WRITE(6,3020)
0026                  DO 10 I = 1,N
0027                 10   WRITE(6,3030) I,X(I),Y(I)
0028                  WRITE(6,3040)
0029                  DO 15 I=1,J
0030                 15   WRITE(6,3050) I,AINT(I),APER(I),ATOT(I),PNL(I)
                C
0031                  WRITE(6,3060)
```

```
C
0032            S=1.0
0033            RHOL=ALPHA+BETA*0.2
0034            JLESS=J-1
0035            V=J
0036            DONE(1)=0.0
0037         70 DO 100 I=1,N
0038            GAMMA=1.0+RHOL
0039         80 IF(Y(I).LE.GAMMA.AND.X(I).GT.10000.0)  BEST=X(I)*2/(V+1)
0040         90 IF(Y(I).LE.GAMMA.AND.X(I).GT.10000.0) GO TO 110
0041        100 CONTINUE
0042        110  CONTINUE
0043            DO 120 I=1,J
0044            L=I-1
0045            W=L
0046            DONE(I)=W*BEST

0047        120 CONTINUE
C
0048        130 DO 140 I=1,J
0049            F(I) = (APER(I)+AINT(I))/ATOTAL
0050        140 CONTINUE
C
0051        190 DO 200  I=1,J
0052            B(I)=DONE(I)
0053        200 CONTINUE
0054            GO TO 330
C
C
0055        210 CONTINUE
0056            NUMB = NUMB + 1
0057            WRITE(6,3070)NUMB ,RHOL
0058            WRITE(6,3080) FPER
0059            WRITE(6,3090) (B(I),I=1,J)
0060            WRITE (6,3100) (F(I),I=1,J)
0061            IF(DABS(TELL).LE.CONVRG) GO TO 11
C
C
0062            TSTEP = STORE
0063            S=0.0
0064        220 DO 230  I=1,J
0065            L=I-1
0066            IF (I.NE.1)  DONE(I)=B(L)
0067        230 CONTINUE
0068            GO TO 190
C
```

```
                C
0069              330 DO 370  I=1,J
0070                  XARG=B(I)
                C     THIS SECTION WILL LOCATE XARG RELATIVE TO THE TABLE VALUES
                C     INPUT AND CENTER THE INTERPOLATION POLYNOMIAL ABOUT XARG
                C     IT CAN ALSO SET UP THE POLYNOMIAL FOR EXTERPOLATION
0071              340 DO 350 L=1,N
0072                  IF (L.EQ.N.OR.XARG.LE.X(L)) GO TO 360
0073              350 CONTINUE
0074              360 MAX = L+IDEG/2
0075                  IF (MAX.LE.IDEG) MAX = IDEG+1
0076                  IF (MAX.GE.N) MAX=N
0077                  MIN = MAX-IDEG
                C     THE VALUE OF MIN HAS NOW BEEN DETERMINED FOR FLAGR TO USE
                C
                C
0078                  YINTER = FLAGR ( X,Y,XARG,IDEG,MIN,N )
0079                  K(I)=YINTER
0080              370 CONTINUE
                C
                C
                C
                C
0081                  KINV=0.0


0082              380 DO 390  I=1,J
0083                  KINV=KINV+(F(I)/K(I))
0084              390 CONTINUE
0085                  RHO=1-KINV
0086                  IF (TSTEP.GT.0.1) GO TO 400
0087                  IF (RHO.LE.RHOL)  GO TO 460
0088              400 IF (RHO.GT.RHOL)  GO TO 440
0089              410 DO 420 I=1,J
0090                  B(I)=B(I)-((ATOTAL/(APER(I)+AINT(I)))*F(I)*TSTEP)
0091              420 CONTINUE
0092                  TSTEP=TSTEP/2
                C
                C
0093              440 DO 450  I=1,J
0094                  B(I)=B(I)+((ATOTAL/(APER(I)+AINT(I)))*F(I)*TSTEP)
0095              450 CONTINUE
                C
```

```
C
0096        PTOTAL = 0.0
0097      470 DO 480  I=1,J
0098        PTOTAL=PTOTAL+APER(I)*(PNL(I)*K(I))**THETAP +
          $       AINT(I)*K(I)**THETAI
0099      480 CONTINUE
C
C
0100      490 DO 500 I=1,J
0101        PPER(I)=(APER(I)*(PNL(I)*K(I))**THETAP)/PTOTAL
0102        PINT(I)=(AINT(I)*K(I)**THETAI)/PTOTAL
0103        F(I)=PPER(I)+PINT(I)
0104      500 CONTINUE
0105        FPER=0.0
0106      510 DO 520 I=1,J
0107        FPER=FPER+PPER(I)
0108      520 CONTINUE
0109        RHOL=ALPHA+BETA*FPER
0110        GO TO 330
0111      460  CONTINUE
0112      540 IF (J.EQ.1)  GO TO 560
0113      550 DO 560 I=1,JLESS
0114        M=I+1
0115        TELL=B(I)-DONE(M)
0116        IF (DABS(TELL).GT.CONVRG) GO TO 210
0117        IF (S.EQ.1) GO TO 210
0118      560 CONTINUE
0119        GO TO 210
0120       990 STOP
C
C         FORMATS FOR INPUT AND OUTPUT STATEMENTS
0121      1000  FORMAT (2X,I3)
0122      1010  FORMAT (8F10.4)
0123       1020  FORMAT (8X,I2,8X,I2,2F10.4)
0124      1030  FORMAT(2F10.2)
0125       1040 FORMAT (8F10.3)
```

```
0126            1050 FORMAT (8F10.1)
0127            1060 FORMAT (2F10.4)
0128            3000 FORMAT(1H1,9X,'THE INPUT PARAMETERS ARE :'///1H )
0129            3010 FORMAT(5X,1HJ,10X,17HNUMBER OF BATCHES,16X,I5//
                    $       5X,6HATOTAL,5X,26HTOTAL NUMBER OF ASSENBLIES,7X,F5.1//
                    $       5X,4HIDEG,7X,19HORDER OF REGRESSION,17X,I2//
                    $       5X,5HTSTEP,6X,18HTIME STEP (MWD/MT),15X,F5.1//
                    $       5X,6HCONVRG,5X,30HCONVERGENCE CRITERION (MWD/MT),3X,F5.1//
                    $       5X,6HTHETAI,5X,14HINTERNAL THETA,19X,F5.1//
                    $       5X,6HTHETAP,5X,16HPERIPHERAL THETA,17X,F5.1//
                    $      5X,5HALPHA,6X,19HLEAKAGE COEFFICIENT,12X,F7.4//
                    $      5X,4HBETA,7X,19HLEAKAGE COEFFICIENT,13X,F6.4/1H1)
0130            3020 FORMAT(10X,'THE READ IN VALUES OF K-EFFECTIVE VS. BURNUP'///20X,
                    $       14HBURNUP(MWD/MT),15X,5HK-EFF/20X,14(1H*),14X,7(1H*)/1H0)
0131            3030 FORMAT(8X,I2,11X,F10.2,16X,F7.4)
0132            3040 FORMAT (1H1,4X,'NON-LEAKAGE PROBABILITY AND THE DISTRIBUTION OF
                    $ASSEMBLIES IN THE BATCHES'///20X,8HINTERNAL,7X,
                    $       10HPERIPHERAL,5X,5HTOTAL,1X,5HBATCH,4X,11HNON-LEAKAGE/
                    $       10X,5HBATCH,3(5X,10HASSEMBLIES),5X,11HPROBABILITY/
                    $       10X,5(1H*),3(5X,10(1H*)),5X,11(1H*)/1H0)
0133            3050 FORMAT(11X,I2,9X,F5.1,2(10X,F5.2),12X,F5.3/1H0)
0134            3060    FORMAT(1H1,4X' THE VALUES OF LEAKAGE (RHOL), PERIPHERAL BATCH
                    $POWER FRACTION (FPER),'/      5X,' BATCH BURNUP B(I) IN MWD/MT AND
                    $ BATCH POWER FRACTION F(I) ARE ARRANGED'/    5X,' IN THE FOLLOWING
                    $ ORDER AFTER EACH ITERATION'///13X,4HRHOL/13X,4HFPER//13X,4HB(1),
                    $     9X,4HB(2), 9X,4HB(3), 9X,4HB(4), 9X,4HB(5), 9X,4HB(6),
                    $    6X,3HETC/13X,4HF(1), 9X,4HF(2), 9X,4HF(3), 9X,4HF(4),
                    $     9X,4HF(5), 9X,4HF(6),6X,3HETC///)
0135            3070  FORMAT(/3X,I3,2X,F10.4)
0136            3080  FORMAT (8X,F10.4)
0137            3090  FORMAT (5X,8(3X,F10.1))
0138            3100  FORMAT (5X,8(3X,F10.4)/1H )
                C
0139                  END
```

```
0001                  FUNCTION FLAGR ( X,Y,XARG,IDEG,MIN,N )     *
                C
                C       FLAGR USES THE LAGRANGE FORMULA TO EVALUATE THE INTERPOLATING
                C       POLYNOMIAL OF DEGREE IDEG FOR ARGUMENT XARG USING THE DATA
                C       VALUES X(MIN)...X(MAX) AND Y(MIN)...Y(MAX) WHERE
                C       MAX = MIN + IDEG. NO ASSUMPTION IS MADE REGARDING ORDER OF
                C       THE X(I) AND NO ARGUMENT CHECKING IS DONE. TERM IS
                C       A VARIABLE WHICH CONTAINS SUCCESSIVELY EACH TERM OF THE
                C       LAGRANGE 'FORMULA. THE FINAL VALUE OF YEST IS THE INTERPOLATED
                C       VALUE.
                C
0002                  IMPLICIT REAL*8(A-H, O-Z)
0003                  REAL*8 X,Y,XARG,FLAGR
0004                  DIMENSION X(N), Y(N)
                C
0005                  FACTOR = 1.0
0006                  MAX = MIN + IDEG
0007                  DO 3002 J=MIN,MAX
0008                  IF (XARG.NE.X(J)) GO TO 3002
0009                  FLAGR = Y(J)
0010                  RETURN
0011           3002 FACTOR = FACTOR*(XARG - X(J))
                C
                C       EVALUATE THE INTERPOLATING POLYNOMIAL
0012                  YEST = 0.
0013                  DO 3005  I=MIN,MAX
0014                  TERM = Y(I)*FACTOR/(XARG - X(I))
0015                  DO 3004  J=MIN,MAX
0016           3004 IF (I.NE.J) TERM = TERM/(X(I)-X(J))
0017           3005 YEST = YEST + TERM
0018                  FLAGR = YEST
0019                  RETURN
                C
0020                  END
```

* REF. (C-7)

TABLE E.3 SAMPLE PROBLEM INPUT CARDS

```
99
 1.0165   0.9785   0.9422   0.9083   0.8513
 1.3195   1.3076   1.2956   1.2385   1.1872   1.1407   1.0978   1.0561
35000.0  40000.0  45000.0  50000.0  60000.0
 3000.0   4000.0   5000.0  10000.0  15000.0  20000.0  25000.0  30000.0
13
    2.00     2.00
  0.0023   0.3010
     8.0     36.0      4.0      0.0      0.0      0.0
    40.0     12.0     44.0     48.0     48.0      1.0
    0.77     0.77     0.77     0.77     0.77     0.77
       6        4     10.0      5.0
```

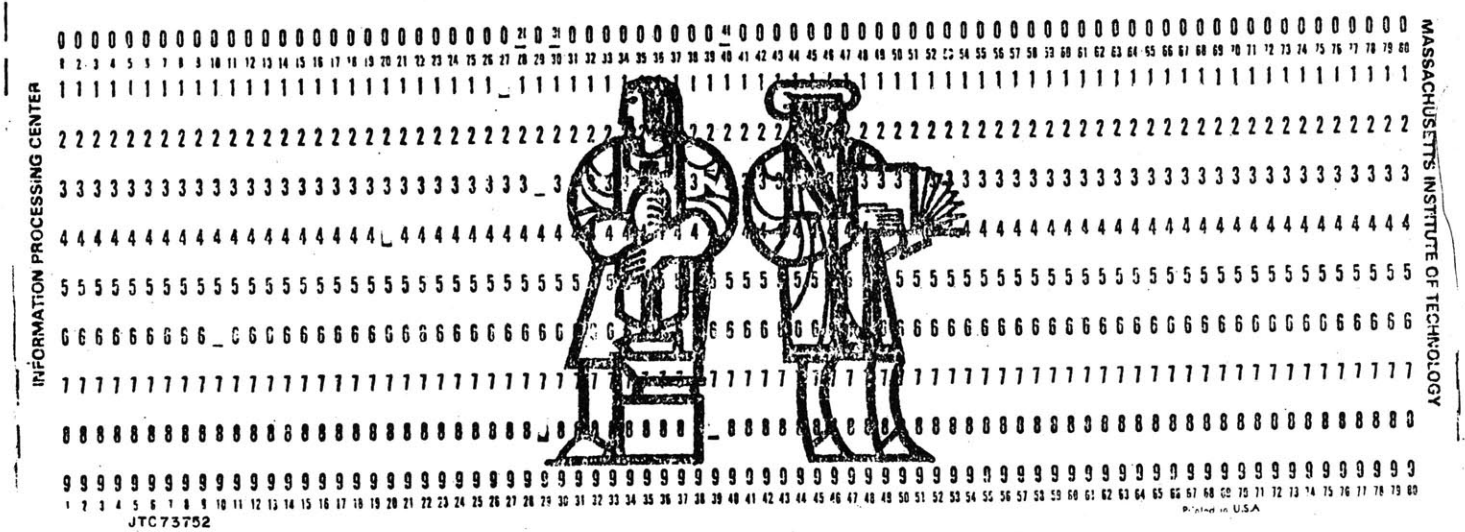

TABLE E.4 ALARM CODE OUTPUT

THE INPUT PARAMETERS ARE :

J	NUMBER OF BATCHES	6
ATOTAL	TOTAL NUMBER OF ASSENBLIES	241.0
IDEG	ORDER OF REGRESSION	4
TSTEP	TIME STEP (MWD/MT)	10.0
CONVRG	CONVERGENCE CRITERION (MWD/MT)	5.0
THETAI	INTERNAL THETA	2.0
THETAP	PERIPHERAL THETA	2.0
ALPHA	LEAKAGE COEFFICIENT	0.0023
BETA	LEAKAGE COEFFICIENT	0.3010

THE READ IN VALUES OF K-EFFECTIVE VS. BURNUP

	BURNUP(MWD/MT)	K-EFF
	**********	*******
1	3000.00	1.3195
2	4000.00	1.3076
3	5000.00	1.2956
4	10000.00	1.2385
5	15000.00	1.1872
6	20000.00	1.1407
7	25000.00	1.0972
8	30000.00	1.0561
9	35000.00	1.0165
10	40000.00	0.9785
11	45000.00	0.9422
12	50000.00	0.9083
13	60000.00	0.8513

NON-LEAKAGE PROBABILITY AND THE DISTRIBUTION OF ASSEMBLIES IN THE BATCHES

BATCH	INTERNAL ASSEMBLIES	PERIPHERAL ASSEMBLIES	TOTAL BATCH ASSEMBLIES	NON-LEAKAGE PROBABILITY
1	40.0	8.00	48.00	0.770
2	12.0	36.00	48.00	0.770
3	44.0	4.00	48.00	0.770
4	48.0	0.0	48.00	0.770
5	48.0	0.0	48.00	0.770
6	1.0	0.0	1.00	0.770

THE VALUES OF LEAKAGE (RHOL), PERIPHERAL BATCH POWER FRACTION (FPER), BATCH BURNUP B(I) IN MWD/MT AND BATCH POWER FRACTION F(I) ARE ARRANGED IN THE FOLLOWING ORDER AFTER EACH ITERATION

	RHOL FPER B(1) F(1)	B(2) F(2)	B(3) F(3)	B(4) F(4)	B(5) F(5)	B(6) F(6)	ETC ETC
1	0.0474 0.1499 18095.4 0.2475	20835.7 0.1766	31746.6 0.2077	39097.5 0.1922	46170.6 0.1727	53423.7 0.0032	
2	0.0455 0.1435 14030.1 0.2659	26236.4 0.1634	31475.9 0.2098	41158.9 0.1874	47577.2 0.1702	53858.3 0.0032	
3	0.0474 0.1500 13077.5 0.2695	22055.9 0.1739	35394.4 0.1971	40252.1 0.1895	48804.3 0.1668	54575.1 0.0032	
4	0.0478 0.1512 13524.5 0.2674	21511.9 0.1753	32120.4 0.2072	43991.8 0.1790	48276.0 0.1680	55941.3 0.0031	

5	0.0476					
	0.1505					
	13635.0	21974.7	31741.3	41205.2	51673.8	55525.5
	0.2671	0.1742	0.2085	0.1869	0.1602	0.0032
6	0.0473					
	0.1495					
	14011.9	22316.9	32429.9	41140.8	49424.9	58821.7
	0.2653	0.1732	0.2063	0.1869	0.1653	0.0030
7	0.0473					
	0.1494					
	13757.9	22480.4	32525.2	41560.8	49210.1	56635.5
	0.2665	0.1728	0.2060	0.1858	0.1658	0.0031
8	0.0474					
	0.1499					
	13670.8	22201.9	32597.8	41583.0	49528.9	56391.8
	0.2668	0.1735	0.2058	0.1857	0.1650	0.0031
9	0.0474					
	0.1499					
	13728.1	22163.1	32403.7	41686.1	49584.0	56713.2
	0.2666	0.1736	0.2064	0.1854	0.1649	0.0031
10	0.0474					
	0.1498					
	13751.0	22228.1	32388.3	41533.0	49689.7	56776.0
	0.2665	0.1734	0.2064	0.1859	0.1647	0.0031
11	.0474					
	0.1498					
	13760.1	22253.9	32450.8	41526.0	49559.4	56877.0
	0.2665	0.1734	0.2062	0.1859	0.1650	0.0031

12	0.0474					
	0.1498					
	13741.9	22250.0	32458.8	41567.7	49541.9	56748.5
	0.2665	0.1734	0.2062	0.1858	0.1650	0.0031
13	0.0474					
	0.1498					
	13737.2	22231.0	32451.8	41571.4	49576.0	56730.0
	0.2666	0.1734	0.2062	0.1858	0.1649	0.0031
14	0.0474					
	0.1498					
	13742.9	22230.7	32440.0	41569.3	49582.8	56764.2
	0.2665	0.1734	0.2063	0.1858	0.1649	0.0031
15	0.0474					
	0.1498					
	13744.8	22236.9	32441.2	41560.3	49582.1	56771.4
	0.2665	0.1734	0.2063	0.1858	0.1649	0.0031
16	0.0474					
	0.1498					
	13744.3	22238.2	32446.1	41561.0	49573.9	56770.5
	0.2665	0.1734	0.2062	0.1858	0.1649	0.0031
17	0.0474					
	0.1498					
	13743.0	22237.0	32446.3	41564.4	49573.6	56762.3
	0.2665	0.1734	0.2062	0.1858	0.1649	0.0031

APPENDIX F

CYCLE SCHEDULE INDICES FOR NON-INTEGER BATCH NUMBERS

Consider a reactor with total number of assemblies N_{tot}, of which $3N_A$ assemblies are run in a three batch mode and $2N_B$ assemblies are run in a two batch mode. Hence, at every shutdown N_A assemblies of type A are loaded and discharged and N_B assemblies of type B are loaded and discharged. The governing reactivity equations can be written as:

$$\rho_{A1} = \rho_{OA} - A_A B_C \frac{f_1}{(N_A/N_{tot})}$$

$$\rho_{A2} = \rho_{OA} - A_A B_C \frac{(f_1 + f_2)}{(N_A/N_{tot})}$$

$$\rho_{A3} = \rho_{OA} - A_A B_C \frac{(f_1+f_2+f_3)}{(N_A/N_{tot})}$$

$$\rho_{B1} = \rho_{OB} - A_B B_C \frac{f_4}{(N_B/N_{tot})}$$

$$\rho_{B2} = \rho_{OB} - A_B B_C \frac{(f_4 + f_5)}{(N_B/N_{tot})} \qquad \text{(F.1)}$$

where ρ_{Ai} (and ρ_{Bi}) are the reactivities of sublots A (and B) during cycle i of in-core residence, ρ_{OA} (and ρ_{OB}) are the initial reactivities of fuel types A (and B), A_A (and A_B) are the slopes of the reactivity vs. burnup curves for fuel types A (and B), and B_C represents the core average cycle burnup (MWD/MTP). The quantity $f_1/(N_A/N_{tot})$ can be interpreted as the relative energy generated in batch 1 of sublot A in an equilibrium burnup cycle; and similarly for the other

analogous terms. Application of the criticality condition:

$$\rho_L = \sum_{i=1}^{N} f_i \rho_i \tag{F.2}$$

gives:

$$B_C = \frac{(f_1+f_2+f_3)\ \rho_{OA}+(f_4+f_5)\rho_{OB}-\rho_L}{A_A\left\{\frac{N_{tot}}{N_A}\sum_{i=1}^{3}\sum_{j=i}^{3} f_i f_j\right\}+\left\{\frac{N_{tot}}{N_B}\sum_{i=4}^{5}\sum_{j=i}^{5} f_i f_j\right\} A_B} \tag{F.3}$$

If we assume that type A and type B fuel are identical then:

$$B_C = \frac{\rho_o - \rho_L}{A\left[\frac{N_{tot}}{N_A}\left[\sum_{i=1}^{3}\sum_{j=i}^{3} f_i f_j\right]+\frac{N_{tot}}{N_B}\left[\sum_{i=4}^{5}\sum_{j=i}^{5} f_i f_j\right]\right]} \tag{F.4}$$

The discharge burnup of type A fuel (three residence cycles) is given by:

$$B_{dis,A} = B_c \frac{N_{tot}}{N_A}(f_1+f_2+f_3) \tag{F.5}$$

and the discharge burnup for type B fuel (two residence cycles) is given by

$$B_{dis,B} = B_C \frac{N_{tot}}{N_B}(f_4+f_5) \tag{F.6}$$

The average discharge burnup is the assembly weighted average of $B_{dis,A}$ and $B_{dis,B}$; namely:

$$B_{dis,avg} = \frac{N_A\ B_{dis,A} + N_B\ B_{dis,B}}{N_A + N_B} \tag{F.7}$$

Combining Eqs. F.5 through F.7 gives:

$$B_{dis,avg} = B_C \frac{N_{tot}}{N_A+N_B} \tag{F.8}$$

In terms of Eq. F.4:

$$B_{dis,avg} = \frac{\rho_o - \rho_L}{A\left[\frac{N_A+N_B}{N_A}\left[\sum_{i=1}^{3}\sum_{j=i}^{3} f_i f_j\right] + \frac{N_A+N_B}{N_B}\left[\sum_{j=4}^{5}\sum_{j=i} f_i f_j\right]\right]} \tag{F.9}$$

The following constituent equations:

$$N_{reload} = N_A + N_B$$

$$N_A = N_{tot} - 2N_{reload}$$

$$N_B = 3N_{reload} - N_{tot}$$

$$N_{reload} = N_{tot} \frac{B_c}{B_{dis,avg}} \tag{F.10}$$

can be combined with Eq. F.9 to give

$$B_{dis,avg} = \frac{\rho_o - \rho_L}{A\left[\frac{1}{(B_{dis}/B_c-2)}\left[\sum_{i=1}^{3}\sum_{j=i}^{3} f_i f_j\right] + \frac{1}{(3-B_{dis}/B_c)}\left[\sum_{i=4}^{5}\sum_{j=i} f_i f_j\right]\right]} \tag{F.11}$$

Consider the case $N_A = N_B$, which gives $B_{dis}/B_c = 2.5$. Then the average discharge burnup becomes:

$$B_{dis,avg} = \frac{\rho_o - \rho_L}{A \cdot 2\left[\left[\sum_{i=1}^{3}\sum_{j=i}^{3} f_i f_j\right] + \left[\sum_{i=4}^{5}\sum_{j=i} f_i f_j\right]\right]} \tag{F.12}$$

and the CSI (cycle schedule index) is:

$$CSI = 2\left\{\left[\sum_{i=1}^{3}\sum_{j=i}^{3} f_i f_j\right]+\left[\sum_{i=4}^{5}\sum_{j=i}^{5} f_i f_j\right]\right\} \qquad (F.13)$$

The cycle schedule index for equal power sharing ($f_1 = f_2 = f_3 = f_4 = f_5$) is 0.72. However, the minimum cycle schedule index (which maximizes burnup and minimizes natural uranium usage) occurs when $f_1 = f_2 = f_3$ and $f_4 = f_5$, but the two sets of f_i's are <u>not</u> equal. For this case ($N_A = N_B$) the minimum occurs when:

$$f_1 = f_2 = f_3 = 0.1766$$
$$f_4 = f_5 = 0.2350$$

and the CSI is 0.7059, 2% lower than the equal-power-sharing case. Recall, that for integer batch numbers (N=2,3,4...) with equal power sharing the CSI was equal to $\frac{N+1}{2N}$. One might be tempted to apply this relation to the non-integer problem of present concern: N=2.5, in which case $\frac{N+1}{2N} = 0.700$, about 0.85% lower than the true optimum (and hence physically unreachable). This example reinforces the observation that an accurate computation of the cycle schedule index is essential to determine discharge burnups and hence uranium savings, particularly when one is trying to distinguish among subtle variations in design or fuel management strategy.

APPENDIX G

MATHEMATICAL EQUIVALENCE OF COOLANT VOID SPECTRAL SHIFT WITH SPECTRAL SHIFT BY PIN-PULLING AND BUNDLE RECONSTITUTION

Spectral shift in a reactor can be accomplished by pitch variation (corresponding to pin-pulling and bundle reconstitution) or by varying the void content of the coolant. While slight differences may occur in the ρ vs. B values for the two systems because of the difference in Dancoff shadowing factors, the two approaches can be made identical for all practical purposes.

Consider spectral shift accomplished by pin-pulling and bundle reconstitution (see Fig. 7-10).

Suppose the reactor contains N_1 assemblies of batch one fuel, each assembly containing M' metric tons of heavy metal and N_2 (N_3) assemblies of batch 2 (3) fuel, each assembly containing M" metric tons of heavy metal. The spectral shift unit cell (or assembly) calculation determines the values of ρ_o', A' and A", where ρ_o' is the initial extrapolated reactivity of the "dry" assembly, A' is the slope of the reactivity vs. burnup curve $(MWD/MT)^{-1}$ for the "dry" assembly and A" is the slope of the ρ vs. burnup curve $(MWD/MT)^{-1}$ for the "wet" assembly. The reactivity equations for the assemblies in the three batches can be written as:

$$\rho_1 = \rho_o' - \frac{A'(P_{avg}t)\ P_1}{M'}$$

$$\rho_2 = \rho_o' - \frac{A'(P_{avg}t)P_1}{M'} - \frac{A''(P_{avg}t)P_2}{M''} + \Delta\rho_\omega$$

$$\rho_3 = \rho_o' - \frac{A'(P_{avg}t)P_1}{M'} - \frac{A''(P_{avg}t)P_2}{M''} - \frac{A''(P_{avg}t)P_3}{M''} + \Delta\rho_\omega$$

(G.1)

where P_{avg} is the average assembly power, P_i is the relative power in assemblies of type i, and the product $P_{avg}t$ can be identified as the average energy generated per assembly in one cycle. The power fraction for each batch is given by:

$$f_1 = \frac{N_1P_1}{N_{tot}} \qquad f_2 = \frac{N_2P_2}{N_{tot}} \qquad f_3 = \frac{N_3P_3}{N_{tot}} \tag{G.2}$$

Applying the criticality equation:

$$\rho_L = \sum_{i=1}^{3} f_i\rho_i \tag{G.3}$$

gives

$$\bar{P}t = \frac{\rho_o' - \rho_L + \Delta\rho_\omega \left[\frac{N_2P_2 + N_3P_3}{N_{tot}}\right]}{\frac{A'P_1}{M'} + \frac{A''}{M''}\left[\frac{N_2P_2^2}{N_{tot}} + \frac{N_3P_3^2}{N_{tot}} + \frac{N_3P_3^2}{N_{tot}}\right]} \tag{G.4}$$

or:

$$\bar{P}t = \frac{\rho_o' - \rho_L + \Delta\rho_\omega\ (f_2+f_3)}{\frac{A'}{M'}\ \frac{N_{tot}}{N_1}\ f_1 + \frac{A''}{M''}\left[\frac{N_{tot}}{N_2}\ f_2^2 + \frac{N_{tot}}{N_2}\ f_2f_3 + \frac{N_{tot}}{N_3}\ f_3^2\right]} \tag{G.5}$$

The cycle burnups for each batch are given by:

$$B_{c1} = \frac{\bar{P}t\ P_1}{M'};\quad B_{c2} = \frac{\bar{P}t\ P_2}{M''};\quad B_{c3} = \frac{\bar{P}t\ P_3}{M''} \tag{G.6}$$

The cycle average burnup is the mass-weighted value of the batch burnups, hence:

$$B_{c,avg} = \frac{N_1 M' (\frac{\bar{P}t}{M'}) P_1 \quad N_2 M'' (\frac{\bar{P}t}{M''}) P_2 \quad N_3 M'' (\frac{\bar{P}t}{M''}) P_3}{M_{total}} \tag{G.7}$$

and so:

$$B_{c,avg} = \frac{\bar{P}t \quad N_{tot}}{M_{tot}} \tag{G.8}$$

In the ideal case, pins are pulled and the batch two bundles are manufactured immediately during the refueling outage, to permit reinsertion of the reconstituted bundles before startup. (Actually this is not essential: one could postpone reinsertion one cycle and obtain the same steady-state condition.) All mass is preserved, so that $N_1M' = N_2M'' = N_3M''$. The reload mass is N_1M'' and the reload feed (MTF) is $(\frac{F}{P})\ N_1M'$ where F/P is the feed to product ratio. The total energy generated per cycle is given by:

$$E = B_{c,avg}\ (M_{tot}) = \bar{P}t\ N_{tot} \tag{G.9}$$

and the total energy per metric ton of feed is given by:

$$U = \frac{E}{F} = \frac{\bar{P}t\ N_{tot}}{(\frac{F}{P})\ N_1M'} \tag{G.10}$$

where U is the uranium utilization (MWD/MTF). Inserting Eq. G.5 and making use of the fact that $N_1M' = N_2M'' = N_3M''$ gives:

$$U = \frac{\rho_o' - \rho_L + \Delta\rho_\omega \, (f_2 + f_3)}{\left[A' f_1 + A''(f_2^2 + f_2 f_3 + f_3^2)\right] \left(\frac{F}{P}\right)} \qquad \text{(G.11)}$$

Eq. G.11 is identical to the corresponding relation developed for coolant spectral shift in Chapter 7. As shown in Chapter 7, the choice of transition burnup, B_{tran}, specifies f_1 (P_1), and hence the optimum uranium utilization occurs when $f_2 = f_3$, which in the pin-pulling and bundle reconstitution case corresponds to $P_2 = P_3$. Optimizing for f_1, f_2, f_3 in the coolant spectral shift case (and, hence, P_1, P_2, P_3 in the pin-pulling case) does not imply that such optimal power profiles can be achieved in actual practice.

REFERENCES

A-1 Adamsam, E. G., et al., "Computer Methods for Utility Reactor Physics Analysis", Reactor and Fuel Processing Technology, 12(2):225-241 (Spring 1969).

A-2 Amster, H. and Suarez, R., "The Calculation of Thermal Constants Averaged Over A Wigner-Wilkins Flux Spectrum: Description of the SOFOCATE Code", WAPD-TM-39, January, 1957.

A-3 Amouyal, A., Benoist, P. and Horowitz, J. J., Nucl. Energy 6, 79,(1957).

A-4 Adams, C. H., "Current Trends in Methods for Neutron Diffusion Calculations", Nucl. Sci. Eng., 64:552 (1977).

B-1 Badruzzaman, A., "Economic Implications of Annular Fuel in PWRs", Trans. Am. Nucl. Soc., 34:384 (June 1980).

B-2 Barry, R. F., "LEOPARD - A Spectrum Dependent Non-Spatial Depletion Code", WCAP-3269-26, September 1973.

B-3 Bohl, H., Gelbard, E., and Ryan, G., "MUFT-4-Fast Neutron Spectrum Code for the IBM-704", WAPD-TM-72, July 1957.

B-4 Breen, R. J., "A One-Group Model for Thermal Activation Calculations", Nucl. Sci. Eng., 9:91 (1961).

B-5 Breen, R. J., et al., "HARMONY: System for Nuclear Reactor Depletion Computation", WAPD-TM-478, January 1965.

B-6 Bergeron, P. A., Maine Yankee Fuel Thermal Performance Evaluation Model, YAEC-1099P, February 1976 (Proprietary).

C-1 Chang, Y. I., et al., "Alternative Fuel Cycle Options: Performance Characteristics and Impact on Nuclear Power Growth Potential", RSS-TM-4, Argonne National Laboratory, Argonne, Illinois, January 1977.

C-2 Correa, F., Driscoll, M. J., and Lanning, D.D., "An Evaluation of Tight Pitch PWR Cores", MITNE-227, August 1979.

C-3 Cacciapouti, R.J., et al., "CHIMP-II, A Computer Program for Handling Input Manipulation and Preparation for PWR Reload Core Analysis", YAEC-1107, May 1976.

C-4 Cadwell, W. R., "PDQ-7 Reference Manual", WAPD-TM-678, January 1967.

C-5 Crowther, R. L., et al., "BWR Fuel Management Improvements for Once Through Fuel Cycles", Trans. Am. Nucl. Soc., 33:369 (1979).

C-6 Crowther, R. L., Personal Communication, January 1981.

C-7 Carnahan, B., Luther, H. R., Wilkes, J. O., Applied Numerical Methods, John Wiley and Sons, New York, 1969.

D-1 Decher, U., and Shapiro, N. L., et al., "Improvements in Once-Through PWR Fuel Cycles", Interim Progress Report, U. S. D.O.E. Contract No. E476-C-02-2426005, January 1979.

D-2 Driscoll, M. J., Pilat, E. E., Correa, F., "Routine Coastdown in LWRs as an Ore Conservation Measure", Trans. Am. Nucl. Soc., 33:399 (November 1979).

D-3 Duderstadt, J. J. and Hamilton, L. J., Nuclear Reactor Analysis, John Wiley and Sons, New York, 1976.

D-4 Dooley, George, Yankee Atomic Electric Company, Personal Communication, Spring 1980.

F-1 Fujita, E. K., Driscoll, M. J. and Lanning, D. D., "Design and Fuel Management of PWR Cores to Optimize the Once-Through Fuel Cycle", MITNE-215, August 1978.

F-2 Fullmer, G. C., BWR End of Cycle/Cycle Length Flexibility Trans. Am. Nucl. Soc., 35:99, 1980.

G-1 Garel, K. C., et al., "A Comparative Assessment of the PWR, SSCR, and PHWR Concepts", Trans. Am. Nuc. Soc., 31: 301 (November 1978).

G-2 Garel, K. C. and Driscoll, M. J., "Fuel Cycle Optimization of Thorium and Uranium Fueled PWR Systems", MITNE-204, October 1977.

G-3 Graves, H.W., Nuclear Fuel Management, John Wiley and Sons, New York, 1979.

H-1 Henry, Alan F., Nuclear Reactor Analysis, M.I.T. Press Cambridge, Mass. 1975.

H-2 Honeck, H. C., "THERMOS, A Thermalization Transports Theory Code for Reactor Lattice Calculations", BNL-5826, 1961.

H-3 Hageman, L. A., "Numerical Methods and Techniques Used in the Two-Dimensional Neutron Diffusion Program PDQ-5", WAPD-TM-364, 1963.

H-4 Hellstrand, E., "Measurements of the Effective Resonance Integral in Uranium Metal and Oxide in Different Geometries", J. Appl. Phys., 28:1493 (1957).

I-1 INFCE, Report of the International Nuclear Fuel Cycle Evaluation, IAEA, Vienna, 1980.

K-1 Kamal, A., "The Effects of Axial Power Shaping on Ore Utilization in Pressurized Water Reactors", S. M. Thesis, M.I.T. Department of Nuclear Engineering, January, 1980.

L-1 Lobo, L., "Coastdown in Light Water Reactors as a Fuel Management Strategy", S. M. Thesis, M.I.T. Department of Nuclear Engineering, December 1980.

M-1 Matzie, R. A., et al., "The Benefits of Cycle Stretchout in PWR Extended Burnup Fuel Cycles", TIS-6469, Combustion Engineering Power Systems, Windsor, Conn., November 1979.

M-2 Macnabb, W. V., "Two Near-Term Alternatives for Improved Nuclear Fuel Utilization", Trans. Am. Nucl. Soc., 33:398, (November 1979).

M-3 Matzie, R. A., et al., "Uranium Resource Utilization Improvements in the Once-Through PWR Fuel Cycle", CEND-380, April 1980.

M-4 Mildrum, C. M. and Henderson, W. B., "Evaluation of Annular Fuel Economic Benefits for PWRs", Trans. Am. Nuc. Soc., 33:806 (November 1979).

M-5 Mildrum, C. M., "Economic Evaluation of Annular Fuel for PWRs", Trans. Am. Nucl. Soc., 35:78 (November 1980).

N-1 "Nuclear Proliferation and Civilian Nuclear Power", Report of the Nonproliferation Alternative System Assessment Program (NASAP), DOE/NE-0001, June 1980.

N-2 Nuclear News, 23(10), August 1980.

N-3 Naft, B. N., "The Effect of Regionwise Power Sharing on PWR In-Core Fuel Management", Trans. Am. Nucl. Soc., 15 (2) (November 1972).

R-1 Robbins, T., "Preliminary Evaluation of a Variable Lattice Fuel Assembly and Reactor Design Concept", Draft Report under Subcontract No. 11Y13576V for Oak Ridge National Laboratory, Pickard, Lowe and Garrick, Inc., Washington, D.C., February 1979.

R-2 Rampolla, D. S., et al., "Fuel Utilization Potential in Light Water Reactors with Once-Through Fuel Irradiation." WAPD-TM-1371 (1978).

S-1 Solan, G. M., Handschuh, J. A., Bergeron, P.A., "Maine Yankee Cycle 4 Design Report", YAEC-1171, January 1979.

S-2 Sider, F. M., "An Improved Once-Through Fuel Cycle for Pressurized Water Reactors", TIS-6529, Combustion Engineering Power Systems, Windsor, Conn., June 1980.

S-3 Smith, M. L., Franklin, C. B., Schleicher, T. W., "Extended Burnup and Extended Cycle Design", Trans. Am. Nucl. Soc., 34:389-390 (June 1980).

S-4 Strawbridge, L. E. and Barry, R. F., "Criticality Calculations for Uniform Water-Moderated Lattices", Nuc. Sci. Eng., 23:58 (1965).

S-5 Suich, J. E. and Honeck, H. C., "The HAMMER System-Heterogeneous Analysis by Multigroup Methods of Exponentials and Reactors", DP-1064, TID-4500, January 1967.

S-6 Sesonke, A., "Extended Burnup Core Management for Once-Through Uranium Fuel Cycles in LWRs", DOE/ET/34021-1, August 1980.

S-7 Silvennoinen, P., Reactor Core Fuel Management, Pergamon Press, Oxford, England, 1976.

S-8 Scherpereel, L. R. and Frank, F. J., "Fuel Cycle Cost Considerations of Increased Discharge Burnup," Trans. Am. Nuc. Soc., 35:72 (1980).

W-1 Williamson, E. A., Terney, W. B. and Huber, D. J., "Interactive Fuel Management Using a CRT", Trans. Am. Nucl. Soc., 30:341 (November 1978).